

file

SSC-129

**A NUMERICAL SOLUTION FOR THE TRANSIENT
STRAIN DISTRIBUTION IN A RECTANGULAR
PLATE WITH A PROPAGATING CRACK**

by
M. P. Gaus

SHIP STRUCTURE COMMITTEE

SHIP STRUCTURE COMMITTEE

MEMBER AGENCIES:

BUREAU OF SHIPS, DEPT. OF NAVY
MILITARY SEA TRANSPORTATION SERVICE, DEPT. OF NAVY
UNITED STATES COAST GUARD, TREASURY DEPT.
MARITIME ADMINISTRATION, DEPT. OF COMMERCE
AMERICAN BUREAU OF SHIPPING

ADDRESS CORRESPONDENCE TO:

SECRETARY
SHIP STRUCTURE COMMITTEE
U. S. COAST GUARD HEADQUARTERS
WASHINGTON 25, D. C.

September 5, 1961

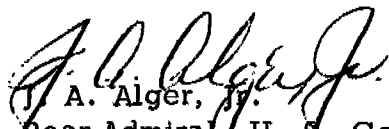
Dear Sir:

As part of its research program related to the improvement of hull structures of ships, the Ship Structure Committee is sponsoring an investigation of Brittle Fracture Mechanics at the University of Illinois. Herewith is a copy of the Fifth Progress Report, Serial No. SSC-129, A Numerical Solution for the Transient Strain Distribution in a Rectangular Plate with a Propagating Crack by M. P. Gaus.

This project is being conducted under the advisory guidance of the Committee on Ship Structural Design of the National Academy of Sciences-National Research Council.

This report is being distributed to individuals and groups associated with or interested in the work of the Ship Structure Committee. Comments concerning this report are solicited.

Sincerely yours,


J. A. Alger, Jr.
Rear Admiral, U. S. Coast Guard
Chairman, Ship Structure
Committee

SSC-129

Fifth Progress Report
of
Project SR-137

to the

SHIP STRUCTURE COMMITTEE

on

A NUMERICAL SOLUTION FOR THE TRANSIENT STRAIN DISTRIBUTION
IN A RECTANGULAR PLATE WITH A PROPAGATING CRACK

by

M. P. Gaus

University of Illinois
Urbana, Illinois

now with

Pennsylvania State University
University Park, Pennsylvania

under

Department of the Navy
Bureau of Ships Contract NObs-65790
BuShips Index No. NS-731-034

transmitted through

Committee on Ship Structural Design
Division of Engineering and Industrial Research
National Academy of Sciences-National Research Council

under

Department of the Navy
Bureau of Ships Contract NObs-72046
BuShips Index No. NS-731-036

Washington, D. C.
National Academy of Sciences-National Research Council
September 5, 1961

ABSTRACT

A physical lattice model that approximates a continuous material by reducing it to a series of rigid bars and deformable connections is used in this report to investigate the transient-strain redistribution associated with a crack propagating through a rectangular plate.

Equations are developed for equilibrium of the lattice model in terms of displacements using plane-stress conditions. A complete set of equations is given to cover all cases of boundary conditions that ordinarily would be encountered in applications of this lattice model. Results of several examples of statically loaded plates analyzed with the lattice model show excellent agreement when compared with an energy method solution.

The differential equations expressing the dynamic behavior of the lattice model are developed, and numerical solution of these equations is discussed. Examples are given of application of these equations to a steady-state condition and the calculation of natural frequencies of lattice models. Several examples of the transient-strain redistribution associated with a crack propagating through a plate in finite jumps are presented. Two methods of numerical integration that are suitable for transient solutions of the differential equations are described and applied to the same problem with resulting comparable satisfactory solutions.

An immense amount of calculation is involved in solving transient strain-wave propagation problems with the lattice model, and a high speed digital computer is virtually a necessity for numerical solution of problems of any complexity by this method.

CONTENTS

	<u>Page</u>
Introduction	1
Object and Scope	1
Brief Review of Some Mathematical Solutions	3
Acknowledgment	4
Notation	5
A Model for Studies of Two-Dimensional Wave Propagation	6
General	6
Description of Model	7
Equilibrium as Related to the Airy Stress Function	11
Equilibrium Equations in Terms of Displacements	16
Boundary Conditions	19
Representation of a Crack-Type Discontinuity	25
Summary of Static Equilibrium Equations for the Lattice Model . .	28
Numerical Results for Static Loading	34
General	34
Square Plate with Parabolically Distributed End Tension	35
Square Plate with Concentrated Loads	41
Uniformly Loaded Plates with Cracks	41
Checking of Bar Stresses	43
Solution of Problems Involving Time Dependence	45
Differential Equations	45
Natural Frequencies	47
General Approach for Solving Strain Wave or Crack Propagation Problems	50
Numerical Integration of Equations	52
Newmark Beta-Method of Integration	52
Runge-Kutta Method of Integration	54
Numerical Results for Transient Strains	57
General Remarks and Problems Considered	57
Variables Entering Into the Calculation	57
Possible Difficulties in Solving Dynamic Problems with a Lat- tice Model	60
Solutions for Transient Strains with a Coarse Lattice Model . . .	60
Summary and Conclusions	73
References	77

BRITTLE FRACTURE MECHANICS ADVISORY COMMITTEE

for the

COMMITTEE ON SHIP STRUCTURAL DESIGN
Division of Engineering & Industrial Research
National Academy of Sciences-National Research Council

Chairman:

N. J. Hoff
Head of Department of Aeronautical Engineering
Stanford University

Members:

D. S. Clark
Professor of Mechanical Engineering
California Institute of Technology

Morris Cohen
Department of Metallurgy
Massachusetts Institute of Technology

F. J. Feely, Jr.
Esso Research & Engineering Company

Martin Goland
Vice President
Southwest Research Institute

G. R. Irwin
Head, Mechanics Division
Naval Research Laboratory

Egon Orowan
Department of Mechanical Engineering
Massachusetts Institute of Technology

W. R. Osgood
Department of Civil Engineering
Catholic University

M. P. White
Head, Civil Engineering Department
University of Massachusetts

INTRODUCTION

Object and Scope

The purpose of this investigation was to develop a physical model that would approximate a continuous material and be suitable for the investigation of transient two-dimensional strain wave propagation. It was desired that this model be able to represent a crack-type discontinuity in a plate and provide a picture of the strain redistribution resulting from the release of internally stored strain energy as a crack is initiated and grows in size.

The investigation was undertaken as a part of a study of the rapid propagation of brittle fracture in low-carbon steel plates. The mechanics of brittle-fracture initiation, propagation, and arrest have been the subject of intensive study for many years. Under certain conditions of stress, temperature, rate of loading, type and nature of material, and geometry, low-carbon steels often fracture in a brittle rather than a ductile manner.

From the structural point of view, the term brittle fracture has become associated with a fracture that is primarily of the cleavage type, with little apparent deformation, and one that proceeds at a very rapid rate once initiated. Such a fracture can propagate through a steel plate at velocities of as much as 5000 fps or more. Usually there is no warning of impending failure, and in many instances where no barrier was present to stop a propagating crack, the results have been catastrophic.¹

This rapid brittle fracture in which a crack somehow initiates and rapidly propagates is the result of an inherent instability of the material. On the basis of present understanding, the gross situation might be pictured as follows: The elastic energy stored in the material, while not sufficient to cause general yielding of the material, may be, below certain temperatures, more than sufficient to cause cleavage fracture in the zone around the moving crack tip once the crack has started to propagate. After a rapidly propagating brittle crack is initiated, there is an intense transient strain field associated with the crack front.²

In the fracture zone at the head of the moving cracks, a combination of

extremely high strain rate and very high tensile stress exists. This combination of conditions produces brittle fracture of the material in the immediate fracture zone, and the released elastic energy in excess of that needed to produce the fracture is carried away from the fracture zone in the form of strain waves. The velocity of the strain wave propagation is greater than the net rate at which the crack grows, so that the zone of high strain rate and high tensile stress extends ahead of the immediate fracture zone. This extension of the intense transient strain zone ahead of the crack causes additional fracturing which releases more energy, and the whole system travels along as a self-sustaining phenomenon until something brings it to a halt. It is emphasized that a comprehensive understanding of the brittle-fracture phenomenon still does not exist.

A finite model that divides a continuous material into a definite number of pieces that behave according to certain rules can only provide an approximate representation of the continuous material. If the stress or strain gradients existing in the continuous material are small, the approximation with even a coarsely divided model will be fairly good. However, if the gradients are large, a finely divided model is required to provide a good representation of the distribution of strains.

Representing a cracked plate with a finite model has two important disadvantages. First, the strain gradients associated with a crack are quite steep, and a very finely divided model would be required to provide accurate qualitative information in the vicinity of the crack. Second, the model can only simulate a crack having a length which is some multiple of the model division, and if the crack is to extend, it must do so in jumps of finite length. In spite of these disadvantages, an investigation with a model of this type has value in that it provides to some degree a quantitative picture of strain redistribution for a propagating crack.

How finely the model is divided depends on the computing facilities available; because there is an immense amount of calculation involved, solution of wave propagation problems by this method is contingent upon the

availability of a high-speed digital computer.

Brief Review of Some Mathematical Solutions

A number of mathematical solutions have been devised to find the stress or strain distribution associated with an elongated hole or crack in an elastic material. The earliest of these solutions was given by Inglis,³ who considered the case of an elliptical hole in a thin plate (where plane stress or plane strain conditions may be assumed to apply) and solved the problem in terms of curvilinear coordinates. The limiting case, consisting of the minor axis of the hole going to zero, represents the solution for a plate containing a crack having a length equal to the major axis of the hole.

By using a complex variable stress function, Westergaard⁴ arrived at the same result as Inglis but in a more easily treated form. Westergaard's method also covers cases of cracks subject to splitting forces, internal pressure, and several other situations.

Griffith⁵ investigated the cracking phenomenon and derived an equation for the length of a crack that would become unstable in a brittle material. Griffith's theory considers the strain energy stored in a material and determines the stability of a crack of given length by comparing the decrease in strain energy resulting from the formation of the crack with the work required to form new crack surfaces in the material. When more strain energy is released than is required to form new crack surfaces, the crack becomes unstable and should grow in size. Orowan⁶ extended Griffith's theory to the case of cracks in steel by replacing the surface tension term with a plastic work factor, and Irwin⁷ showed a parallel for certain ductile materials.

Neuber⁸ developed methods for computing stresses in notched bars and presented a cracking mechanism theory. Irwin,⁹ using Westergaard's method, expressed the stress environment at the end of a crack in terms of a "crack extension force" for plane stress or plane strain conditions. McClintock¹⁰ considered a crack within a field of uniformly applied elastic shear stress and calculated the plastic field at the crack root as well as the general elastic stress field.

All of the solutions which have been mentioned so far considered stationary cracks. Mott¹¹ extended Griffith's theory and suggested that the expression for balance of energy should contain a term including the kinetic energy of the material as well as available elastic energy and surface tension. Through the application of dimensional analysis, Mott arrived at an expression containing a kinetic energy term. Roberts and Wells¹² used Mott's work as a starting point, Westergaard's solution for the kinetic energy distribution of the material and the distance a stress wave could extend away from the crack tip as limited by the velocity of longitudinal elastic waves to arrive at a limiting velocity for a crack propagation in an elastic material.

Yoffe¹³ considered a moving Griffith crack of constant length $2a$ translated at a constant velocity through an infinite plate. This steady-state solution was based on elastic surface waves and Westergaard's static solution. It was concluded that a critical velocity exists beyond which a crack will tend to curve or form branches.

Only a few of the more prominent references pertaining to the stress or strain distribution associated with a crack have been mentioned here. Since the report is concerned with the development of a method for calculating transient strain effects associated with an extending crack, no attempt has been made in this brief review to give a comprehensive survey of published literature. The few references reviewed here are only intended to provide background information on available solutions for the stresses and strains associated with cracks in plates.

Acknowledgment

The work described in this report was conducted in the Structural Research Laboratory of the Department of Civil Engineering, University of Illinois. The research program is sponsored by the Ship Structure Committee, and the members of the Brittle Fracture Mechanics Advisory Committee under the Committee on Ship Structural Design of the National Academy of Sciences-National Research Council have acted in an advisory

capacity in the planning of this program.

The program is under the general direction of N. M. Newmark, Professor and Head of the Department of Civil Engineering, and under the immediate direction of W. J. Hall, Professor of Civil Engineering. This report is based in part on a doctoral dissertation by the author submitted to the Graduate College, University of Illinois.

Notation

The notation that follows has been adopted in this report. Each term is defined when first introduced but is summarized here for convenience.

- |A| = Matrix of stiffness coefficients
- a = Acceleration
- |B| = Mass matrix
- C = Amplitude
- D = $-(1 - \nu^2)/Ed$
- d = Plate thickness
- E = Young's modulus = 30×10^6 psi for all examples
- F = Extensional force
- G = Shear modulus = $E/2(1 + \nu)$
- h = Integration time interval
- i = Variable subscript
- j = Variable subscript
- m = Mass
- n = n-th bar, n-th time interval, etc.
- P = Concentrated load or load factor for parabolic load
- p = Natural frequency = $\omega/2\pi$
- S = Shear force
- T = Period of vibration
- t = Time
- u = Displacement in x-direction
- v = Displacement in y-direction

- \bar{X} = Body force in x-direction
- \bar{Y} = Body force in y-direction
- x = Direction of axis or variable
- y = Direction of axis or variable
- α = Undetermined coefficient
- β = Parameter used in Newmark method of integration
- γ = Shear strain
- δ = Phase angle
- ϵ = Extensional strain
- λ = Grid or bar spacing, eigenvalue
- ν = Poisson's ratio = 0.30 for all examples
- σ = Extensional stress
- τ = Shear stress
- ϕ = Airy stress function
- ψ = Stress function in energy method
- ω = Circular frequency
- ∇^4 = Biharmonic operator

A MODEL FOR STUDIES OF TWO-DIMENSIONAL WAVE PROPAGATION

General

Sometimes it is necessary to resort to an approximate method in order to investigate the strain and stress distribution in a body. Among the approximate procedures previously used for the investigation of two-dimensional elasticity problems, which are not readily treated by exact methods, are finite differences and physical analogies such as lattice, bar, or framework methods.

Usually the lattice or framework methods used for solution of two-dimensional problems involving plane stress or plane strain conditions can be shown to be the physical representation of the finite difference formulation of some set of elasticity equations. Even though there is an equivalence between the finite difference procedure and the lattice analogy procedure, each of these methods can be derived independently and each is subject to certain peculiari-

ties. The use of a physical model is convenient because the model provides something which is easily visualized and facilitates the treatment of difficult boundary conditions.

Hrennikoff¹⁴ and McHenry¹⁵ have described the development and application of several lattice* or framework analogies for solution of two-dimensional static elasticity problems. Their analogies consist of replacing a plate of continuous material with a network of elastic bars, pin-connected to each other at the ends, to form a lattice whose deformation in any direction under any form of loading duplicates the deformation of certain points on the original plate. Any distributed loading acting on the plate is replaced by statically equivalent loads acting at joints of the lattice. Each bar forming the lattice is considered as an elastic member, and the areas of these bars are selected so that there are identical deformations at a certain number of points in the continuous plate and the analogous lattice. One peculiarity of the lattices described by Hrennikoff and McHenry is that the value of Poisson's ratio must be taken as one third in order to satisfy identically equilibrium and compatibility conditions. Hrennikoff suggests several lattices that may overcome this difficulty; however, the use of these lattices would be quite cumbersome.

The lattice model developed in this report is shown to be the physical analog of an Airy stress function expressed in terms of finite differences. The report describes the lattice model, as well as the correspondence between the model and continuous plate that it replaces. The equations of equilibrium for the lattice model are developed in terms of Airy's stress function, and the stress-strain relationships of linear elasticity are then used to develop equilibrium equations in terms of displacements of the lattice model bars.

Description of Model

The particular model used for this investigation of two-dimensional wave propagation and to represent a crack-type discontinuity was suggested by Dr.

*The term "lattice" or "lattice model" will hereafter be used to refer to a physical model made up of a system of bars and is to be considered to include the terms "bar" or "framework."

N. M. Newmark. This model replaces a thin plate with a number of discrete units composed of rigid bars, each having a definite mass, which are linked together through massless deformable connections. Displacements, deformations, and forces in the lattice model formed by the discrete bar units are made to agree as closely as possible at definite points with the displacements, deformations, and forces at the equivalent points in the thin plate that the model replaces.

In order to illustrate and identify different parts of the model easily, it is convenient to use a schematic drawing. Such a schematic drawing of a model that replaces a square plate is shown in Fig. 1. The model illustrated divides the original square plate into sixteen square units having a width of λ on each side, where λ equals the plate width divided by the number of units (four) into which the plate width is divided. It will be assumed that the dimensions of any rectangular plate to be represented with this model are such that the plate can be divided into some number of square units. Each unit of the model is composed of four interconnected rigid bars which are drawn to a convenient width in Fig. 1 for ease of visualization. In an undeformed condition, the lattice of bars forming the model are either parallel or perpendicular to each other and have their centerlines spaced at the distance λ .

A system of notation is needed to describe the lattice model and readily identify different lattice model parts and their locations. The system of notation used is shown in Fig. 1 and consists of a grid of lines parallel to the indicated x- and y-axes. The lines are spaced at a distance of $\lambda/2$ and are arranged so that in the undeformed lattice model these lines either form the centerline of bars or pass midway between the bars. Each bar is then bisected by two lines, one forming the centerline of the bar and the other laterally dividing the bar length into two equal sections. Starting at the lower left-hand corner and proceeding in the positive direction of the x- and y-axes, the lines forming the bar centerlines are assigned numbers. The remaining grid lines, situated between bars, are similarly assigned letters. If the numbers and letters are used as x- and y- coordinates, the point formed by the intersection of any

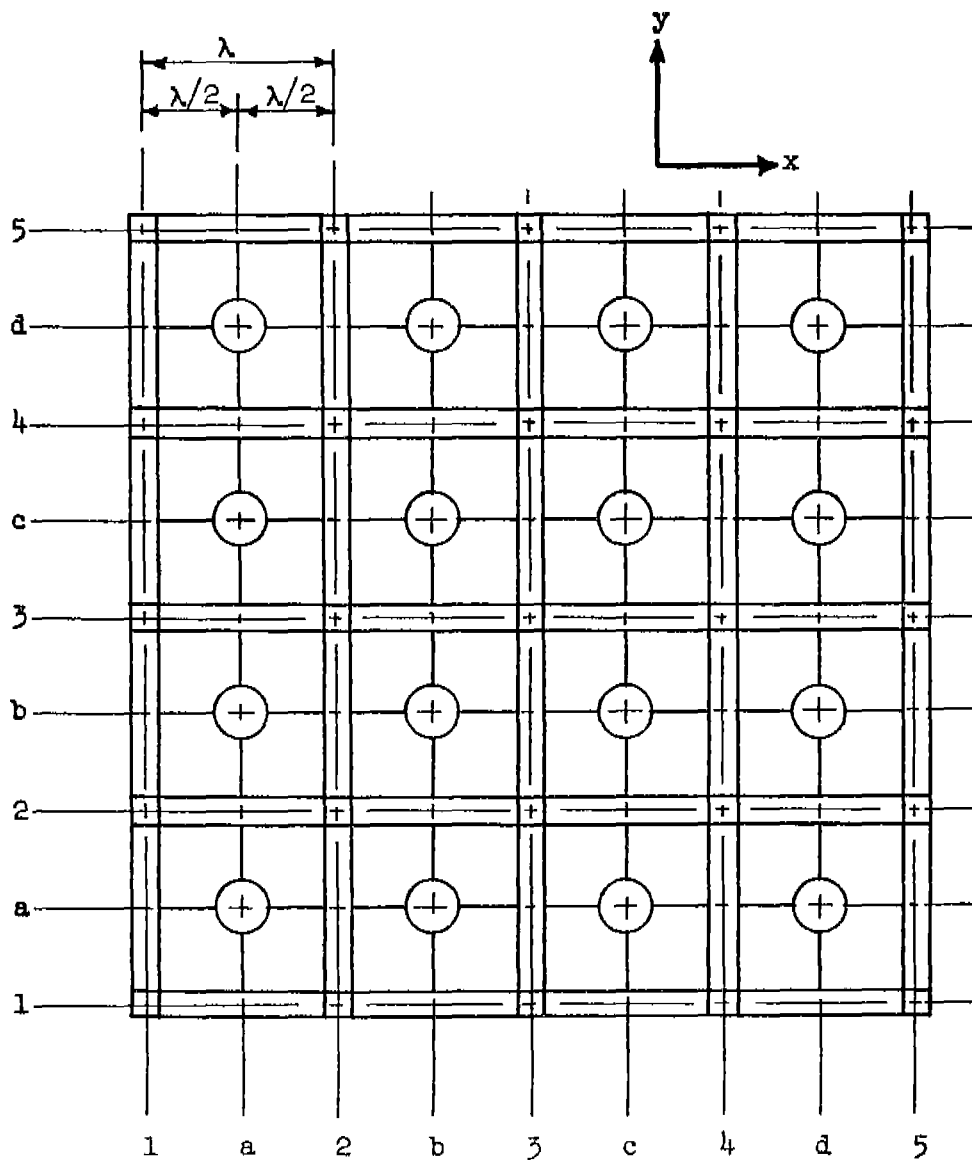


FIG. 1 LATTICE MODEL OF RECTANGULAR PLATE

two grid lines can be identified with a combination of letters, numbers, or a letter and a number. Only points formed by the intersection of grid lines are considered to have meaning in the lattice model, and when reference to such a point is made, it is done so by either giving the appropriate letters and numbers or using them as subscripts of terms defined at that point.

The following definitions are used with the lattice model as shown in Fig. 1.

- λ - Spacing between lattice model bars
- d - Thickness of plate represented by the lattice model.
- u and v - Displacement of a point, from the initial position in the lattice model, in the x - and y -directions, respectively. Positive displacement is in the positive x - or y -directions.
- bar - A rigid bar drawn to any convenient size for purposes of illustration. The mass of each bar is equivalent to a section of plate having the dimensions $\lambda^2 d$ or $\lambda^2 d/2$ depending upon whether the bar is in the interior or at the edge of the model. A typical interior bar is b-3 and a typical edge bar is 5-b.
- displacement point - The point at the center of a bar coinciding with the intersection of two grid lines. Displacement is only defined at these points and is in the direction of the x - or y -axes. This is the displacement u or v and the bar referred to is identified by letter and number subscripts such as u_{b3} for displacement of bar b-3.
- node - A point at the intersection of two or more bars. All extensional deformation or strain and associated extensional forces or stresses are concentrated at the node points. For illustrative purposes, the nodes are drawn as small squares the same width as the bars such as node 3-2.
- shear point - A point midway between the bars making up the lattice model. All shear deformation or strain and associated shear stresses and forces are concentrated at these points. A typical shear point is c-b.
- extensional force F - A force which acts on the end of and along the axis of a lattice model bar. This force is the statical equivalent of the force acting across a section of the plate that the bar replaces. Positive force, positive stress σ , and positive strain ϵ are associated with a linear extension of a piece of elastic material. The

extensional forces are applied to bars at node points.

- shear force S - A force that is applied to a lattice model bar at the displacement point whose lines of action are along the axis of the bar. This shear force is the statical equivalent of the shear force acting along a section of the plate replaced by the bar. Positive shear force is associated with positive shear stress and strain as defined in books on theory of elasticity, for example, as in Timoshenko and Goodier.¹⁶
- body force - Force resulting from gravity or any other time independent effect. A body force is considered to act at the displacement point and along the axis of a bar. Body forces in an x -direction are denoted by \bar{X} and body forces in the y -direction are denoted by \bar{Y} . The positive direction of a body force is in a direction opposite to the positive direction of the x - and y -axes.

Deformation behavior of the continuous plate is approximated in the lattice model by stretching or compressing the deformable nodes for extensional strains and changing the angles between bars for shear strain. The shearing resistance of the lattice can be visualized as a set of elastic rods connecting the bars at their deformation points as shown in Fig. 2, or as a four-armed spring device that opposes changes in the angles between its arms, which are connected to four-bar displacement points, as shown in Fig. 3. The four-armed spring is used in Fig. 1 because it is easier to visualize.

Typical interior bars such as $b-3$ and $3-b$ in Fig. 1 are taken as free bodies in Figs. 4 and 5 to show the forces that could be acting on the bars. The line of action of all the forces actually must pass through the displacement point at the center of the bar--the shear forces are drawn at the sides of the bars for clarity. The directions of the forces as shown are for positive strains and a positive body force.

Equilibrium as Related to the Airy Stress Function

Equilibrium of the model can be developed in terms of finite differences

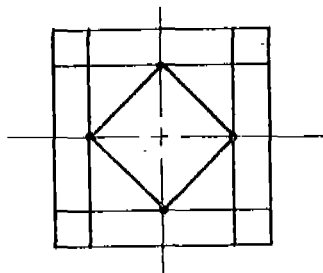


FIG. 2 SHEAR DEFORMATION WITH DEFORMABLE RODS

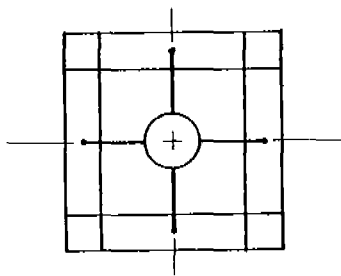


FIG. 3 SHEAR DEFORMATION WITH FOUR ARMED SPRING

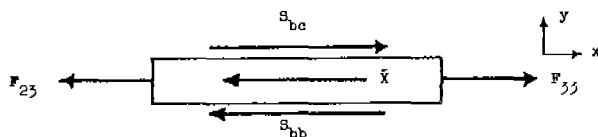


FIG. 4 FORCES ACTING ON x-DIRECTION BAR

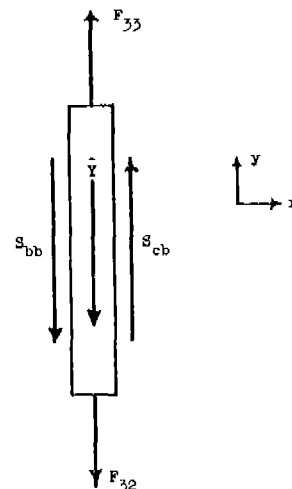


FIG. 5 FORCES ACTING ON y-DIRECTION BAR

of Airy's stress function. Such a development shows that the lattice model can be thought of as a finite physical representation of the Airy stress function method for solving an elasticity problem.

The general solution to an elasticity problem must satisfy three sets of equations: equilibrium, compatibility, and boundary conditions. Simplifying assumptions are made regarding one of the displacements or one of the stresses to obtain the plane strain or plane stress conditions and thereby reduce a three-dimensional problem to one of two dimensions.

The Airy stress function has been shown¹⁶ to provide a convenient solution for problems of plane stress or plane strain. If a function* $\phi(x, y)$, which hereafter is called the Airy stress function, satisfies the biharmonic equation $\nabla^4 \phi = 0$, then the equilibrium and compatibility equations are exactly satisfied for plane strain conditions and approximately satisfied for plane stress conditions. The approximation in plane stress problems occurs because for plane stress conditions it is assumed $\sigma_z = \tau_{xz} = \tau_{yz} = 0$ and that σ_x , σ_y , and τ_{xy} are independent of z . These assumptions imply that ϵ_x , ϵ_y , ϵ_z , and γ_{xy} are independent of z and that γ_{xz} and γ_{yz} are zero. The compatibility equation

*Unless otherwise noted the symbols for stress, strain, and the Airy stress function are the same as those defined in Theory of Elasticity by Timoshenko and Goodier.¹⁶

$$\partial^2 \epsilon_x / \partial y^2 + \partial^2 \epsilon_y / \partial x^2 = \partial^2 \gamma_{xy} / \partial x \partial y \quad (1)$$

is then satisfied by the strain components ϵ_x , ϵ_y , and γ_{xy} ; however, in the general three-dimensional case there are five other compatibility equations which must be satisfied with the above assumptions. All five of these remaining compatibility equations are satisfied only if ϵ_z is a linear function of x and y . The strain ϵ_z must satisfy the condition

$$\epsilon_z = -\nu(\sigma_x + \sigma_y)/E = ax + by + c \quad (2)$$

where a , b , c are constants.

This condition is not always satisfied in plane stress problems. Generally, for such problems, γ_{xz} , γ_{yz} , and σ_z are different from zero and vary through the thickness of the plate. It is shown in Timoshenko and Goodier,¹⁶ however, that for thin-plate problems the solutions obtained from the plane strain approximation to the plane stress problem are reasonably good approximations to the "exact" solution. It will be assumed in this report that the plates considered are thin enough so that a satisfactory plane stress solution will be obtained from an Airy stress function that satisfies $\nabla^4 \phi = 0$.

When a stress function $\phi(x, y)$ is known for a particular problem the stresses are found from the following relations.

$$\sigma_x = \partial^2 \phi / \partial y^2 \quad (3.1)$$

$$\sigma_y = \partial^2 \phi / \partial x^2 \quad (3.2)$$

$$\tau_{xy} = -\partial^2 \phi / \partial x \partial y \quad (3.3)$$

One interpretation of the stress function $\phi(x, y)$ is to consider this function to represent a three-dimensional surface extending over the plate.

The stresses can then be interpreted as being represented by the curvature or twist of this stress surface.

Assume some stress function that satisfies both $\nabla^4 \phi = 0$ and the boundary conditions is known for a rectangular plate subject to some form of loading. If the magnitude of the stress function at any point is represented by an ordinate perpendicular to the surface of the plate, these ordinates will form a three-dimensional stress surface over the plate. As the plate is to be represented by a lattice model, it is marked with a grid of spacing λ as shown in Fig. 1. Equilibrium of a typical lattice bar will now be shown to exist by using finite differences of the Airy stress function.

Consider a typical bar of the lattice model (shown in Fig. 1) such as b-3 which extends in the direction of the x-axis. Neglecting the body force there are four forces which act on the bar. These forces are F_{23} and F_{33} , corresponding to extensional forces in the plate, and S_{bc} and S_{bb} , corresponding to shear forces in the plate. All of these forces acting in their positive directions are shown in Fig. 4.

Each of the forces acting on bar b-3 represents the total force in a section of plate having an area λd . If σ_{23}^x is considered to be the average stress in the x-direction of a plate section extending from point 2-c to point 2-b, which the bar b-3 replaces, the bar force F_{23}^x is given by the relation

$$F_{23}^x = \sigma_{23}^x \lambda d \quad (4)$$

In the lattice model the stress σ_{23}^x is at point 2-3. Defining the stresses σ_{33}^x , τ_{bc} , and τ_{bb} as the average stresses along a width of plate replaced by the lattice bar, the remaining three forces are given by the relations

$$F_{33}^x = \sigma_{33}^x \lambda d \quad (5.1)$$

$$S_{bc} = \tau_{bc} \lambda d \quad (5.2)$$

$$S_{bb} = \tau_{bb} \lambda d \quad (5.3)$$

In order to have a state of equilibrium for the bar b-3, the following equation must be satisfied.

$$F_{23}^x - F_{33}^x + S_{bb} - S_{bc} = 0 \quad (6)$$

Referring to Eqs. 3 it can be seen that the plate stresses can also be expressed in terms of finite differences of the Airy stress function. The same grid points are used for the finite difference equations as are used for the lattice model (points 2-4, 2-3, etc.). Denoting the value of the stress function at the grid points by a subscript, the plate stresses in terms of finite differences are given by the following equations:

$$\sigma_{23}^x = (\phi_{24} - 2\phi_{23} + \phi_{22})/\lambda^2 \quad (7.1)$$

$$\sigma_{33}^x = (\phi_{34} - 2\phi_{33} + \phi_{32})/\lambda^2 \quad (7.2)$$

$$\tau_{bc} = (\phi_{24} + \phi_{33} - \phi_{34} - \phi_{23})/\lambda^2 \quad (7.3)$$

$$\tau_{bb} = (\phi_{23} + \phi_{32} - \phi_{33} - \phi_{22})/\lambda^2 \quad (7.4)$$

The stresses expressed in terms of finite differences are taken to be the average stresses in a width of plate equal to the grid spacing λ . If the stresses given by Eqs. 7 are substituted in Eqs. 4 and 5, the lattice model bar forces are given in terms of finite differences of Airy's stress function in the following equations:

$$F_{23}^x = d(\phi_{24} - 2\phi_{23} + \phi_{22})/\lambda \quad (8.1)$$

$$F_{33}^x = d(\phi_{34} - 2\phi_{33} + \phi_{32})/\lambda \quad (8.2)$$

$$S_{bb} = d(\phi_{23} + \phi_{32} - \phi_{33} - \phi_{22})/\lambda \quad (8.3)$$

$$S_{bc} = d(\phi_{24} + \phi_{33} - \phi_{34} - \phi_{23})/\lambda \quad (8.4)$$

When Eqs. 8 for the bar forces are substituted in bar equilibrium Eq. 6, the following identity is found showing that Eq. 6 is satisfied.

$$\begin{aligned} & d[\phi_{24} - 2\phi_{23} + \phi_{22} - \phi_{34} + 2\phi_{33} - \phi_{32} + \phi_{23} + \phi_{32} \\ & \quad - \phi_{33} - \phi_{22} - \phi_{24} - \phi_{33} + \phi_{34} + \phi_{23}] / \lambda = 0 \quad (9) \end{aligned}$$

An interior lattice model bar is therefore in equilibrium in terms of finite differences of an Airy stress function, which is a solution for the particular problem considered. Because the model is related to an Airy stress function that satisfies the equilibrium and compatibility conditions, the model satisfies the biharmonic equation in finite form in addition to the equilibrium and compatibility conditions.

Equilibrium Equations in Terms of Displacements

Static equilibrium of the lattice model can be expressed in terms of displacements by relating strains in the lattice model to the stress-strain relationship of classical linear elasticity. In the lattice model, strains are calculated from the differences in displacements of adjacent bars divided by the original distance between the displacement points of the bars.

The extensional strains at some typical extensional deformation point in the lattice model, such as deformable node 3-3, are

$$\epsilon_{33}^x = [u_{c3} - u_{b3}]/\lambda \quad (10.1)$$

$$\epsilon_{33}^y = [v_{3c} - v_{3b}]/\lambda \quad (10.2)$$

Shear strains, which are the changes in values of an originally right angle in the unstrained state, are defined in the lattice model in terms of the displacements of four points surrounding the point at which the shear strain is calculated. Thus, for a typical shear point in the lattice model such as b-c the shear strain is

$$\gamma_{bc} = [u_{b4} - u_{b3} + v_{3c} - v_{2c}]/\lambda \quad (11)$$

The stress-strain relationships for linear elasticity and plane stress are given by the following equations:

$$\sigma_x = E [\epsilon_x + \nu\epsilon_y]/(1-\nu^2) \quad (12.1)$$

$$\sigma_y = E [\epsilon_y + \nu\epsilon_x]/(1-\nu^2) \quad (12.2)$$

$$\tau_{xy} = G \gamma_{xy} \quad (12.3)$$

where

E = Young's modulus

G = Shear modulus = $E/2(1 + \nu)$

ν = Poisson's ratio

When the lattice model strains in terms of displacements are substituted in Eqs. 12 for stress, the stresses in the lattice model in terms of displacements are given by the following equations for extensional node 3-3 and shear joint b-c.

$$\sigma_{33}^x = E [u_{c3} - u_{b3} + \nu(v_{3c} - v_{3b})]/\lambda(1 - \nu^2) \quad (13.1)$$

$$\sigma_{33}^Y = E \left[v_{3c} - v_{3b} + \nu(u_{c3} - u_{b3}) \right] / \lambda(1 - \nu^2) \quad (13.2)$$

$$\tau_{bc} = G \left[u_{b4} - u_{b3} + v_{3c} - v_{2c} \right] / \lambda \quad (13.3)$$

Each of the forces acting on a typical bar can be expressed in terms of displacements by substituting the stress given in terms of displacements into the relations $F = \sigma \lambda d$ and $S = \tau \lambda d$. If the forces expressed in this manner are substituted into the equilibrium equation for a lattice model bar, the equilibrium equation will then be formulated in terms of displacements. The equilibrium equations will hereafter also include the body force terms \bar{X} or \bar{Y} .

The equilibrium equation for the typical interior lattice model bar b-3 is

$$F_{23}^X - F_{33}^X + S_{bb} - S_{bc} + \bar{X} = 0 \quad (14)$$

When the forces in Eq. 14 are formulated in terms of displacements the following equilibrium equation results.

$$\begin{aligned} & Ed \left[u_{b3} - u_{a3} + \nu(v_{2c} - v_{2b}) \right] / (1 - \nu^2) - Ed \left[u_{c3} - u_{b3} + \nu(v_{3c} - v_{3b}) \right] / (1 - \nu^2) \\ & + Gd \left[u_{b3} - u_{b2} + v_{3b} - v_{2b} \right] - Gd \left[u_{b4} - u_{b3} + v_{3c} - v_{2c} \right] + \bar{X} = 0 \end{aligned} \quad (15)$$

Substituting the relation $G = E/2(1 + \nu)$ and simplifying leads to the equation

$$\begin{aligned} & Ed \left[(3 - \nu) u_{b3} - u_{c3} - u_{a3} - 1/2 (1 - \nu)(u_{b4} + u_{b2}) \right. \\ & \left. + 1/2 (1 + \nu)(v_{2c} - v_{2b} + v_{3b} - v_{3c}) \right] / (1 - \nu^2) + \bar{X} = 0 \end{aligned} \quad (16)$$

This is the equilibrium equation for bar b-3 in terms of displacements with body-force terms not enumerated. Similar equations can be found for other

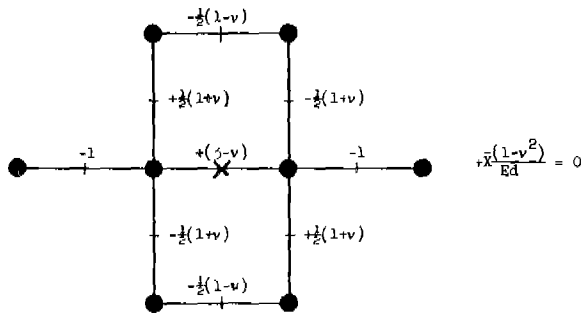


FIG. 6 DISPLACEMENT—EQUILIBRIUM EQUATION FOR
x-DIRECTION INTERIOR BAR

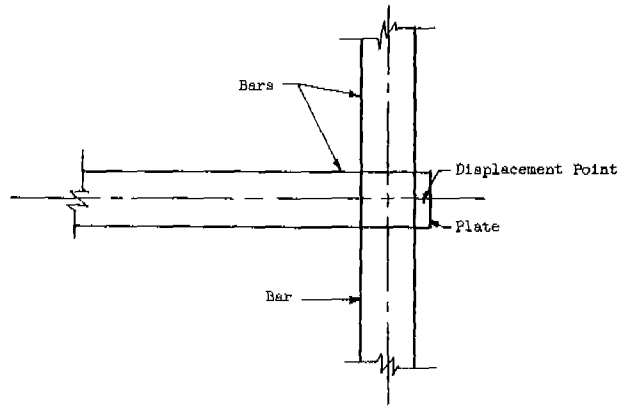


FIG. 7 PHYSICAL REPRESENTATION OF BOUNDARY DISPLACEMENT

interior bars extending in the horizontal or vertical directions.

Because the form of the equations is the same for all internal bars, with only the subscripts changing, it is convenient to represent the equations in a schematic form. This is accomplished by making a line drawing consisting of only the centerline of the bars whose displacements enter into the equilibrium equation (Eq. 15) and marking the displacement points on the centerlines at the appropriate points. The coefficients of each displacement point are written next to the corresponding displacement point on the line drawing. A cross mark is drawn at the displacement point of the bar to which the equilibrium equation applies. Then if this skeleton line drawing is imagined to have the same scale as a lattice model and is superposed over any interior bar with the cross-marked point over the center of the bar, the coefficients would be placed next to their proper displacement points. The equations may also be multiplied by $(1 - \nu^2)/Ed$ or some other constant, so these terms do not have to be carried with each coefficient. The equilibrium equation in skeleton form for a typical interior bar running in the x-direction is shown in Fig. 6.

Boundary Conditions

Boundary conditions for the lattice model must be established such that the bars along the boundary are in equilibrium and provide a satisfactory representation of the boundary conditions in the plate represented by the lattice model. The types of boundary conditions to be considered are (1) free edge with or without applied loads, (2) edge given a specified dis-

placement, or (3) any combination of these two conditions.

Consider a typical section along the boundary of the lattice model as shown in Fig. 1. In order to provide a smooth boundary for the model, a displacement point must be defined on the boundary with the displacement taking place perpendicular to the boundary. If a physical interpretation of this displacement point is desired, it can be imagined that there is a small plate placed over the deformable node on the boundary as shown in Fig. 7 and that a displacement point is defined at the midpoint of this plate. Any normal components of loads acting on the boundary will be applied through this point. If the normal components of the loads are distributed along the boundary they are concentrated into statically equivalent loads using the Newmark formula for equivalent loads.¹⁷ If the normal components of the loads are concentrated forces that fall between boundary displacement points, the forces are distributed to the displacement points on each side of the force. Boundary loads that do not act perpendicular to the boundary are resolved into normal and tangential components, which are then concentrated into statically equivalent forces. These statically equivalent forces act through the displacement point of the bar parallel to the boundary if it is a tangential force and at the edge displacement point if it is a normal force.

With the boundary displacement points just described, the strains in a deformable node along a boundary such as node 5-3 in Fig. 1 will be

$$\epsilon_{53}^x = 2 \left[u_{53} - u_{d3} \right] / \lambda \quad (17.1)$$

$$\epsilon_{53}^y = \left[v_{5c} - v_{5b} \right] / \lambda \quad (17.2)$$

Shear strains along the boundary of the lattice model expressed in terms of displacements are not directly affected by the boundary conditions.

When the edge of the plate is free to move but has some distribution of loading in the form of normal and shear stress along the boundary, the

plane stress elasticity stress-strain condition at a y-direction boundary is

$$\sigma_x = \bar{\sigma}_{\text{Boundary}} = E(\epsilon_x + \nu\epsilon_y)/(1 - \nu^2) \quad (18.1)$$

$$\sigma_y = E(\epsilon_y + \nu\epsilon_x)/(1 - \nu^2) \quad (18.2)$$

or, because boundary stress only is specified,

$$\epsilon_x = \frac{1 - \nu^2}{E} \bar{\sigma}_x - \nu\epsilon_y \quad (19)$$

Substituting Eq. 19 in Eq. 18.2, we have

$$\sigma_y = E\left[\epsilon_y + \nu\left(\frac{1 - \nu^2}{E} \bar{\sigma}_x - \nu\epsilon_y\right)\right]/(1 - \nu^2) = E\epsilon_y + \nu\bar{\sigma}_x \quad (20)$$

The forces applied to bars on or terminating at the boundary would be

$$F^x = \lambda d \bar{\sigma}_x = \text{Equivalent Concentrated Normal Force} \quad (21.1)$$

$$F^y = \frac{\lambda d}{2} E\epsilon_y + \nu \frac{\lambda d}{2} \bar{\sigma}_x + \bar{\tau} \lambda d \quad (21.2)$$

where

$\bar{\sigma}_x$ = Average uniform normal force equal to the concentrated force found by applying the Newmark parabolic formula divided by λd

$\bar{\tau}$ = Average uniform shear force applied to the boundary

Equilibrium of a bar that intersects the boundary, such as bar d-3 in Fig. 1, can be written in terms of displacements and equivalent concentrated boundary loads. Substituting the expressions for strain in terms of displacements into the appropriate bar force equations and writing the equilibrium condition in terms of these forces gives the equation

$$\begin{aligned}
 & \text{Ed} \left[u_{d3} - u_{c3} + \nu(v_{4c} - v_{4b}) \right] / (1 - \nu^2) - F_{53}^x \\
 & + \text{Gd} \left[u_{d3} - u_{d2} + v_{5b} - v_{4b} \right] \\
 & - \text{Gd} \left[u_{d4} - u_{d3} + v_{5c} - v_{4c} \right] + \bar{X} = 0
 \end{aligned} \tag{22}$$

or, by substituting $G = E/2(1 + \nu)$ and combining,

$$\begin{aligned}
 & \frac{\text{Ed}}{1 - \nu^2} \left[(2 - \nu)u_{d3} - u_{c3} + \frac{1}{2}(1 + \nu)(v_{4c} - v_{4b}) \right. \\
 & \left. - \frac{1}{2}(1 - \nu)(u_{d4} + u_{d2} - v_{5c} + v_{4b}) \right] \\
 & - F_{53}^x + \bar{X} = 0
 \end{aligned} \tag{23}$$

This equation is shown in skeleton form in Fig. 8. Equations for bars of the same type but of different orientation will be presented later.

A bar lying along a free edge would be one similar to bar 5-b in Fig 1. Considering the equilibrium of the bar in terms of forces and then expressing the forces in terms of displacements or concentrated boundary loads gives the equation

$$\begin{aligned}
 & \frac{\text{Ed}}{2} \left[v_{5b} - v_{5a} \right] + \frac{\nu}{2} F_{52}^x - \frac{\text{Ed}}{2} \left[v_{5c} - v_{5b} \right] \\
 & - \frac{\nu}{2} F_{53}^x + \text{Gd} \left[u_{d3} - u_{d2} + v_{5b} - v_{4b} \right] \\
 & + \bar{Y} = 0
 \end{aligned} \tag{24}$$

where any tangential boundary force is included in \bar{Y} . This may be rewritten as

$$\begin{aligned} & Ed \left[(3 + 2\nu)v_{5b} - (1 + \nu)(v_{5a} + v_{5c}) + u_{d3} \right. \\ & \left. - u_{d2} - v_{4b} \right] + \nu(1 + \nu)(F_{52}^x - F_{53}^x) \\ & + 2(1 + \nu) \bar{Y} = 0 \end{aligned} \quad (25)$$

This equation is shown in skeleton form in Fig. 9.

Should the x-direction boundary displacement be required, this could be computed with the following formula:

$$\begin{aligned} u_{53} = u_{d3} + \frac{1}{2} \left[\frac{1 - \nu^2}{Ed} F_{53}^x - \nu(v_{5c} \right. \\ \left. - v_{5b}) \right] \end{aligned} \quad (26)$$

A second boundary condition, which for convenience is called here the fixed-edge condition, is the case where boundary displacements must be included in the equilibrium equations. This condition occurs when a boundary is given an initial displacement and then held fixed, or when it is desirable to find boundary displacements as a result of loading elsewhere in the plate.

When the boundary displacement is considered for a bar such as d-3 (Fig. 1), which is perpendicular to the edge, the equilibrium equation in terms of displacements is

$$\begin{aligned} & Ed \left[u_{d3} - u_{c3} + \nu(v_{4c} - v_{4b}) \right] / (1 - \nu^2) - Ed \left[2(u_{53} - u_{d3}) + \nu(v_{5c} - v_{5b}) \right] \\ & / (1 - \nu^2) + Gd \left[u_{d3} - u_{d2} + v_{5b} - v_{4b} \right] - Gd \left[u_{d4} - u_{d3} + v_{5c} - v_{4c} \right] + \bar{X} = 0 \end{aligned} \quad (27)$$

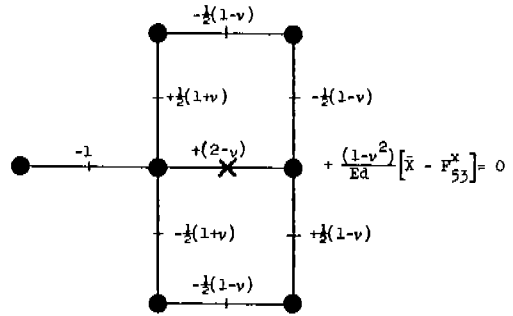


FIG. 8 SKELETON EQUATION FOR BAR INTERSECTING A FREE BOUNDARY

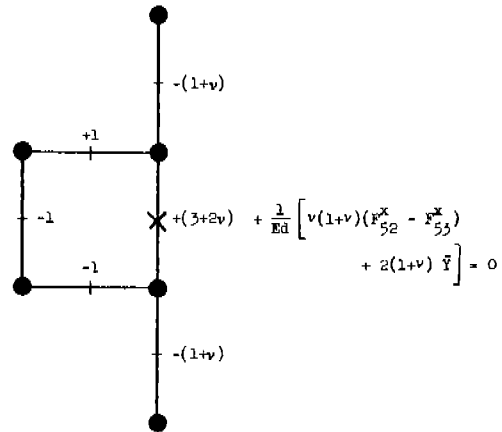


FIG. 9 SKELETON EQUATION FOR BAR ALONG A FREE BOUNDARY

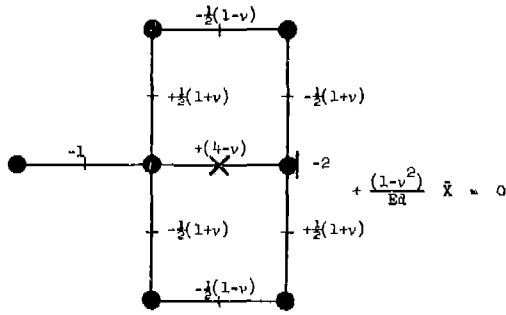


FIG. 10 SKELETON EQUATION FOR BAR INTERSECTING A FIXED BOUNDARY

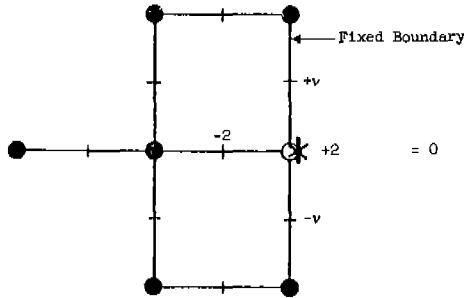


FIG. 11 SKELETON EQUATION FOR FIXED BOUNDARY POINT

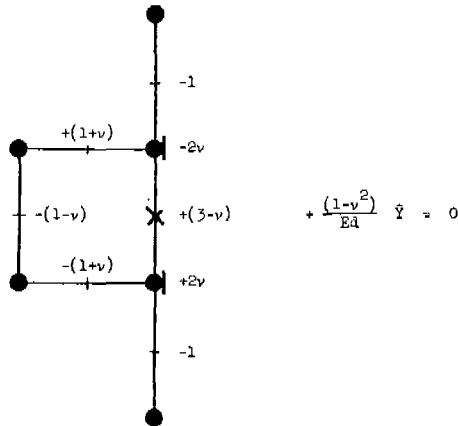


FIG. 12 SKELETON EQUATION FOR BAR ALONG A FIXED BOUNDARY

or

$$\frac{Ed}{1-\nu^2} \left[(4-\nu)u_{d3} - u_{c3} + \frac{1}{2}(1+\nu)(v_{4c} - v_{4b} - v_{5c} + v_{5b}) - \frac{1}{2}(1-\nu)(u_{d2} + u_{d4}) - 2u_{53} \right] + \bar{X} = 0 \quad (28)$$

This is shown in skeleton form in Fig. 10.

The boundary force resulting from the specified displacement of boundary point 5-3 is

$$F_{\text{Boundary}}^X = F_{53}^X \quad (29)$$

and can be found from the calculated displacements as follows:

$$F_{53}^X = \frac{Ed}{1-\nu^2} \left[2(u_{53} - u_{d3}) + \nu(v_{5c} - v_{5b}) \right] \quad (30)$$

If it is desirable to calculate the displacement of a point along a boundary, an equation must be written for this point in the

same manner as those written for bars. Equation 30, which is the equation for the boundary point, is shown in skeleton form in Fig. 11.

When the additional displacement points are included for a bar such as 5-b which is lying along the boundary, the equilibrium equation will be

$$\frac{Ed}{2(1-\nu^2)} \left[v_{5b} - v_{5a} + 2\nu(u_{52} - u_{d2}) \right] - \frac{Ed}{2(1-\nu^2)} \left[v_{5c} - v_{5b} + 2\nu(u_{53} - u_{d3}) \right] + Gd \left[u_{d3} - u_{d2} + v_{5b} - v_{4b} \right] + \bar{Y} = 0 \quad (31)$$

or

$$\frac{Ed}{2(1-\nu^2)} \left[(3-\nu)v_{5b} - v_{5a} - v_{5c} + 2\nu(u_{52} - u_{53}) \right. \\ \left. + (1+\nu)(u_{d3} - u_{d2}) - (1-\nu)v_{4b} \right] + \bar{Y} = 0 \quad (32)$$

This is shown in skeleton form in Fig. 12.

Similar equations can be developed for bars having a different orientation forming the corners of the lattice model. Because development of these equations is just a repetition of the methods already illustrated, only the results will be given in a later section of this report.

Representation of a Crack-Type Discontinuity

A crude representation of a crack-type discontinuity may be made in the model by considering certain of the rigid bars to be split down the middle and attached at their ends to the extensionally deformable nodes. This requires that the shear stress on each side of the discontinuity be the same so that the displacements of the midpoints of the two halves are identical, or, in other words, so that no shear stress can be transmitted across or exist on the surface of the crack.

The requirements of equal shear will be satisfied if the axis of the crack extends along a line of symmetry in the plate. Thus, the axis of the crack could extend along the centerline A-A of the plate shown in the upper part of Fig. 13. Minimum length of the crack is one lattice spacing for an edge crack or two lattice spacings for an interior crack. The actual formation of the crack takes place because of a separation or fracture of the extensionally deformable nodes, with one-half of each node remaining with one bar half, as shown in Fig. 13.

By using the assumption of zero shear on the crack surface, it is possible to write displacement-equilibrium equations that satisfy the boundary conditions for the bars forming the crack. First consider a lattice model rep-

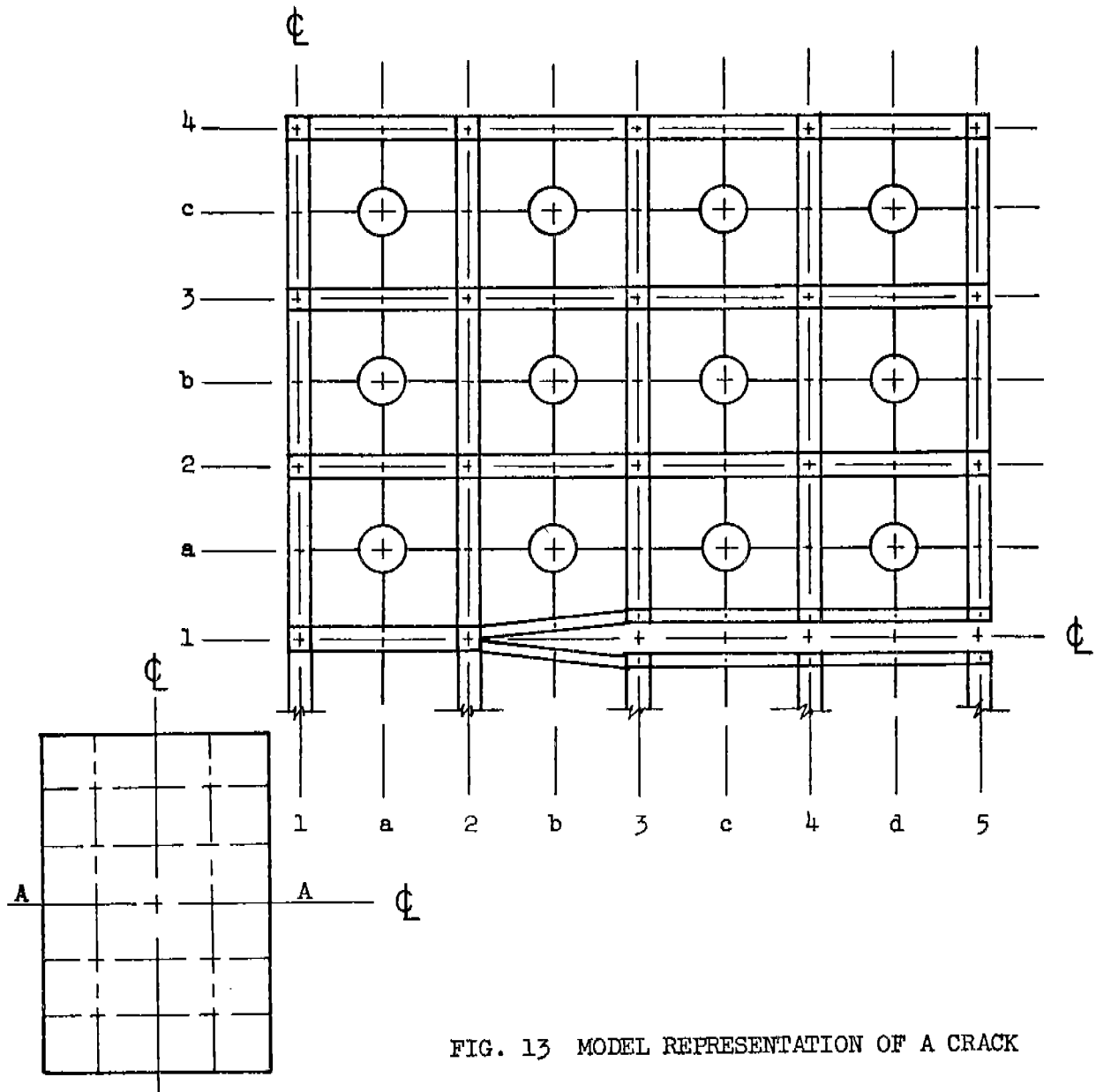


FIG. 13 MODEL REPRESENTATION OF A CRACK

representing a cracked plate as shown in Fig. 13. Here the crack extends from the edge up to node 2-1. Both halves of each bar will be considered to contribute equally to each equilibrium equation and to have identical displacements. With both surfaces of the crack free from loads, the equilibrium of a split bar forming the end of a crack such as b-1 in Fig. 13 will be

$$F_{21}^x - F_{31}^x - 2S_{ba} + \bar{X} = 0 \quad (33)$$

When expressed in terms of displacements, it becomes

$$\begin{aligned} & \frac{Ed}{1-\nu^2} [u_{b1} - u_{a1} + \nu(2v_{2a})] - Ed[u_{c1} \\ & - u_{b1}] - 2Gd[u_{b2} - u_{b1} + v_{3a} - v_{2a}] \\ & + \bar{X} = 0 \end{aligned} \quad (34)$$

which can be simplified to the following relation:

$$\begin{aligned} & \frac{Ed}{1-\nu^2} [(3-\nu-\nu^2)u_{b1} - u_{a1} + (1+\nu)v_{2a} \\ & - (1-\nu)(u_{b2} - v_{3a}) - (1-\nu^2)u_{c1}] \\ & + \bar{X} = 0 \end{aligned} \quad (35)$$

This is shown in skeleton form in Fig. 14.

A bar forming the surfaces of the crack but not at the tip or intersecting a boundary is one such as bar c-1 in Fig. 13. The equilibrium equation for this bar in terms of displacement is

$$Ed[u_{c1} - u_{b1}] - Ed[u_{d1} - u_{c1}] - 2Gd[u_{c2} - u_{c1} + v_{4a} - v_{3a}] + \bar{X} = 0 \quad (36)$$

or

$$\frac{Ed}{1+\nu} [(3+2\nu)u_{c1} - (1+\nu)(u_{b1} - u_{d1}) - u_{c2} - v_{4a} + v_{3a}] + \bar{X} = 0 \quad (37)$$

This equation is shown in skeleton form in Fig. 15.

A bar forming the surface of the crack and intersecting a free edge is one such as bar d-1 in Fig. 13. The equilibrium equation for this bar in terms of displacements is

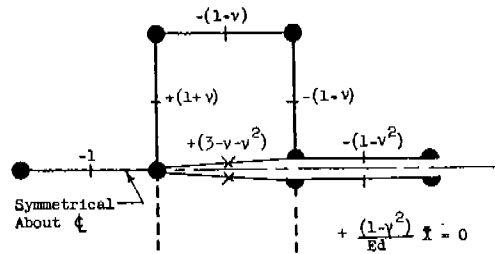


FIG. 14 SKELETON EQUATION FOR BAR FORMING THE END OF A CRACK

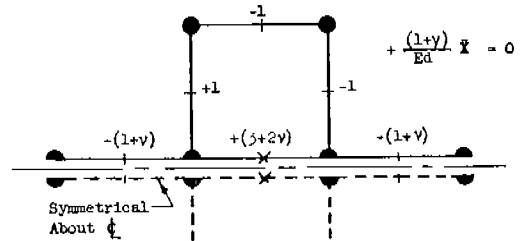


FIG. 15 SKELETON EQUATION FOR BAR FORMING SURFACE OF A CRACK

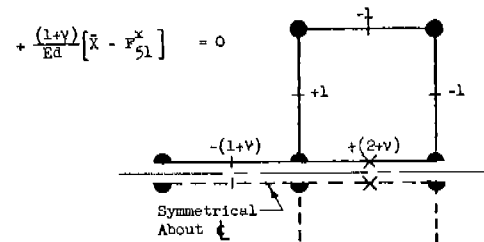


FIG. 16 SKELETON EQUATION FOR BAR FORMING SURFACE OF A CRACK AND INTERSECTING A FREE EDGE

$$Ed[u_{d1} - u_{c1}] - F_{51}^x - 2Gd[u_{d2} - u_{d1} + v_{5a} - v_{4a}] + \bar{X} = 0 \quad (38)$$

or

$$\frac{Ed}{1 + \nu} [(2 + \nu)u_{d1} - (1 + \nu)u_{c1} - u_{d2} - v_{5a} + v_{4a}] - F_{51}^x + \bar{X} = 0 \quad (39)$$

This equation is shown in skeleton form in Fig. 16.

Because the surface of the crack is the same as an unloaded free edge, bars that terminate at this boundary (such as bar 3-a in Fig. 13) have the same equilibrium equation as a bar that terminates at a free boundary. Similarly a bar such as 5-a in Fig. 13 is the same as a corner bar along a free edge.

Summary of Static Equilibrium Equations for the Lattice Model

Using the assumptions of plane-stress conditions, equilibrium equations in terms of displacements have been developed in previous sections of this chapter for several bars forming various parts of the lattice model. In each case an equation was developed for a particular bar having a certain orientation and using the notation, as shown in Fig. 1, for displacement points involved in the equilibrium of the bar. After the equation was developed in terms of definite displacement points, the equation was expressed graphically in a skeleton form so that the equation can be universally applied to any other bar of the same type and orientation.

When the lattice model is used for the approximate solution of thin plate plane-stress problems, the plate is replaced by the model. Solution of the problem is thus reduced to solving for stresses and strains in the model, which approximate the stresses and strains in the plate. The first step in the analysis is to determine the number of units (and therefore the number of bars) in the model. After the number of bars is known, one equilibrium equation, expressed in terms of displacements, is written for each bar of the lattice model. Solution of the set of bar equilibrium equations determines the bar displacements for the particular boundary and loading conditions specified. Strain and stress can then be calculated in the lattice model, at points where these quanti-

ties are defined, from the bar displacements.

Displacement-equilibrium equations are therefore required for every type of bar, boundary condition, and bar orientation that may be encountered in solving problems with the lattice model. A summary of bar equilibrium equations for most of the conditions that may be encountered in solving static problems with the lattice model is given in Figs. 17 to 60 in graphical skeleton form. Derivation of these equations (except for cases derived in preceding sections) is not given because of space limitations and to avoid repetition. Some of the equations in Figs. 17 to 60 have been multiplied by a constant so that the matrix of coefficients of the unknown displacements for any set of these equations, written for a particular lattice model, will be a symmetric positive definite matrix.

The standard notation used in Figs. 17 to 60 is as follows:

$$D = - (1 - \nu^2) / Ed$$

F = Statically equivalent concentration of forces applied at a boundary displacement point which is marked with a capital letter and which is also used as a subscript of F to indicate that F has been applied. A superscript x or y is also used to indicate in which direction the force acts.

\bar{X} and \bar{Y} = Body forces acting on the section of plate replaced by a bar. Surface forces and tangential components of boundary loads are included in the body-force terms.

As previously explained, the graphical skeleton form of illustrating an equation utilizes only the centerlines of bars involved in the equation. A cross mark on one of the centerlines indicates the bar to which the equation applies. If a scale drawing of the model is made and the skeleton equations are drawn to the same scale, the skeleton equation for a type of bar could be superposed, physically or by imagination, over any bar of the same type and orientation. The coefficients on the skeleton equation are then placed next to the proper displacement points on the lattice model and their identification can be made.

Hereafter only the centerlines of lattice model bars will be drawn in the

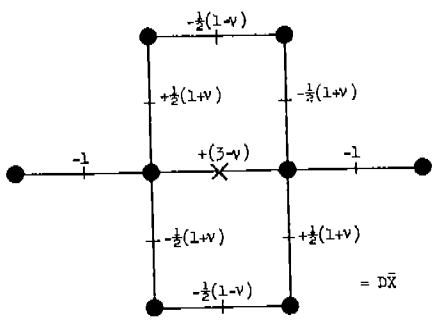


FIG. 17 INTERIOR x-DIRECTION BAR

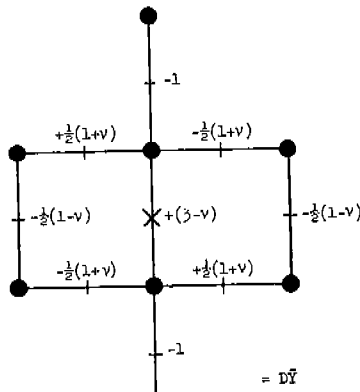


FIG. 18 INTERIOR y-DIRECTION BAR

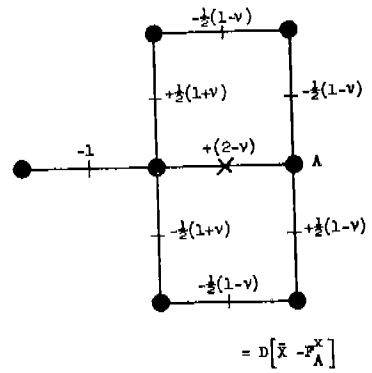


FIG. 19 BAR INTERSECTING RIGHT SIDE FREE EDGE

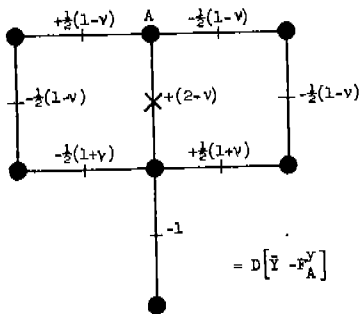


FIG. 20 BAR INTERSECTING UPPER FREE EDGE

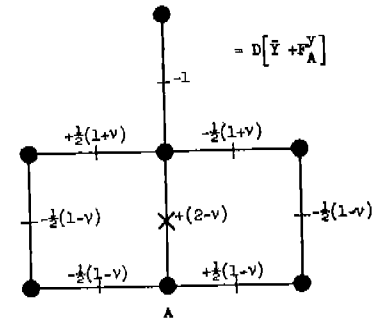
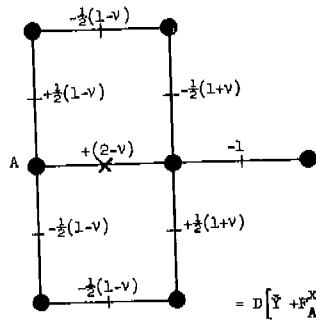


FIG. 22 BAR INTERSECTING LOWER FREE EDGE

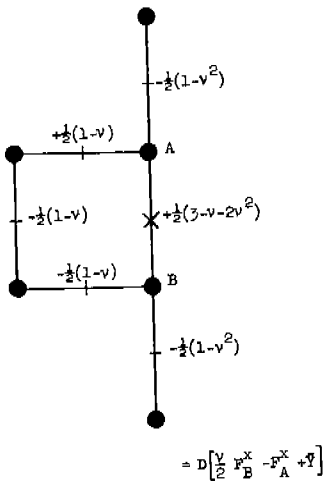


FIG. 23 RIGHT SIDE FREE EDGE BAR

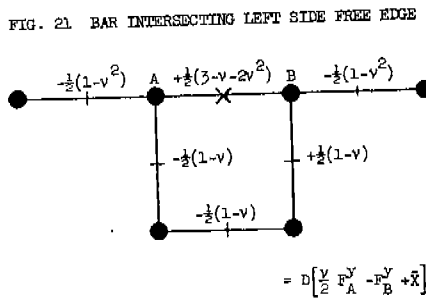


FIG. 24 UPPER SIDE FREE EDGE BAR

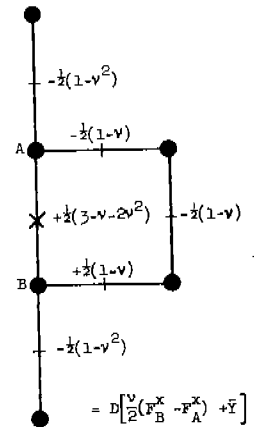


FIG. 25 LEFT SIDE FREE EDGE BAR

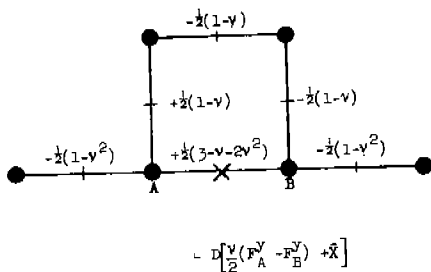


FIG. 26 LOWER SIDE FREE EDGE BAR

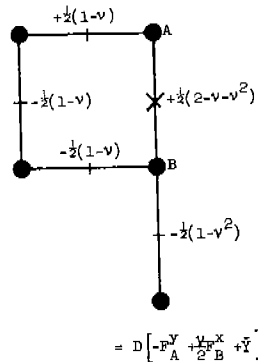


FIG. 27 RIGHT SIDE CORNER BAR ALONG A FREE EDGE

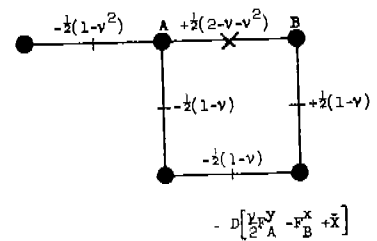


FIG. 28 UPPER RIGHT SIDE CORNER BAR ALONG A FREE EDGE

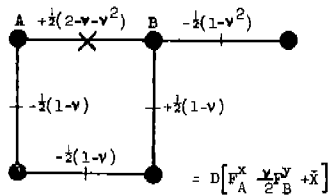


FIG. 29 UPPER LEFT SIDE CORNER BAR ALONG A FREE EDGE

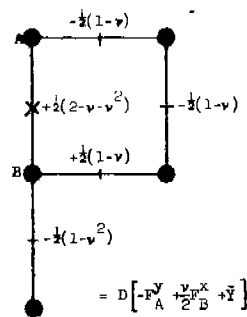


FIG. 30 LEFT SIDE CORNER BAR ALONG A FREE EDGE

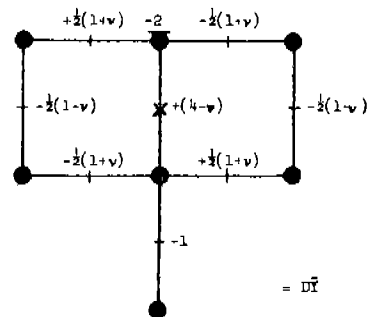


FIG. 31 BAR INTERSECTING UPPER FIXED EDGE

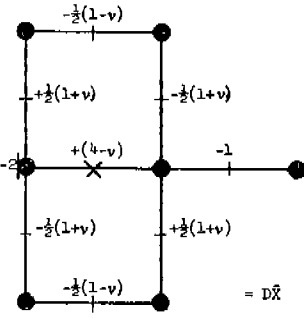


FIG. 32 BAR INTERSECTING LEFT SIDE FIXED EDGE

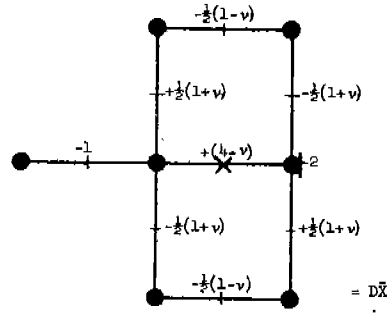


FIG. 33 BAR INTERSECTING RIGHT SIDE FIXED EDGE

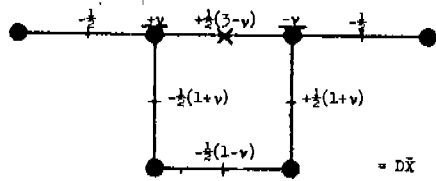


FIG. 34 FIXED EDGE BAR ALONG UPPER SIDE

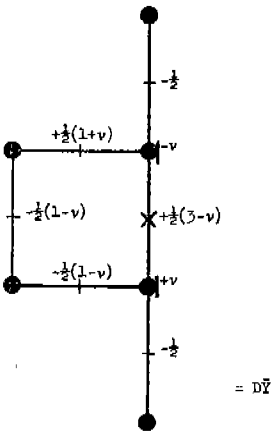


FIG. 35 FIXED EDGE BAR ALONG RIGHT SIDE

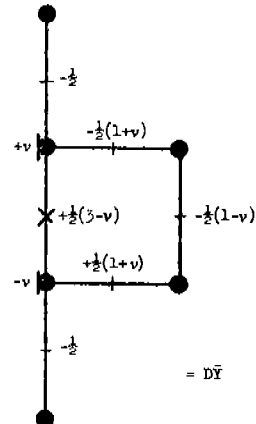


FIG. 36 FIXED EDGE BAR ALONG LEFT SIDE

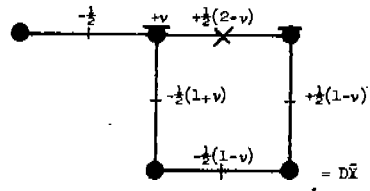


FIG. 37 UPPER RIGHT SIDE FIXED EDGE CORNER BAR INTERSECTING A FREE EDGE

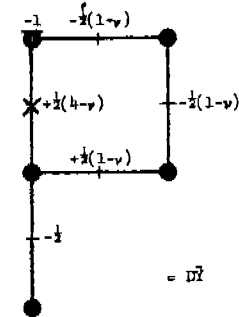


FIG. 40 LEFT SIDE FREE EDGE CORNER BAR INTERSECTING A FIXED EDGE

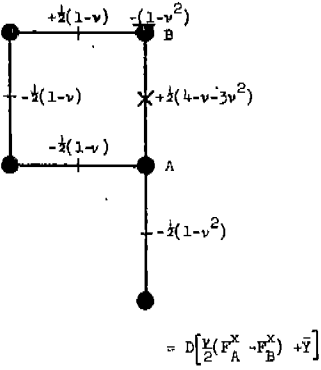


FIG. 38 RIGHT SIDE FREE EDGE CORNER BAR INTERSECTING A FIXED EDGE

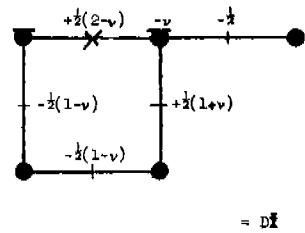


FIG. 39 UPPER LEFT SIDE FIXED EDGE CORNER BAR INTERSECTING A FREE EDGE

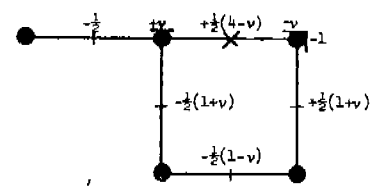


FIG. 41 UPPER RIGHT SIDE FIXED EDGE CORNER BAR INTERSECTING A FIXED EDGE

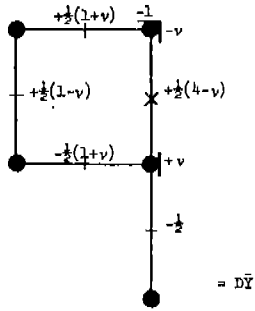


FIG. 42 RIGHT SIDE FIXED EDGE CORNER BAR
INTERSECTING A FIXED EDGE

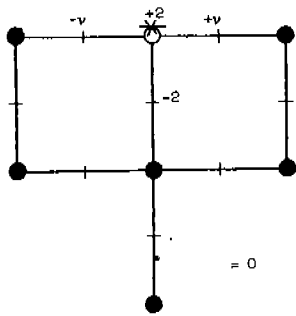


FIG. 43 BOUNDARY POINT ON UPPER EDGE

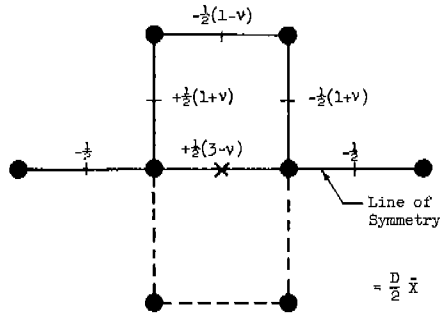


FIG. 44 INTERIOR x-DIRECTION BAR ON LINE OF
SYMMETRY

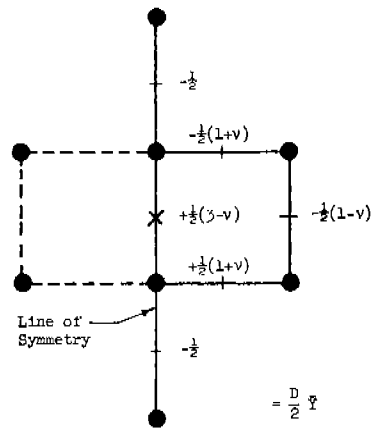


FIG. 45 INTERIOR y-DIRECTION BAR ON
LINE OF SYMMETRY

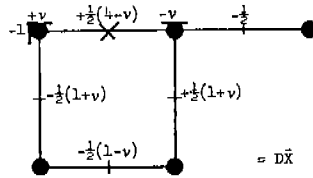


FIG. 45 UPPER LEFT SIDE FIXED EDGE CORNER BAR
INTERSECTING A FIXED EDGE

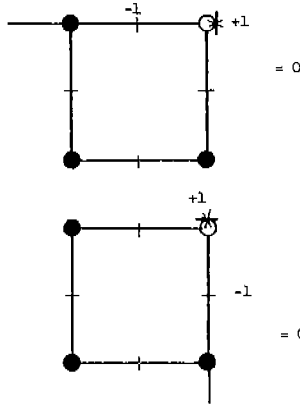


FIG. 46 CORNER BOUNDARY POINTS WITH ONE
EDGE FIXED AND ONE EDGE FREE

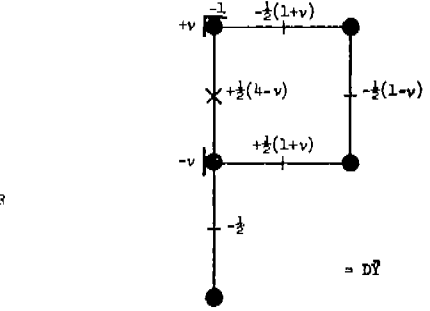
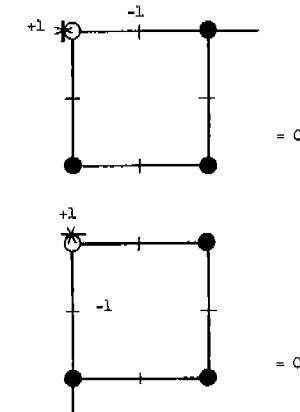


FIG. 44 LEFT SIDE FIXED EDGE CORNER BAR
INTERSECTING A FIXED EDGE

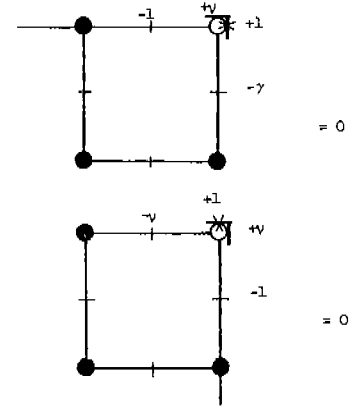


FIG. 47 CORNER BOUNDARY POINTS WITH
BOTH EDGES FIXED

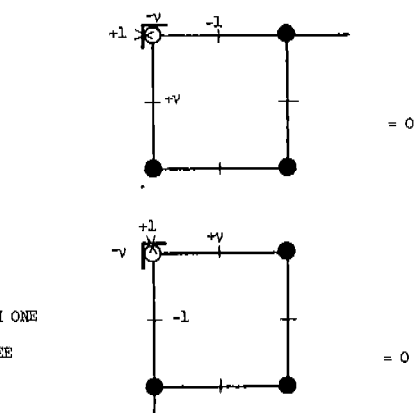


FIG. 51 INTERIOR x-DIRECTION BAR
INTERSECTING A LINE OF SYMMETRY

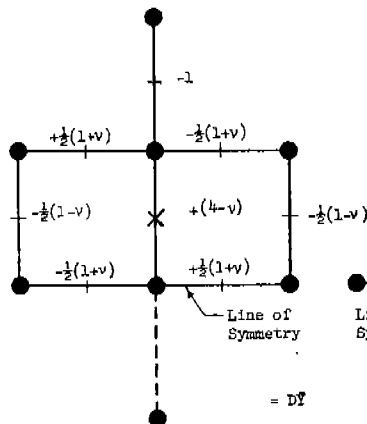
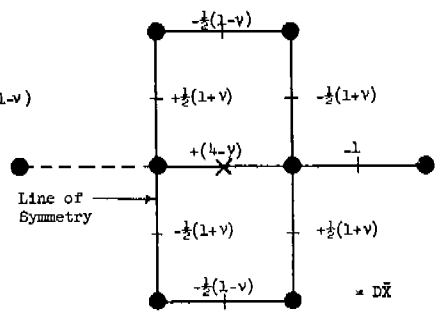


FIG. 50 INTERIOR y-DIRECTION BAR
INTERSECTING A LINE OF SYMMETRY



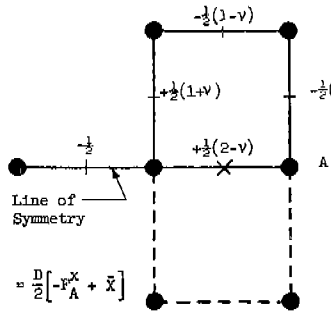


FIG. 52 BAR INTERSECTING RIGHT SIDE OF FREE EDGE AND LYING ON A LINE OF SYMMETRY

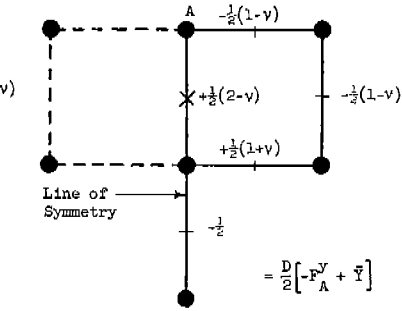


FIG. 53 BAR INTERSECTING UPPER FREE EDGE AND LYING ON A LINE OF SYMMETRY

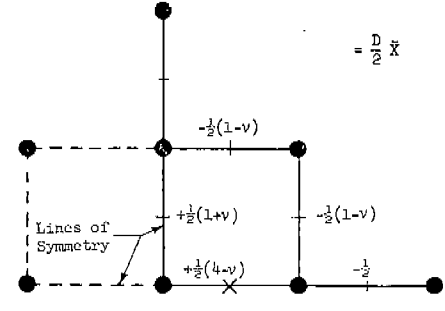


FIG. 54 INTERIOR x-DIRECTION BAR AT INTERSECTION OF TWO LINES OF SYMMETRY

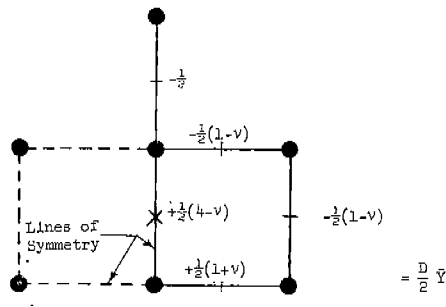


FIG. 55 INTERIOR y-DIRECTION BAR AT INTERSECTION OF TWO LINES OF SYMMETRY

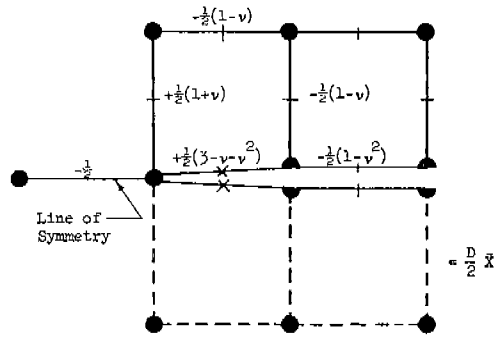


FIG. 56 SPLIT BAR FORMING CRACK TIP

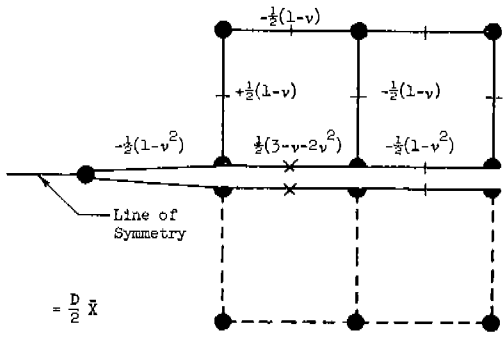


FIG. 57 BAR FORMING SURFACE OF CRACK

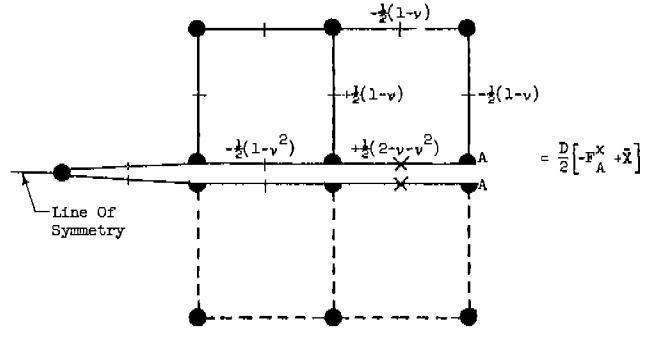


FIG. 58 BAR FORMING SURFACE OF CRACK AND INTERSECTING A FREE EDGE

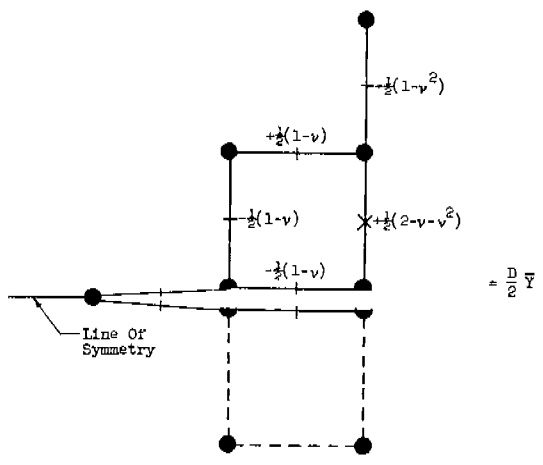


FIG. 59 FREE EDGE BAR INTERSECTING CRACK

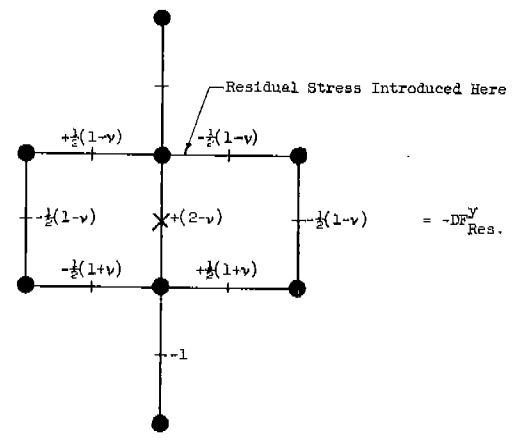


FIG. 60 EXAMPLE OF INTERIOR BAR WITH RESIDUAL STRESS INTRODUCED

figures, and the simpler notation of assigning a number to bars, nodes, and shear points will be used. A few comments pertaining to groups of equations which apply to various boundary conditions are given below.

Figs. 17 and 18 - Equations applicable to all interior bars of the lattice model.

Figs. 19 and 30 - Equations applicable to edges of the lattice model that are free to move but may have applied loads.

Figs. 31 to 47 - Equations applicable to boundaries that are fixed in position, or to some combination of fixed and free edges.

Figs. 48 to 55 - Equations applicable to points in the lattice model that are at lines of symmetry.

Figs. 56 to 59 - Equations applicable to points on or adjoining a crack.

Fig. 60 - This equation is a sample equation of the type that would apply if residual stress was introduced in one of the nodes of the lattice model. The internal force resulting from the residual stress is F_{res}^Y .

NUMERICAL RESULTS FOR STATIC LOADING

General

Analyses of several cases of rectangular plates involving several different boundary conditions are presented in this chapter. A comparison is made, in one case, between the lattice-model analysis and the solution of the same problem with an energy method. Several of the examples analyzed also indicate the effect of changing the number of divisions, or "fineness," in the lattice model.

The procedure followed in each case is similar. The plate is divided into the appropriate number of divisions for the lattice model representation; applied loads are converted into statically equivalent loads applied to the bars of the model; appropriate equations, developed and summarized in the preceding chapter, are written for each bar of the model; and the result is a set of simultaneous linear equations with bar displacements as unknowns. For plate and loads symmetrical about two axes, only one quarter of the plate need be considered; for plate and loads with one axis of symmetry, only one half of the plate need be considered;

and if there is no axis of symmetry with respect to the plate and loads, then the entire plate must be considered. Solution of the linear equations determines the bar displacements from which strain and stress can be calculated, if desired, by using the formulas of the preceding chapter.

Square Plate with Parabolically Distributed End Tension

The case of a square plate loaded with parabolically distributed end tension was selected for comparison of stresses calculated by two methods (discussed subsequently) because a fairly good energy-method solution is available for this problem. Solutions were obtained for lattice models that represented the same plate but had different degrees of division to determine the effect of fineness of division on calculated stresses and strains as shown in Figs. 61-71.

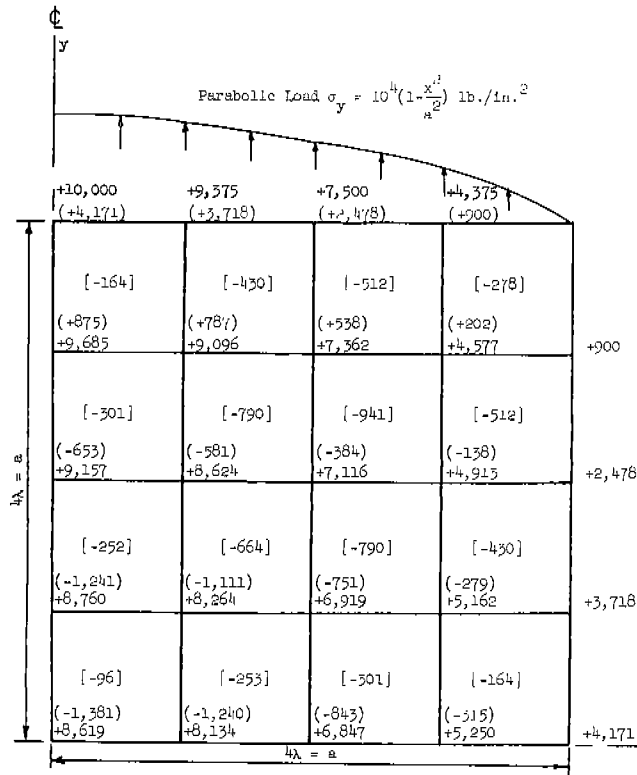
The energy-method solution is taken from the work of Timoshenko and Goodier.¹⁶ A principle of "least work" is used, in which an expression is written for the strain energy of a plate of unit thickness, using a stress function assumed in the form of the following series.

$$\psi = \psi_0 + \alpha_1 \psi_1 + \alpha_2 \psi_2 + \alpha_3 \psi_3 + \dots \quad (40)$$

where ψ is the stress function that satisfies the boundary conditions and α represent constants to be determined. The minimum of the strain energy expression is found by variational calculus. The notation here has been changed from that used in the Timoshenko and Goodier book.¹⁶

A parabolically loaded plate has two axes of symmetry, so that only one quarter of the square of total dimensions $2a$ must be considered. Such a quarter plate is shown in Figs. 61 and 65, along with the loading and direction of axes. By use of the first three terms of the series in Eq. 40, the following stress function is found:

$$\psi = \frac{Px^2}{2} \left[1 - \frac{1}{6} \frac{x^2}{a^2} \right] + \frac{P}{6} (x^2 - a^2)^2 (y^2 - a^2)^2 \left[0.04040 + 0.01174 \frac{x^2 + y^2}{a^2} \right] \quad (41)$$



Stresses In lb./in.² From Energy Method

xxx - σ_y
(xxx) - σ_x
[xxx] - τ_{xy}

FIG. 61 STRESSES AT EIGHTH POINTS OF SQUARE PLATE

WITH PARABOLICALLY DISTRIBUTED END TENSION

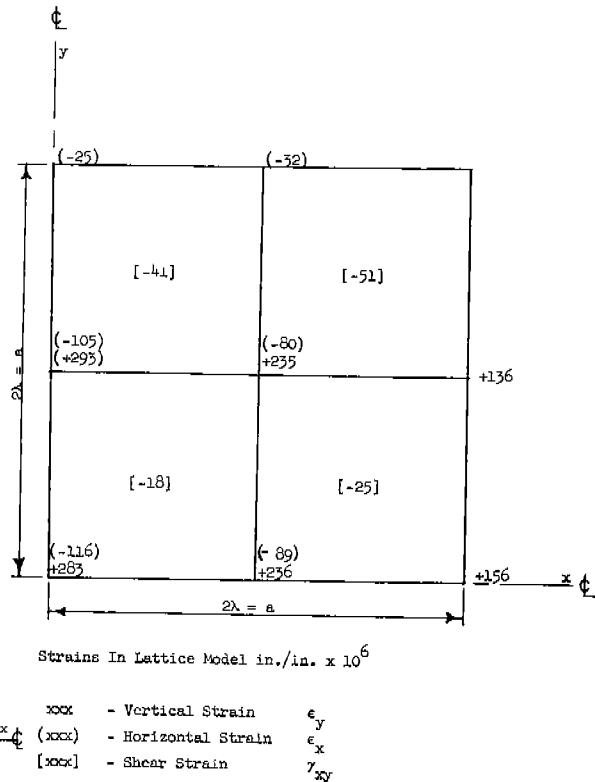
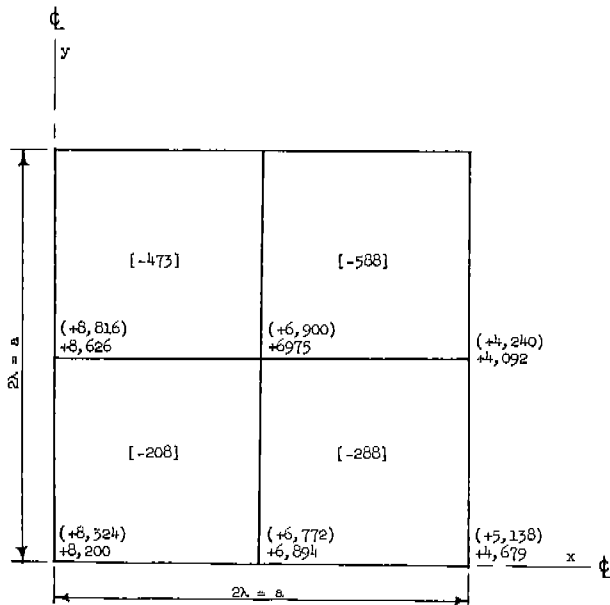


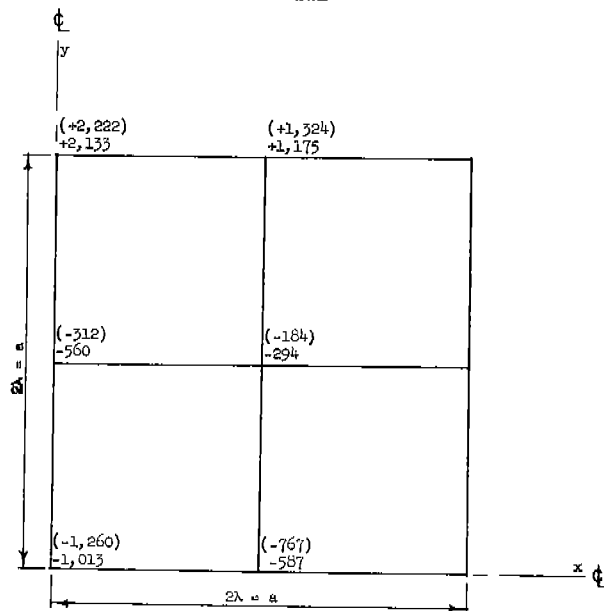
FIG. 62 STRAINS IN 2-DIVISION LATTICE MODEL WITH PARABOLIC LOAD



Stress In lb./in.²

xxx - σ_y From Lattice Model
(xxx) - σ_y Averaged From Energy Method Solution
[xxx] - τ_{xy} From Lattice Model

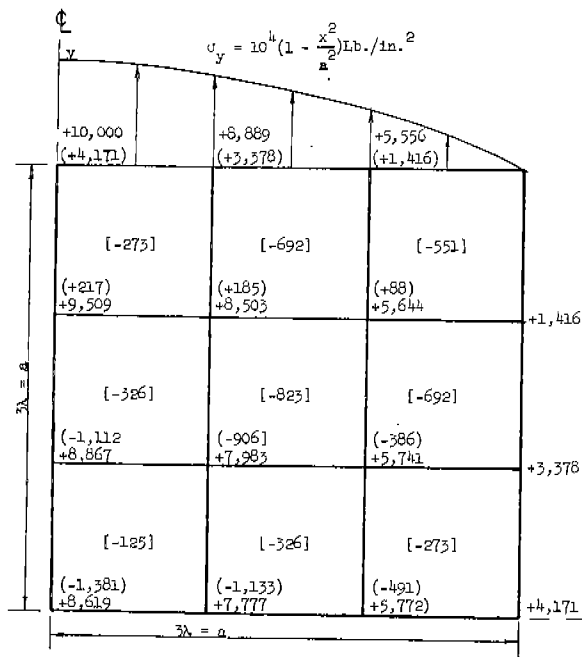
FIG. 63 COMPARISON OF σ_y IN 2-DIVISION LATTICE MODEL WITH PARABOLIC LOAD



Stresses In lb./in.²

xxx - σ_x From Lattice Model
(xxx) - σ_x Averaged From Energy Method Solution

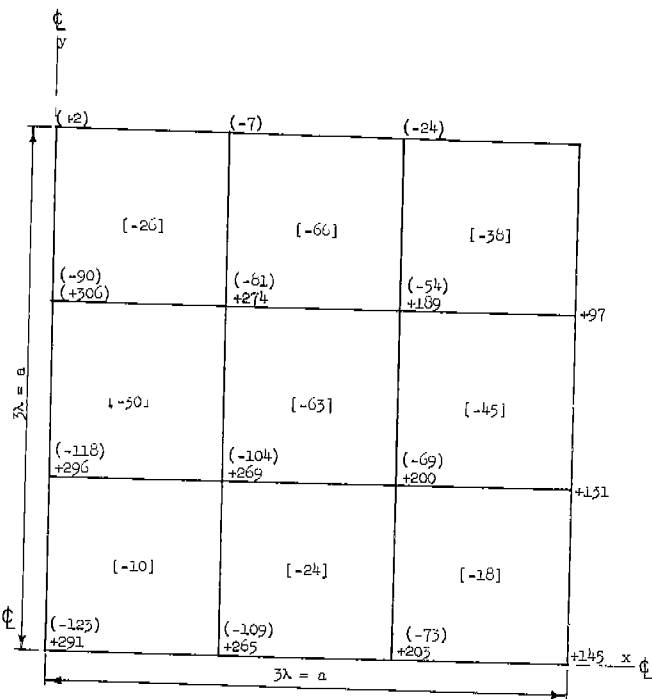
FIG. 64 COMPARISON OF σ_x IN 2-DIVISION LATTICE MODEL WITH PARABOLIC LOAD



Stresses In lb./in.² From Energy Method

xxx - σ_y
(xxx) - σ_x
[xxx] - τ_{xy}

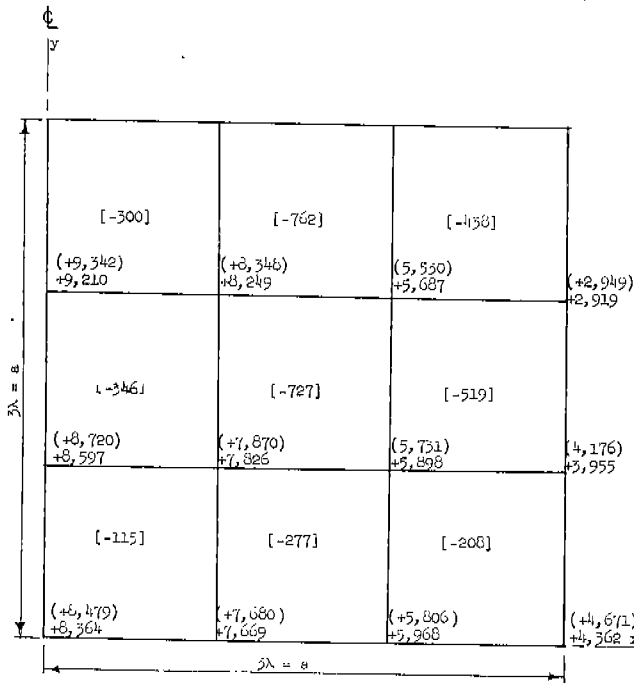
FIG. 65 STRESSES AT SIXTH POINTS OF SQUARE PLATE WITH PARABOLICALLY DISTRIBUTED END TENSION



Strains In Lattice Model in./in. $\times 10^6$

xxx - Vertical Strain ϵ_y
(xxx) - Horizontal Strain ϵ_x
[xxx] - Shear Strain γ_{xy}

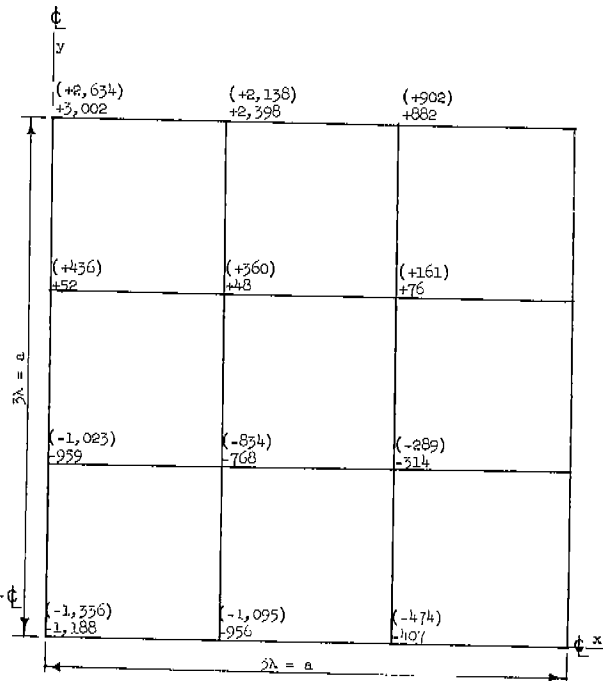
FIG. 66 STRAINS IN 3-DIVISION LATTICE MODEL WITH PARABOLIC LOAD



Stresses Due To Load of $\sigma_y = 10^4 \left(1 - \frac{x^2}{a^2}\right) \text{lb./in.}^2$

xxx - σ_y From Lattice Model
(xxx) - σ_y Averaged From Energy Solution
[xxx] - τ_{xy} From Lattice Model

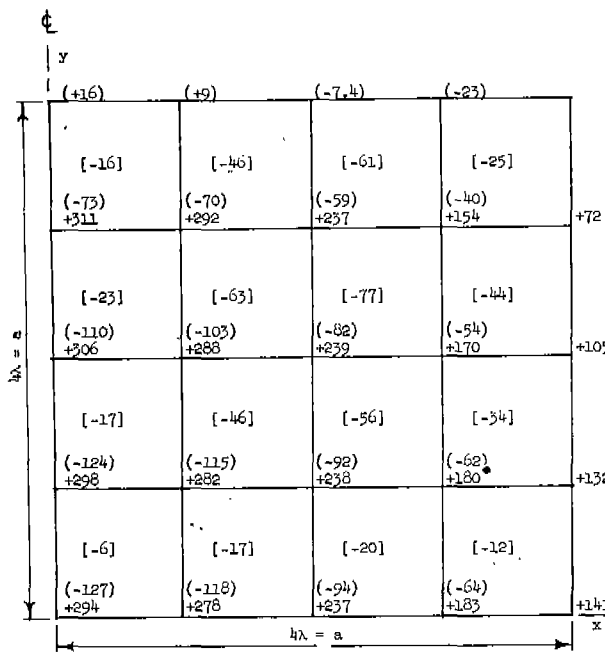
FIG. 67 COMPARISON OF σ_y IN 3-DIVISION LATTICE MODEL WITH PARABOLIC LOAD



Stresses In lb./in.²

xxx - σ_x From Lattice Model
(xxx) - σ_x Averaged From Energy Method Solution

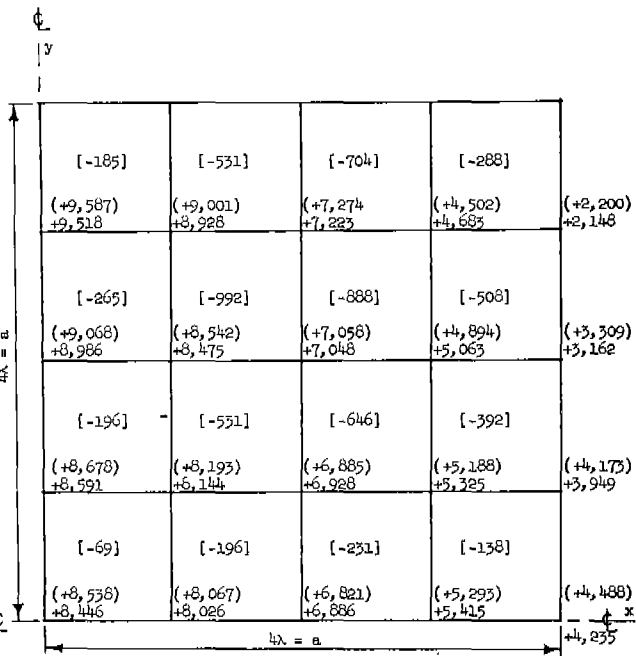
FIG. 68 COMPARISON OF σ_x IN 3-DIVISION LATTICE MODEL WITH PARABOLIC LOAD



Strains In Lattice Model in./in. x 10⁶

xxx - Vertical Strain ϵ_y
 (xxx) - Horizontal Strain ϵ_x
 [xxx] - Shear Strain γ_{xy}

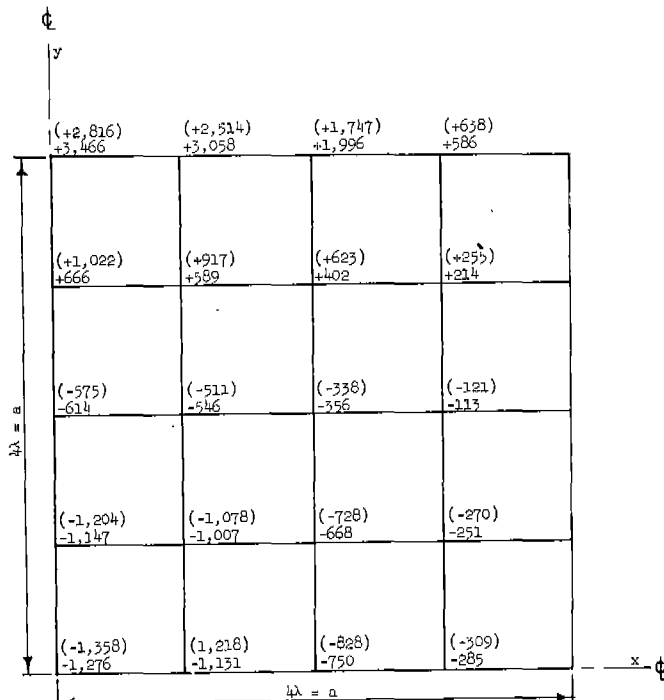
FIG. 69 STRAINS IN 4-DIVISION LATTICE MODEL WITH PARABOLIC LOAD



Stresses In lb./in.²

xxx - σ_y From Lattice Model
 (xxx) - σ_y Averaged From Energy Method Solution
 [xxx] - τ_{xy} From Lattice Model

FIG. 70 COMPARISON OF σ_y IN 4-DIVISION LATTICE MODEL WITH PARABOLIC LOAD



Stresses In lb./in.²

xxx - σ_x From Lattice Model
 (xxx) - σ_x Averaged From Energy Method Solution

FIG. 71 COMPARISON OF σ_x IN 4-DIVISION LATTICE MODEL WITH PARABOLIC LOAD

The stresses are found from this function by partial differentiation and are

$$\frac{\partial^2 \psi}{\partial x^2} = \sigma_y = P \left(1 - \frac{x^2}{a^2}\right) - 0.16160 P \left(\frac{y^2}{a^2} - 1\right)^2 \left(1 - 3 \frac{x^2}{a^2}\right) + 0.02348 P \left(\frac{y^2}{a^2} - 1\right)^2 \left[2 \frac{y^2}{a^2} \left(3 \frac{x^2}{a^2} - 1\right) + 15 \frac{x^4}{a^4} - 12 \frac{x^2}{a^2} + 1\right] \quad (42.1)$$

$$\frac{\partial^2 \psi}{\partial y^2} = \sigma_x = -0.16160 P \left(1 - 3 \frac{y^2}{a^2}\right) \left(\frac{x^2}{a^2} - 1\right)^2 + 0.02348 P \left(\frac{x^2}{a^2} - 1\right)^2 \left(15 \frac{y^4}{a^4} - 12 \frac{y^2}{a^2} + 6 \frac{x^2 y^2}{a^4} - 2 \frac{x^2}{a^2} + 1\right) \quad (42.2)$$

$$-\frac{\partial^2 \psi}{\partial x \partial y} = \tau_{xy} = -\frac{8xy}{a^2} P \left(\frac{x^2}{a^2} - 1\right) \left(\frac{y^2}{a^2} - 1\right) \left[0.03522 \left(\frac{x^2 + y^2}{a^2}\right) + .05732\right] \quad (42.3)$$

These expressions have been evaluated with $P = 10^4$ psi at a number of points that correspond to points where stress is defined in lattice models having various numbers of subdivisions. The results are given in Figs. 61 and 65.

Three different grid sizes were used in dividing the quarter section of the plate for lattice-model analysis. The numbers of divisions on each side of the quarter plate were 2, 3, and 4. Therefore systems of 12, 24, and 40 equations had to be solved for bar displacements. Strains calculated from the bar displacements are summarized in Figs. 62, 66, and 69. In each of these figures the grid lines forming the centerlines of lattice model bars are shown, and the strains are given above and to the right of node points and over shear points using the notation given in the figures. This system of summarizing information is used in all figures giving results of analyses of statically loaded lattice models.

A direct comparison of stresses calculated with the lattice model can be made with the stresses calculated by the energy method; however, such a

direct comparison may not give the best results, because strains and stresses in the model are average values over a bar width. In order to place comparisons of stresses calculated with the methods on a similar basis, the stresses found from the energy method solution have also been averaged. The averaging procedure consisted of (1) finding what the bar force would have been using the energy-method stresses evaluated at node points of the lattice model, (2) concentrating to a force with the Newmark parabolic formulae, and (3) dividing these forces by the area λd .

The vertical σ_y and shear τ_{xy} stresses calculated from the lattice model strains summarized in Figs. 62, 66, and 69 and the vertical stresses from the energy-method solution, averaged as just indicated, are summarized in Figs. 63, 67, and 70. Horizontal stresses σ_x calculated from the strains summarized in Figs. 62, 66, and 69 and the averaged energy-method stresses are summarized in Figs. 64, 68, and 71.

A comparison of stresses calculated with the lattice model and the averaged energy-method stresses is directly made by examining Figs. 63, 64, 67, 68, 70, and 71. By making this comparison it can be seen that on the basis of averaged stresses the lattice model gives very good results for vertical stress even with the coarse two-division lattice model, although better agreement is obtained with the three- and four-division lattice models. The agreement is so good in the four-division lattice model that it is difficult to say which of the values is more accurate because only the first three terms of the series in Eq. 40 were used when the stress function was evaluated for the energy-method solution. Horizontal stresses are somewhat more sensitive to changes in the number of divisions in the lattice model. It can be seen from Figs. 68 and 71 that increasing the number of divisions in the lattice model provides a better picture of deformation and stress.

If it is desired to compare stresses calculated with the lattice model to the unaveraged stresses calculated by the energy method, the lattice model stresses in Figs. 63, 64, 67, 68, 70, and 71 are compared to the energy-method stresses in Figs. 61 and 65. Comparison of shear stress has not been made on

an averaged basis; however, direct comparison of the lattice model shear stresses in Figs. 67 and 70 with the energy-method stresses in Figs. 61 and 65 shows that the lattice model provides a good picture of the distribution of shear stress.

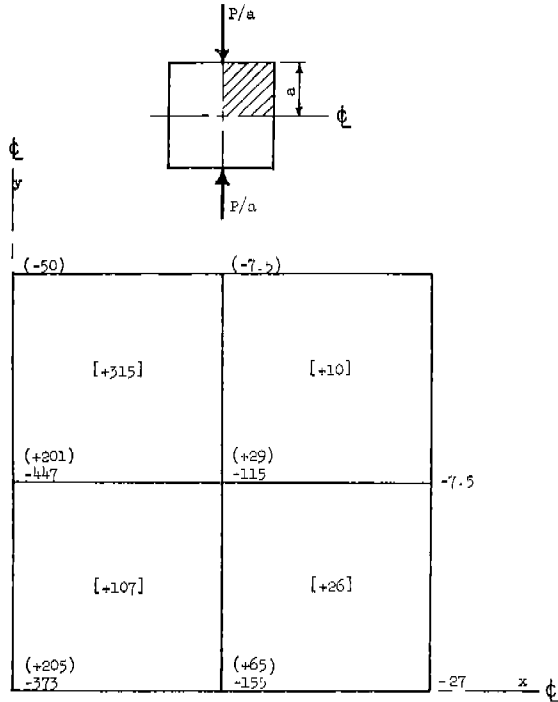
Square Plate with Concentrated Loads

Many of the plate problems for which solutions may be desired involve concentrated effects or effects involving very high strain gradients. In order to illustrate how the model represents such an effect and how the representation changes as the number of plate divisions increases, the case of a square plate loaded with a pair of concentrated loads has been analyzed. The entire plate and the loads are shown at the top of Figs. 72 and 73. With two lines of symmetry, only the shaded quarter of the plate need be considered. The load was taken as $P/a = 10^4$ and the plate thickness as unity so that the specific dimensions of the plate would not have to be considered.

Strain distributions in lattice models that divide the quarter plate into two and four divisions are shown in Figs. 72 and 74. The stress distributions calculated from the strains given in Figs. 72 and 74 are shown in Figs. 73 and 75. It can be seen that across the centerline of the plate both the two-division and the four-division models give similar results, but as the external loads are approached the two-division model is too crude to give a representation of the strain or stress gradient near these points.

Uniformly Loaded Plates with Cracks

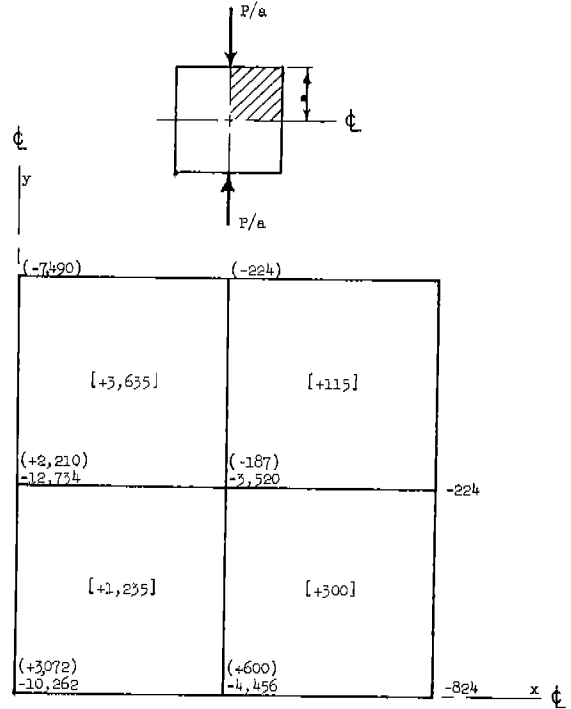
Several cases of plate models containing cracks and loaded with uniform end tension have been analyzed to indicate the static strain distribution resulting from these conditions. Two types of cracked plates have been considered. The first, called the symmetrical case, consists of a square plate with uniform tension on two opposite edges and cracks extending symmetrically from the center of each of the free edges parallel to



Strains In Lattice Model - in./in. $\times 10^6$
Load = $P/a = 10^4$ lb./in.

xxx - Vertical Strain ϵ_y
(xxx) - Horizontal Strain ϵ_x
[xxx] - Shear Strain γ_{xy}

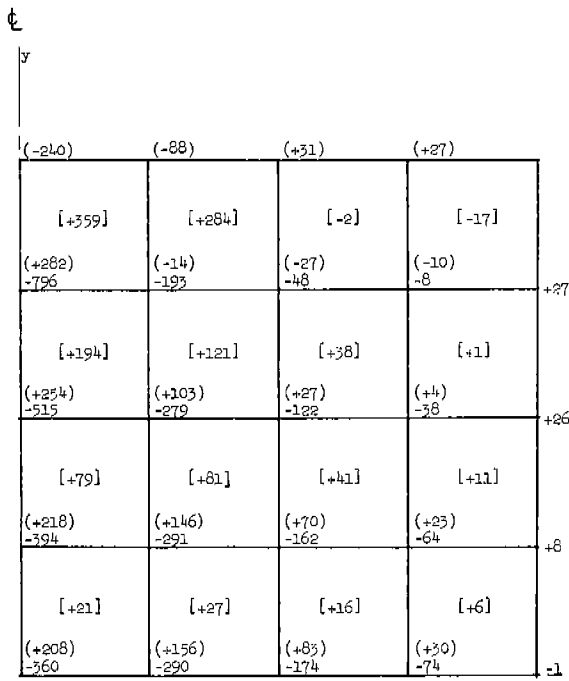
FIG. 72 STRAIN DISTRIBUTION IN
2-DIVISION LATTICE MODEL
WITH CONCENTRATED LOADS



Stresses From Lattice Model - lb./in.²
Load = $P/a = 10^4$

xxx - σ_y
(xxx) - σ_x
[xxx] - τ_{xy}

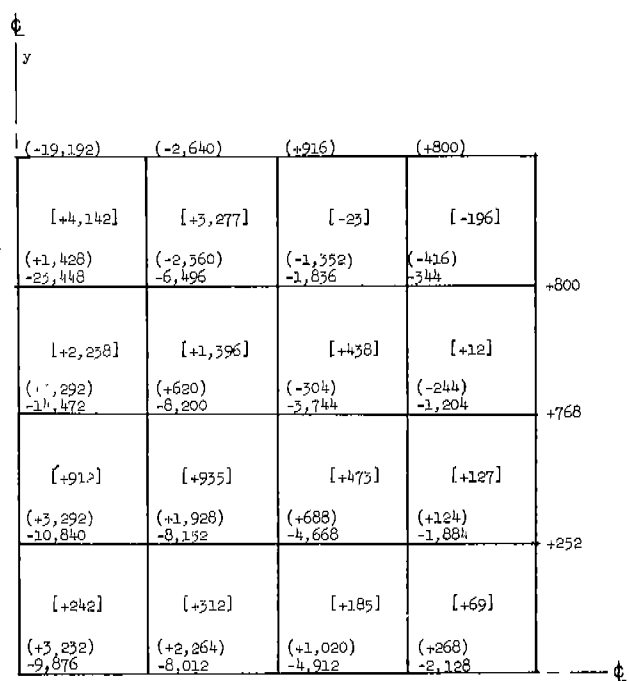
FIG. 73 STRESS DISTRIBUTION IN
2-DIVISION LATTICE MODEL
WITH CONCENTRATED LOADS



Strains In Lattice Model - in./in. $\times 10^6$ With $P/a = 10^4$

xxx - Vertical Strain ϵ_y
(xxx) - Horizontal Strain ϵ_x
[xxx] - Shear Strain γ_{xy}

FIG. 74 STRAIN DISTRIBUTION IN
4-DIVISION LATTICE MODEL
WITH CONCENTRATED LOADS



Stresses In Lattice Model - lb./in.² With $P/a = 10^4$

xxx - σ_y
(xxx) - σ_x
[xxx] - τ_{xy}

FIG. 75 STRESS DISTRIBUTION IN
4-DIVISION LATTICE MODEL
WITH CONCENTRATED LOADS

the loaded edges. The second, called the unsymmetrical case, consists of a plate of the same length as the square plate but only half as wide, with uniform tension applied to the short edges and one crack extending along the centerline of one free edge toward the left edge.

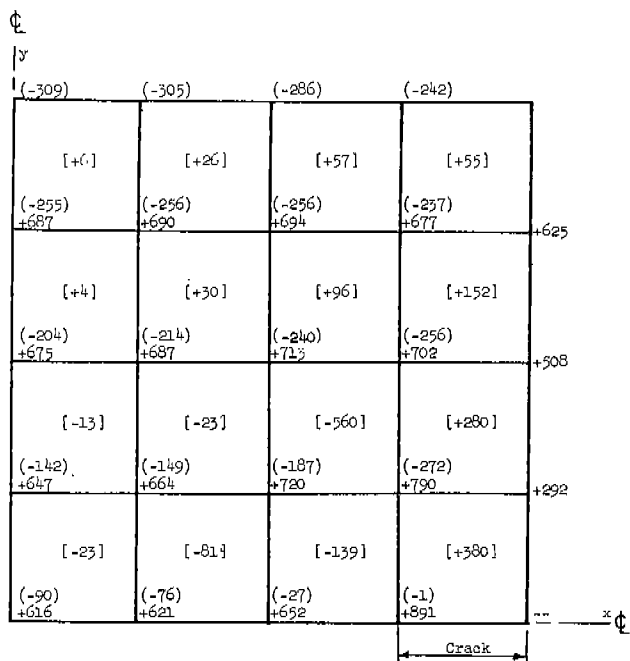
The same number of lattice-model divisions have been used for each case; however, the symmetrical case has two lines of symmetry so that the lattice model need only replace one quarter of the plate, while in the unsymmetrical case there is only one line of symmetry and the lattice model must replace one half of the plate. Four divisions in each direction were used for the lattice models so that the total plate is divided into eight sections on each edge in the symmetrical case, and eight sections on the long edge and four sections on the short edge in the unsymmetrical case.

Strain distributions in the symmetrical, four-division lattice model having cracks with lengths of one, two, and three divisions are shown in Figs. 76, 77, and 78. Strain distributions in the unsymmetrical four divisions are shown in Figs. 79 and 80. Loading in each case was 20,000 psi uniform end tension.

The strain distributions in Figs. 76 and 80 provide only a rough description of the highly concentrated disturbance around the crack tip in an actual plate because the model division is much too coarse. However, interesting trends can be noted in regard to the effect of length of crack and extent of strain redistribution associated with the crack. As would be expected, deformation at the crack tip and the zone of disturbance becomes larger as a crack increases in length. The unsymmetrical cases in Figs. 79 and 80 show the bending in the plane of the plate as a result of the cracks.

Checking of Bar Stresses

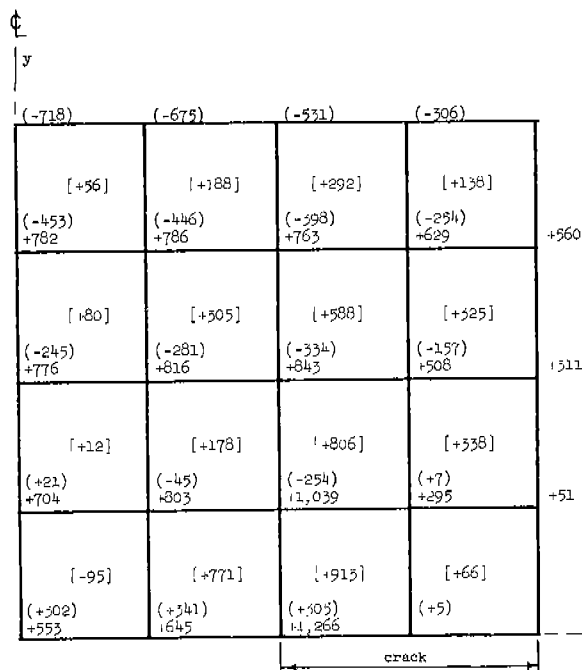
The stress values calculated from the lattice model can be checked for numerical errors by calculating the sum of the forces acting across a section through the lattice model. In the case of a plate loaded on two opposite sides and with the remaining two sides free, the sum of the bar forces across



Strains in Lattice Model - in./in. $\times 10^6$

xxx - Vertical Strain ϵ_y
 (xxx) - Horizontal Strain ϵ_x
 [xxx] - Shear Strain γ_{xy}

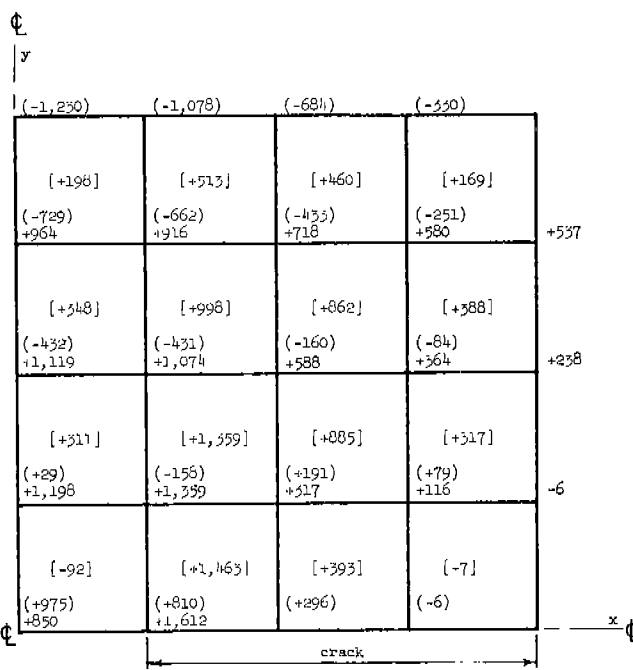
FIG. 76 STRAIN DISTRIBUTION IN A SYMMETRIC 4-DIVISION LATTICE MODEL WITH A 1-DIVISION CRACK



Strains In Lattice Model in./in. $\times 10^6$

xxx - Vertical Strain ϵ_y
 (xxx) - Horizontal Strain ϵ_x
 [xxx] - Shear Strain γ_{xy}

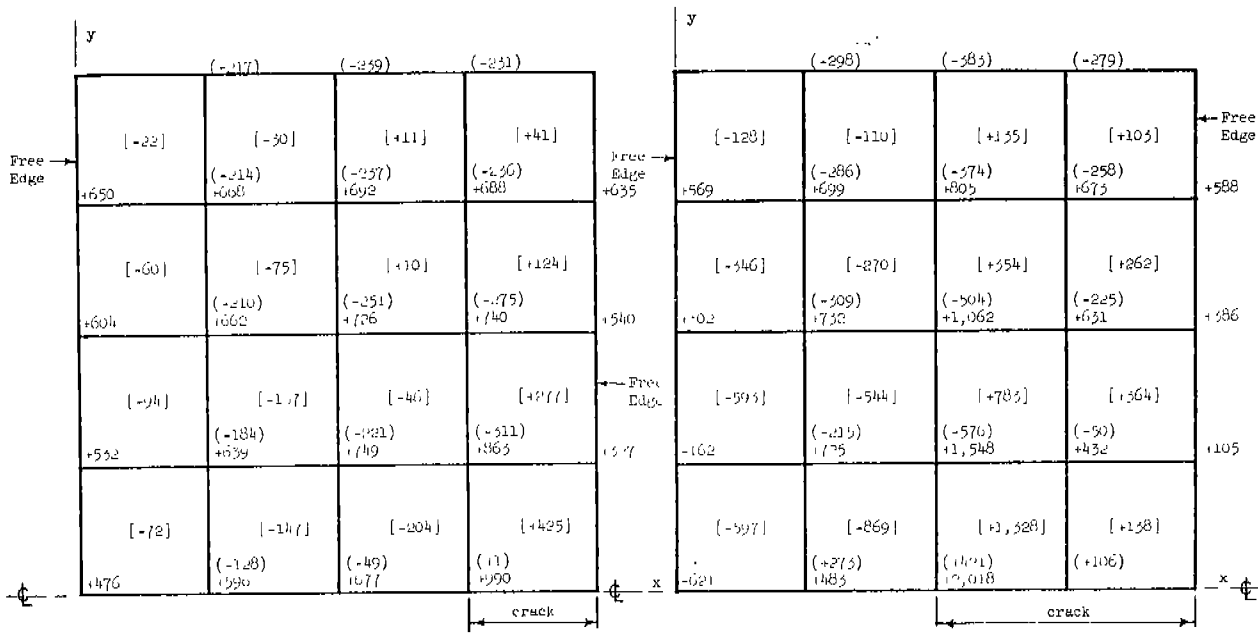
FIG. 77 STRAIN DISTRIBUTION IN A SYMMETRIC 4-DIVISION LATTICE MODEL WITH A 2-DIVISION CRACK



Strains In Lattice Model in./in. $\times 10^6$

xxx - Vertical Strain ϵ_y
 (xxx) - Horizontal Strain ϵ_x
 [xxx] - Shear Strain γ_{xy}

FIG. 78 STRAIN DISTRIBUTION IN A SYMMETRIC 4-DIVISION LATTICE MODEL WITH A 3-DIVISION CRACK



Strains in Lattice Model in./in. $\times 10^6$

xxx - Vertical Strain ϵ_y
 (xxx) - Horizontal Strain ϵ_x
 [xxx] - Shear Strain γ_{xy}

FIG. 79 STRAIN DISTRIBUTION IN AN UNSYMMETRIC 1-DIVISION LATTICE MODEL WITH A 1-DIVISION CRACK

Strains in Lattice Model in./in. $\times 10^6$

xxx - Vertical Strain ϵ_y
 (xxx) - Horizontal Strain ϵ_x
 [xxx] - Shear Strain γ_{xy}

FIG. 80 STRAIN DISTRIBUTION IN AN UNSYMMETRIC 3-DIVISION LATTICE MODEL WITH A 3-DIVISION CRACK

a section parallel to the loaded ends must be equal to the applied load. The sum of the forces on a section parallel to the unloaded edges must equal zero. Bar forces are calculated by multiplying the stress by the bar area $\sigma \lambda d$ for an interior bar or by $\sigma \lambda / 2d$ for an edge bar.

SOLUTION OF PROBLEMS INVOLVING TIME DEPENDENCE

Differential Equations

The static equilibrium equations for the lattice model including body forces were developed in an earlier chapter, which included a complete summary of the equations. Body forces in this case were limited to gravitational or any time-independent forces. Analysis of a static problem consisted in writing the equilibrium equations for each bar of the model, taking into account the boundary conditions. This resulted in a system of simultaneous linear equations the solution of which gave the bar displacements. From the bar displacements, the strains and stresses, at points where these are defined, could be

calculated.

If body forces that are not time-independent are considered, then the equations expressing the behavior of the model will become a system of differential equations. The time-dependent forces to be considered for the model are inertial forces of the plate material or time-dependent external forces. Under dynamic conditions, the instantaneous equilibrium equation for a single-mass system free to move in one dimension only is

$$F = ma \tag{43}$$

where

F = Resultant of all forces acting on mass at time t

m = Mass

a = Acceleration at time t

For the lattice model, each bar has only one degree of freedom, and therefore the acceleration of each bar, considered as a rigid mass, is the second derivative of the displacement with respect to time. The body force acting on each bar can be split into two parts, one time-dependent and one time-independent. Each equilibrium equation will then be of the form

$$- m \frac{d^2(u \text{ or } v)}{dt^2} = \left[\sum f(u_n, v_n) \right] + (\bar{X} \text{ or } \bar{Y}) + f(t) \tag{44}$$

where

m = Mass

u_n, v_n = Displacements

$\sum f(u_n, v_n)$ = Sum of forces resulting from material deformations

\bar{X}, \bar{Y} = Time-independent body forces

f(t) = Time-dependent force

Writing one dynamic equilibrium equation for each bar when each bar represents one degree of freedom will yield a system of simultaneous second-order differential equations. Solution of this set of equations will give the

bar displacement and therefore the stress or strain at a particular time.

Natural Frequencies

A plate considered as a continuous material has an infinite number of degrees of freedom with respect to vibrational motion. In analyzing such a situation, any general harmonic vibration can be treated as the superposition of an infinite number of individual frequencies and associated mode shapes. Usually the most important motion consists of the first few fundamental modes. This is particularly true when considering the lateral vibration of a plate.

Motion in the plane of the plate is much more complex than lateral motion and has not been studied as extensively as lateral motion. The only simply treated cases involving motion in the plane of the plate are flexural vibrations that occur if the plate has a much greater length than its width. Generally the type of motion in the plane of the plate that is of most interest is the propagation of strain or stress waves from some source. Wave propagation in a finite plate seldom achieves a tractable steady-state condition, being subject to dispersion, refraction, and reflection.

The model has a finite number of frequencies of vibration and mode shapes and when assumed to be in harmonic motion oscillates in a steady-state condition. The calculation of the frequencies and mode shapes is of general interest, and the values are useful in other calculations involving wave propagation in the model. If the circular frequency of vibration is assumed to be ω and the amplitude of a particular bar n to be C_n , the displacement of the bar will be

$$u_n \text{ or } v_n = C_n \sin(\omega t + \delta) \tag{45}$$

where

δ = Phase angle

C_n = Amplitude of n -th bar

u_n or v_n = Displacement of n -th bar

Or, considering that the system starts from rest ($\delta = 0$),

$$u_n \text{ or } v_n = C_n \sin(\omega t) \tag{46}$$

Using the latter assumption, the acceleration (the second time derivative) would be

$$\frac{d^2 u_n}{dt^2} \text{ or } \frac{d^2 v_n}{dt^2} = -\omega^2 C_n \sin(\omega t) \tag{47}$$

When the lattice is undergoing steady harmonic motion, the acceleration and displacements in the differential equation (Eq. 44) can be replaced by the values given in Eq. 47 and Eq. 46. When this is done, the equations have the form

$$m_i \omega^2 C_i \sin \omega t = \sum_{j=1}^n a_{ij} C_j \sin(\omega t) \tag{48}$$

where

C = Vibration amplitude of a bar as indicated by subscript

a_{ij} = Coefficient

i = Bar to which equation applies $1 \leq i \leq n$

j = Variable subscript $1 \leq j \leq n$

m_i = Mass of bar i

As $\sin(\omega t)$ appears in every term of the equation, it can be factored out. There then remains a system of equations containing the undetermined factors ω^2 and the amplitudes C_j . The system of equations can be written as follows:

$$\begin{aligned} (a_{11} - m_1 \omega^2) C_1 + a_{12} C_2 + \dots + a_{1n} C_n &= 0 \\ \cdot & \quad \cdot \quad + \dots \quad \cdot \quad \cdot \\ \cdot & \quad \cdot \quad + \dots \quad \cdot \quad \cdot \\ \cdot & \quad \cdot \quad + \dots \quad \cdot \quad \cdot \\ \cdot & \quad \cdot \quad + \dots \quad \cdot \quad \cdot \end{aligned}$$

$$a_{n1}C_1 + a_{n2}C_2 + \dots + (a_{nn} - m_n \omega^2)C_n = 0 \tag{49}$$

In order that these equations have a non-trivial solution, the determinant of the coefficients must equal zero. The matrix equation of the coefficients can be written as

$$|A| - \lambda |B| = 0 \tag{50}$$

where

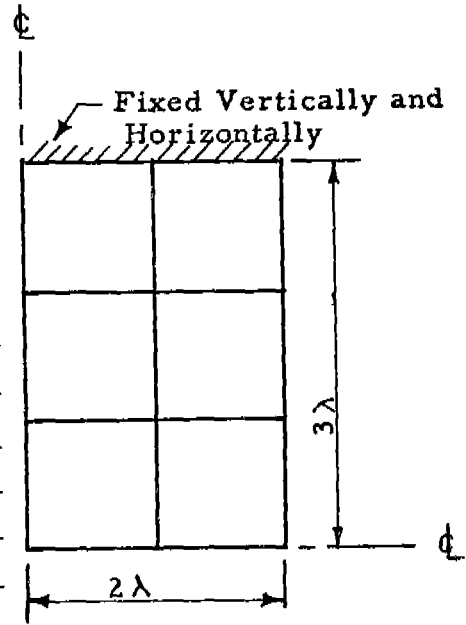
- $|A|$ = Matrix of displacement coefficients
- $|B|$ = Mass matrix
- $\lambda = \omega^2$

This is a characteristic equation which arises in many physical problems and for which methods of solution have been worked out. The solution of the characteristic equation yields the eigenvalues λ_i , from which the frequencies are found, and the eigenvectors, which give the relative magnitudes of the amplitudes of motion.

As an illustration, natural frequencies are presented for two examples in Tables 1 and 2, and the mode shapes are presented for one example in Table 3. The first case is a two-division by three-division symmetric lattice model and is shown in outline form at the bottom of Table 1. It was assumed that the ends of the model are fixed in both the vertical and the horizontal directions. The circular frequencies, natural frequencies, and periods of vibration for the model with a thickness of unity and with $\lambda = 9$ in. are given in Table 1. The second case is a two-division by four-division symmetric model with $\lambda = 9$ in. As in the first case, the ends are assumed fixed both vertically and horizontally. An outline of the model is shown in Fig. 81 along with bar numbers. Frequencies and periods are given in Table 2, and eigenvectors are given in Table 3. Since the eigenvectors, giving the mode shapes, are only relative values, they are normalized so that the sum of their squares equals one. The eigenvectors are considered to be numbered consecutively from one to twenty with each

TABLE 1 FREQUENCIES AND PERIODS FOR 2 x 3 DIVISION
SYMMETRICAL LATTICE MODEL

Vibration Mode	Circular Frequency Rad./sec.	Natural Freq. Cycles/sec.	Period of Vibration sec. X 10 ³
1	5,561	885	1.1299
2	6,776	1,078	0.9276
3	7,525	1,198	0.8347
4	8,571	1,364	0.7331
5	9,534	1,517	0.6592
6	10,788	1,717	0.5824
7	11,618	1,849	0.5408
8	12,672	2,017	0.4958
9	12,836	2,043	0.4895
10	14,647	2,331	0.4290
11	14,720	2,343	0.4268
12	14,877	2,368	0.4223
13	16,755	2,667	0.3750
14	18,072	2,876	0.3477
15	20,138	3,205	0.3120



number corresponding to a bar number in Fig. 81.

It can be seen from Tables 1 and 2 that the highest and lowest frequencies do not differ much in these two examples. The main reason for this is that the values of λ and d (and therefore the bar masses) were the same in each case, and the total size of the plates is only slightly different.

General Approach for Solving Strain Wave or Crack Propagation Problems

The differential equations governing the behavior of the model and an application to a steady-state condition were discussed in the two preceding sections of this chapter. Generally time-dependent behavior of the model or the continuous material that it represents is not of a steady type and cannot be solved as an eigenvalue problem. In such cases it is necessary to treat the problem as an initial-value problem starting with known conditions and determining what conditions exist at some later time.

TABLE 2 FREQUENCIES AND PERIODS

**FOR 2 X 4 DIVISION LATTICE
MODEL OF FIG. 81**

Vibration Mode	Circular Frequency Rad./sec.	Natural Freq. Cycles/sec.	Period of Vibration sec. X 10 ⁻³
1	5.061	806	1.2410
2	5.880	936	1.065
3	6.230	992	1.008
4	7.536	1,199	0.8340
5	8.631	1,374	0.7278
6	8.778	1,397	0.7158
7	9.896	1,575	0.6349
8	10.338	1,645	0.6079
9	10.761	1,713	0.5838
10	11.799	1,878	0.5324
11	12.698	2,021	0.4948
12	13.048	2,077	0.4815
13	13.609	2,166	0.4617
14	14.368	2,287	0.4373
15	14.692	2,338	0.4277
16	15.658	2,492	0.4013
17	16.657	2,651	0.3772
18	16.802	2,674	0.3740
19	18.982	3,021	0.3310
20	20.236	3,221	0.3105

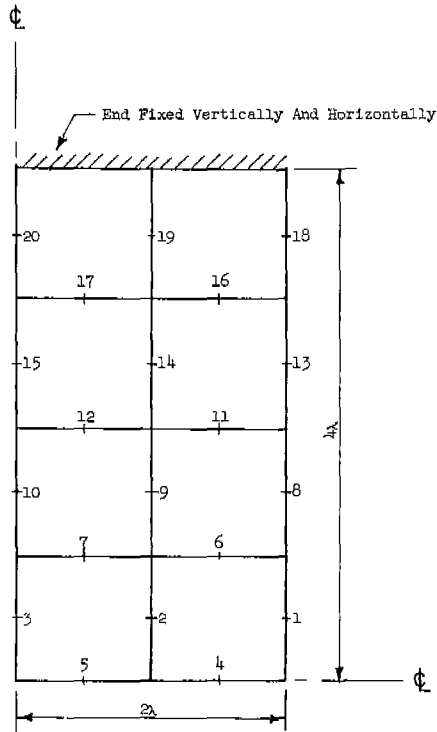


FIG. 81 LATTICE MODEL FOR FREQUENCY ANALYSIS

TABLE 3 EIGENVECTORS FOR LATTICE MODEL SHOWN IN FIG. 81

Mode 1	Mode 2	Mode 3	Mode 4	Mode 5
-0.0136197749	+0.1224708294	-0.2314875790	+0.1176407131	+0.2319286935
-1.297315268	+0.1110536740	-0.0064885298	-0.1219014093	-0.0525236499
-1.740302012	+0.0884891738	+0.0905087637	-0.1403517355	-0.3187646643
+0.4962364786	+0.3222630216	-0.3179879368	+0.5525187329	+0.2407787491
+0.2029156750	+0.1512712737	-0.1531331693	+0.2013325642	+0.2131761370
+0.3601379245	+0.3628938138	-0.0158101001	+0.0989490160	-0.5118790531
+0.1473282466	+0.1624366209	-0.0211967052	-0.0542313882	-0.1212125982
-0.0503604264	+0.3328754138	-0.4746886306	-0.0874162514	+0.0106890686
-0.3070057064	+0.2485261330	-0.0808811827	-0.0607863609	+0.1785709776
-0.4003599434	+0.1799343443	+0.1053990457	+0.0421388700	-0.2792389724
+0.0730495457	+0.3739776482	+0.4384472678	-0.2698143147	+0.2366745136
+0.0305473873	+0.1538546277	+0.1819074231	-0.1076748400	+0.0779550795
-0.0877738113	+0.3883506341	-0.3059469322	-0.3459185290	+0.2203220052
-0.2775765822	+0.2115846394	-0.1892159271	+0.1122623124	+0.0313902155
-0.3585656765	+0.1222024570	-0.0874893700	+0.3229565650	-0.4435394038
-0.1053366326	+0.2247723596	+0.3781127885	+0.4661995236	+0.0462793390
-0.0412590684	+0.0806517528	+0.1703904096	+0.2023627830	-0.0622535766
-0.0740630825	+0.1978638694	-0.0378660794	-0.0010272554	+0.1032041348
-0.0932396033	+0.0634598824	-0.1280286106	-0.0200346261	-0.0252882532
-0.1143500527	+0.0200850452	-0.1328975917	+0.0171449098	-0.1614867779
Mode 6	Mode 7	Mode 8	Mode 9	Mode 10
+0.0647846127	-0.1490872378	-0.3642441012	-0.1637690095	+0.0144482643
-0.1278239288	+0.1897249515	-0.3096599654	+0.0462532936	-0.3215105441
+0.0998651597	-0.0994944307	-0.0196046394	-0.4359843423	+0.4199745293
+0.4700127965	+0.0807663754	+0.0504725660	-0.1903379543	+0.1656495740
+0.0333096711	+0.2931137793	-0.1561559411	+0.2366238255	-0.4552478524
-0.1328802387	+0.0848582888	-0.0042901415	+0.0174607221	-0.1535678291
-0.1479989798	+0.1564688472	+0.0715731164	-0.0790614246	+0.3684104840
-0.2191281420	-0.4347688227	-0.4325984198	-0.1294419364	+0.0174352723
-0.0672188970	+0.3686066477	-0.2303164844	-0.0560244842	+0.2091780146
+0.5822838128	-0.1474213042	-0.1140009820	-0.3235537782	-0.3471753284
+0.2226416615	+0.0749706594	-0.0364568169	+0.1724876722	+0.1210287184
+0.1068450820	-0.0643816040	+0.2078436514	-0.2515943820	-0.2667869386
-0.0115935190	-0.4932666620	+0.2358963079	+0.2649864187	+0.0360084088
-0.1472701764	+0.2137931172	-0.4329632598	-0.1347798867	-0.1153236690
+0.3389238923	-0.0088076040	-0.0841770535	+0.5020262948	+0.1944246841
-0.3319244869	-0.1339812347	-0.0023456789	-0.0316300766	+0.0134756678
-0.0306584286	-0.1811455666	-0.0923650026	+0.1088969717	-0.0105455270
-0.1064876213	-0.2985727816	+0.2788937853	+0.201466812	-0.0111795471
+0.0308437650	+0.0663067397	+0.2935573780	+0.073204518	-0.0749323992
+0.1734954494	+0.1413500932	+0.1363293655	+0.2554829413	+0.1311516012
Mode 11	Mode 12	Mode 13	Mode 14	Mode 15
+0.0982994407	+0.3543485620	+0.4768004457	+0.0328804260	+0.3939262227
-0.0642950873	-0.1199948265	+0.2785894497	+0.0046702199	+0.2250991218
-0.1262181899	-0.1870467164	+0.3277358173	+0.0877001465	+0.2391103776
-0.0604005100	-0.1934603571	+0.0560829934	-0.2297732340	+0.0314440162
-0.1127638560	-0.1113020462	-0.0516883623	+0.5896942594	-0.0435957329
+0.0471298277	-0.0387082036	-0.0172343229	-0.2196050744	-0.0122687951
-0.1553168004	+0.0521672716	+0.0151893512	+0.5067563557	-0.0066659425
+0.1958422981	+0.3775780720	-0.1685671362	-0.0019545871	+0.3783846254
-0.1388627711	-0.1281148461	-0.1108201889	+0.1058736887	-0.2133599084
+0.0013374436	-0.2457742402	-0.1255414379	+0.1070809565	-0.2525450444
+0.1051231558	+0.1579587393	+0.0104085178	-0.1456801989	+0.0226240920
+0.0026688554	+0.2213512918	-0.0331643069	+0.3147169232	-0.0164028653
-0.0309310021	-0.3340071612	-0.1996994066	+0.1053707379	+0.3693644283
+0.0895200601	+0.1037986044	-0.1270179718	-0.1147143277	+0.2219857253
+0.0177595244	+0.1484850484	-0.1460397603	+0.1297714299	+0.2250504253
+0.2325556777	-0.0711348751	+0.0441722026	+0.0110138590	-0.0220932915
-0.5326576412	+0.1944963637	-0.0563399295	+0.0000824091	+0.0296951230
-0.1534026542	-0.4306405251	+0.4929073615	+0.0774371896	-0.3854550959
+0.3061723944	+0.2857759924	+0.2765226118	-0.1746720445	-0.2012442609
+0.6281825843	+0.1526275829	+0.3385223430	+0.2562174284	-0.2320279921
Mode 16	Mode 17	Mode 18	Mode 19	Mode 20
-0.4341185355	+0.0354642883	-0.4191038305	+0.1200254482	-0.1377043334
+0.1678700118	+0.1030803585	+0.1907707608	-0.2491599778	+0.2925744191
+0.3096342330	-0.2851048410	+0.2939370736	+0.3261093498	-0.3818845123
+0.1807386647	+0.1562829787	+0.1787433714	-0.1763090576	+0.1629027756
+0.0970519170	-0.4652136671	+0.0261360578	+0.3769759566	-0.3429677347
-0.0965971688	+0.0818919049	-0.1311384541	+0.0888407209	-0.1535503060
-0.0955678922	-0.0745315623	-0.1158806728	-0.1901406790	+0.3234749703
+0.0992461026	-0.1933070130	+0.3499856366	-0.0006689292	+0.1204218218
-0.0232255188	+0.2547867657	-0.1134198955	+0.0016677064	-0.2593568200
-0.0918736296	-0.2069712911	+0.3593918276	-0.0029347840	+0.3386230909
-0.0436135912	-0.2049461577	+0.0907952731	+0.0665368129	+0.1267740775
-0.0136119118	+0.3732520809	+0.1625723669	-0.1841000864	-0.2671323016
+0.2848736998	+0.0819998212	-0.3137100014	-0.1201515317	-0.0918356791
-0.115335742	-0.0729647846	+0.1209976580	+0.2495000280	+0.1974770826
-0.2413523903	-0.0074372594	+0.2843774422	-0.3239639176	-0.2574921278
+0.1255399660	-0.0969633402	-0.115377920	-0.1710139099	-0.0841490487
+0.1348073784	+0.2670066782	-0.0319775646	+0.3616427526	+0.1764696082
-0.4799801272	+0.1102557201	+0.864719498	+0.1367276159	+0.0570673717
+0.1870140616	-0.2582697055	-0.1587051797	-0.2733257341	-0.1194409484
+0.3935575107	+0.3967869519	-0.1538931292	+0.3513641863	+0.1545382129

The equations of motion for a continuous elastic material have been solved for a number of situations, most of which involve semi-infinite media. In working with the differential equations of motion for a continuous material, the greatest difficulty is encountered in satisfying the boundary conditions. The finite model developed in this report provides an approximate two-dimensional method for treating difficult boundary conditions or types of loading. Use of the model provides a physical system which can easily be visualized and reduces the problem to the solution of a set of linear second-order differential equations which are easily solved by numerical integration.

The general approach for solution of a wave propagation or time-dependent boundary value problem with the model is as follows:

1. Determine model dimensions and layout.
2. Determine initial static displacements.
3. Apply a step-by-step numerical integration procedure for solution of the differential equations.
4. Adjust boundaries and loads as the integration proceeds.

If the boundary conditions are time-independent, it may not be necessary to determine initial displacements for solution of wave-propagation problems. In such cases the transient effects can be determined separately and superposed on the initial conditions. Two methods of numerical integration are presented in the following section.

NUMERICAL INTEGRATION OF EQUATIONS

Newmark Beta-Method of Integration

The Newmark Beta-Method of integration is a step-by-step method for solution of systems of second-order differential equations having initial conditions specified. This method is about the most convenient method available for hand solution of equations. The value of β can be selected to give the best possible results for the values (period, amplitude, etc.) that are considered most important. A complete development and description of the Beta-Method is given in several references. ¹⁸⁻²⁰

The β -integration equations are

$$\ddot{u}_{n+1} = \frac{P}{m} \tag{51.1}$$

$$\dot{u}_{n+1} = \dot{u}_n + \frac{h}{2} (\ddot{u}_n + \ddot{u}_{n+1}) \tag{51.2}$$

$$u_{n+1} = u_n + h \dot{u}_n + h^2 \left(\frac{1}{2} - \beta \right) \ddot{u}_n + h^2 \beta \ddot{u}_{n+1} \tag{51.3}$$

where

P = Unequibrated force acting on the mass

m = Mass

\ddot{u} = Acceleration of mass

\dot{u} = Velocity of mass

u = Displacement of mass

h = Time interval

β = Parameter of β -Method

n = n -th time interval

The β -Method is an iterative method starting with an assumed acceleration. Steps in the calculation for each time interval, considering only one mass at a time, are

1. Assume an acceleration \ddot{u}_{n+1}
2. Calculate \dot{u}_{n+1} and u_{n+1}
3. Using the values of \dot{u}_{n+1} and u_{n+1} from Step 2, calculate P .
4. Calculate a new \ddot{u}_{n+1} from Eq. 51.1
5. Compare the values of \ddot{u}_{n+1} from Steps 1 and 4. If the values differ by more than the desired number of figures, repeat Steps 1 to 5 using \bar{u}_{n+1} from Step 4 as the assumed value.

when two successively calculated accelerations agree to a desired number of significant figures for all masses in the system being considered, one step of integra-

tion has been completed. The values that have just been calculated are then used in the calculation of the next step.

Varying the value of β has the effect of changing the shape of the acceleration-time curve over the integration interval. If β is taken as zero this assumes a constant acceleration pulse for each integration interval which causes an instantaneous jump in velocity at the start of each interval. Taking $\beta = 1/8$ assumes that the acceleration has a constant value equal to the initial value for the first half of the time interval and equal to the final value for the second half of the time interval; $\beta = 1/6$ assumes a linear variation of acceleration over each interval; and $\beta = 1/4$ assumes a uniform acceleration whose value is equal to the average of the acceleration at each time interval.

In order for this procedure to be useful, the successive values calculated in one step must converge toward a definite and correct value. Fairly rapid convergence is also required in order to achieve good accuracy. The convergence and accuracy characteristics of the β -Method have been investigated by considering a single-degree-of-freedom elastic vibratory system. Results from the single-degree-of-freedom system can be applied to the multi-degree-of-freedom systems by considering the various modes of the multi-degree-of-freedom system. Limits have been worked out in terms of frequency (or period) and integration time interval for convergence, stability of a harmonic motion, and error for each value of β .

Truncation errors depend upon the value selected for β . For example, if $\beta = 1/4$, the accuracy will be of the order of h^2 , and if $\beta = 1/6$, the accuracy will be of the order of h^3 .

Runge-Kutta Method of Integration

The Runge-Kutta Numerical Integration Method is a non-iterative step-by-step procedure. This method achieves its accuracy by using several estimates of the dependent variable for each increment of the independent variable. Usually the method is applied to first-order equations, although modifications of the procedure have been developed for higher-order equations.

The specific form in which the Runge-Kutta Method is used with many high-speed computing machines is due to the work of Gill.²² In this form a program is designed to solve n simultaneous first-order differential equations. If it is desired to solve equations of higher order, each higher-order equation is reduced to a number of first-order equations. For example, consider the third-order differential equation

$$\frac{d^3 y}{dx^3} + a(x) \frac{d^2 y}{dx^2} + b(x) \frac{dy}{dx} + c(x)y = g(x) \tag{52}$$

and let

$$\frac{dy}{dx} = u \tag{53.1}$$

$$\frac{du}{dx} = v \tag{53.2}$$

Substitute these into Eq. 52 to get

$$\frac{dv}{dx} = - a(x)v - b(x)u - c(x)y + g(x) \tag{54}$$

Thus solution of the three simultaneous first-order Eqs. 53.1, 53.2, and 54 is equivalent to the solution of the single third-order Eq. 52.

A complete derivation of the Runge-Kutta Method is given elsewhere,^{23, 24} and only the results used in the ILLIAC^{*} library program P-1 are stated here. For a given set of differential equations

$$\dot{y}_i = f_i (y_0, y_1, y_2, \dots, y_{n-1}), \quad i = 0, 1, 2, \dots, n-1 \tag{55}$$

the process used in the integration is defined by the following:

$$k_{i,j} = 2^m h f_i (y_{0j}, y_{1j}, y_{2j}, \dots, y_{n-1j}) \tag{56.1}$$

*ILLIAC is the University of Illinois high-speed electronic digital computer.

$$r_{i, j+1} = (A_{j+1} + 1)(k_{i, j} - B_j q_{ij}) \quad (56.2)$$

$$y_{i, j+1} = y_{i, j} + 2^{-m} r_{i, j+1} \quad (56.3)$$

$$q_{i, j+1} = q_{i, j} + 3r_{i, j} + (c_j - 1)k_{i, j+1} \quad (56.4)$$

with the following table of values

j	A_{j+1}	B_j	C_j
0	-1/2	2	1/2
1	$-(1/2)^{1/2}$	1	$(1/2)^{1/2}$
2	$(1/2)^{1/2}$	1	$-(1/2)^{1/2}$
3	-5/6	2	1/2

Where double subscripts are used, the first subscript indicates which variable is being considered and the second subscript j indicates which of the four parts of one step is being performed. The quantities $r_{i, j}$ are only an intermediate calculation and are not carried from step to step. Only the values of $y_{i, 4}$, the dependent variable at the end of the integration interval, and the values of $q_{i, 4}$, which prevent the rapid accumulation of round-off errors, are carried directly from step to step. Thus for one integration step the order of calculation would be

- j = 0 i = 0, 1, 2, ---, n-1
- j = 1 i = 0, 1, 2, ---, n-1
- j = 2 i = 0, 1, 2, ---, n-1
- j = 3 i = 0, 1, 2, ---, n-1

The truncation error for one integration step is of the order of h^5 . There are no limits for convergence or stability, and the length of the increment of the independent variable may be altered at any step of the calculation.

NUMERICAL RESULTS FOR TRANSIENT STRAINS

General Remarks and Problems Considered

Several examples of the transient strain redistribution associated with a propagating crack are presented in this chapter to indicate the nature of some of the results that have been found with the lattice model and to point out some of the difficulties encountered in applying this method. The lattice models used in these examples are much too coarse to portray adequately strain gradients as steep as those associated with the highly concentrated disturbance surrounding a moving crack tip. Therefore the coarse lattice models do not give quantitative results of practical significance. On the other hand, the solutions do provide to some degree a qualitative picture of strain redistribution for a propagating crack.

As previously mentioned, the solution of problems by this method involves an immense amount of calculation; thus a very high speed digital computer with a large memory capacity is required. By way of illustration, the ILLIAC, the digital computer used for the examples given in this chapter, could not treat lattice models with more than 40 bars without the calculation time becoming excessive.

Two cases of crack propagation are considered here, the unsymmetrical case in which a crack propagates from one side of a plate to the other side, and the symmetrical case in which cracks propagate from both edges of a plate and meet at the center. These two methods of numerical integration described in the preceding chapter are applied to the unsymmetrical case to permit a comparison of solutions by the two methods.

Variables Entering Into the Calculation

A number of variables enter into the transient solution of the set of differential equations expressing the behavior of the lattice mode. The most important of these variables are:

- (a) fineness of subdivision of lattice model
- (b) boundary conditions

- (c) velocity of crack propagation
- (d) integration method
- (e) integration time interval

Lattice model subdivision is very important for two reasons. First, the ability of the lattice model to approximate steep strain gradients is directly dependent on how finely the lattice model is subdivided, and this affects all solutions, either static or dynamic. Second, the periods of the natural frequencies of the lattice model are directly proportional to the square root of the bar masses; the natural periods of vibration are important in dynamic analyses. Some problems associated with the natural frequencies of the model are discussed in the next section.

Boundary conditions define how much energy, if any, can be fed into a plate during crack propagation and also define whether or not the boundaries are able to displace during crack propagation. Two boundary conditions were considered: uniformly loaded boundaries that were free to move with the magnitude of the load always remaining constant, and boundaries that were initially given a displacement equivalent to the movement resulting from a uniformly applied load and thereafter held fixed. It was found that maintaining a uniform load and allowing the boundaries to move tended to increase the magnitudes of peak strains ahead of the crack, this effect being much more pronounced at low crack velocities. The end condition in which the ends were uniformly displaced and then held fixed was used in the case of the examples presented in this chapter. It is believed the fixed-end condition closely duplicates conditions experienced in most plate-fracture experiments made in massive testing machines.

Crack velocity in the lattice model is an artificial concept and in general has no relation to the fracture process in the physical material that the lattice model replaces; this will become apparent from the discussion that follows. Initiation of the crack was carried out by allowing the first node (or nodes in the symmetrical case) to separate. Crack velocity was thereafter determined by the time allowed until the next node was permitted

to separate. In this manner the crack proceeded by jumps of finite length. Transient strain redistribution is dependent upon the crack velocity; if the crack velocity is progressively increased, a point is reached where the strain energy released by separation of the deformed nodes does not have time to propagate ahead of the crack and increase the strain at nodes ahead of the crack.

One of the original objectives of this investigation was to establish theoretical fracture criteria for nodes in the lattice model by considering strain rates, strain magnitudes, previous deformation history, and non-linear elasticity of some of the nodes and to determine at what velocity or velocities a crack would propagate or arrest under such theoretical conditions. However, such a search for fracture criteria was found to be impossible because the available digital computer was too slow to consider a lattice model having subdivisions fine enough to give adequate definition of strain gradients. In the examples of crack propagation in a lattice model presented in this chapter the crack velocity was arbitrarily selected as a convenient value falling in the range of velocities that have been experimentally observed in tests of wide steel plates.³

The integration method used for numerical solution of the differential equations must be considered a variable because of certain peculiarities associated with different methods of step-by-step integration of initial-value problems. Two methods of numerical integration, the Newmark Beta-Method and the Runge-Kutta Method, were presented in the preceding chapter. These two methods were applied to the same problem and the results compared to check whether either method generates a spurious solution and to determine how well the calculated values agree when the same time interval and auxiliary data are used.

The integration time interval is important because truncation errors are proportional to some power of the time interval. Limits of stability and convergence in the Newmark Beta-Method have been worked out in terms of the integration time interval and the natural periods of vibration. Rather ex-

tensive discussions of truncation errors, parasitic or spurious solutions, stability, convergence, and propagation of round-off errors are given in several references.^{18-20, 23}

Possible Difficulties in Solving Dynamic Problems with a Lattice Model

Several difficulties can arise in using a lattice model for the solution of dynamic problems. Most of the difficulties are a result of concentrating a continuous material at definite points and introducing distinct natural frequencies of vibration. When energy in the form of strain waves is passed through the lattice model, reflections take place at boundaries and usually cause oscillations of the adjoining lattice model bars. These oscillations modulate any strain waves that thereafter pass through the section of lattice model where the oscillations have developed. Eventually the oscillations also spread through the lattice model and confuse interpretation of strain values.

Another difficulty can arise because of the finite nature of the lattice model. The mechanical system formed by the lattice model has as an electrical analog and L-C filter. Such filters have been extensively studied for one-dimensional wave propagation, but because they become very complex in two-dimensional analysis, they have not been studied as extensively as the one-dimensional case. It has been shown²⁵ that L-C filters exhibit passing and stopping bands toward electrical disturbances of varying frequencies. Certain frequencies are easily propagated through the filter, while others are strongly attenuated. On the basis of the coarse lattice models used to study transient strains associated with a propagating crack, no such effect has been detected. If the lattice model is used to investigate strain-wave propagation resulting from external loads, a careful investigation would be required to determine if stopping or passing bands exist.

Solutions for Transient Strains with a Coarse Lattice Model

Two cases of crack propagation in the lattice model are presented in this section. The first problem treated (Example 1) is one of unsymmetrical crack

propagation where a crack starts from one edge of a plate and extends toward the opposite edge. This case has been integrated with the Runge-Kutta Method (Example 1) and also with the Newmark Beta-Method; results of the two integration methods are compared in Example 3. The second problem treated (Example 2) is one of symmetrical crack propagation wherein cracks start from two opposite edges of a plate and extend toward the center; the Runge-Kutta Method of integration is used in Example 2. Strains as a function of time are plotted for all nodes and shear points in the unsymmetrical case (Example 1) and for only a few points in the symmetrical case (Example 2).

The lattice model used in each example has four divisions in each direction and therefore has forty bars or forty degrees of freedom. In order to carry out the numerical solution of the examples, some numerical values must be assigned for plate dimensions, loads, and other parameters. It was considered desirable to work with dimensions and parameters that were similar to values used in laboratory experiments.³ On this basis the lattice model division λ was taken equal to nine inches and the thickness of the plate as one inch. Using these dimensions, the unsymmetrical lattice model represents a plate 1-in. thick, 3-ft wide and 6-ft long.

The symmetrical lattice model represents a square plate 1-in. thick and 6 ft on each side. Initial loading was equivalent to a uniform end tension of 20,000 psi applied to each end of the plate, which allowed the ends to move and then held the ends fixed in position vertically. The elastic constants were taken as $E = 30 \times 10^6$ psi and $\nu = 0.30$.

Crack velocity in the lattice model in each case was held constant and consisted of jumps of 0.75 ft in 0.180 millisecc. This represents a step velocity of 4167 fps across the plate width.

The integration time interval was selected as a conservative value, because the purpose of the examples presented is to illustrate characteristics of the lattice model and not to investigate all possible variables associated with the integration methods. The value of h was taken as 2×10^{-6} sec; such a small time interval gives quite accurate results and eliminates to a large degree

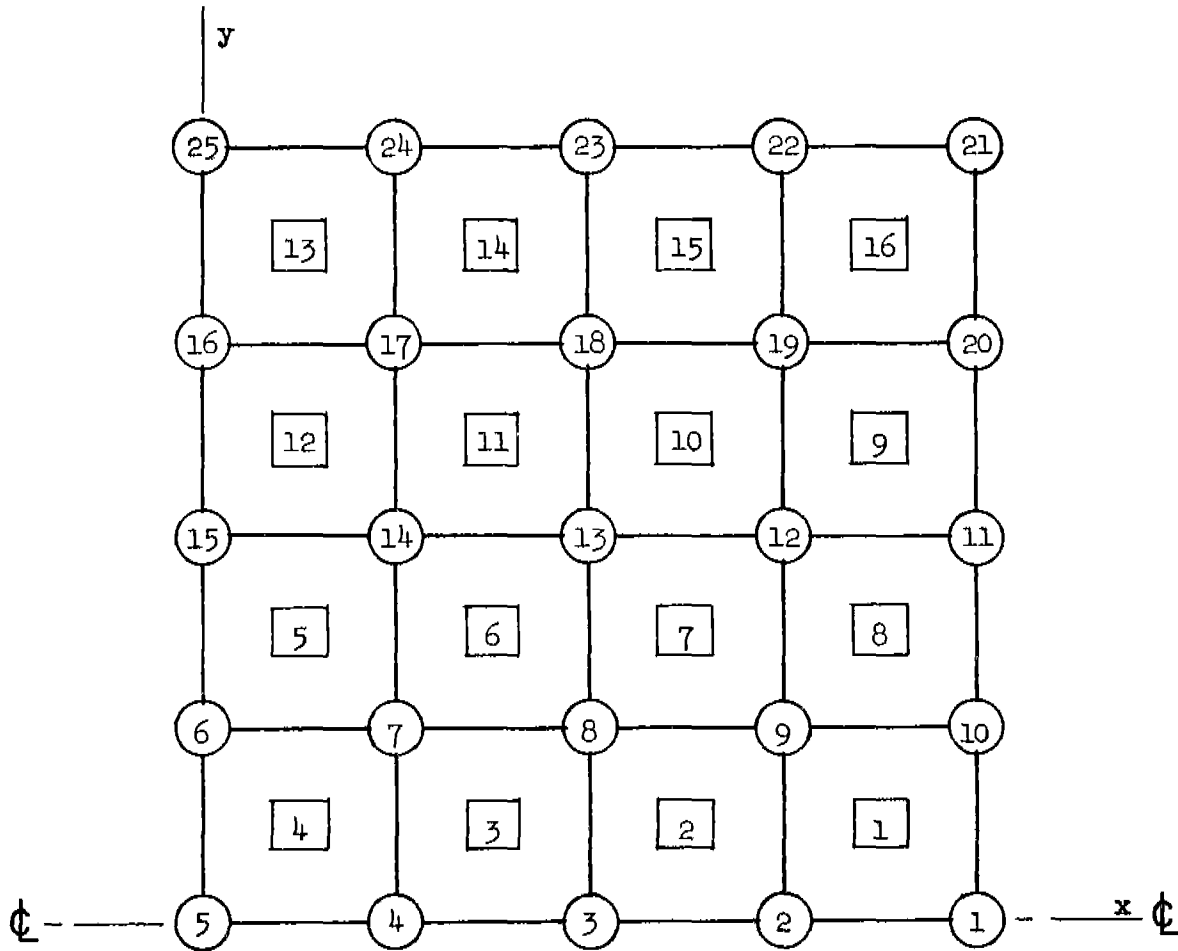


FIG. 82 LATTICE MODEL NOTATION FOR CRACK PROPAGATION EXAMPLES

some of the problems associated with the numerical integration processes. Values of bar displacements and strains were punched out by the computer for every five steps of integration to provide a detailed picture of lattice model behavior.

The notation used for each of the examples that follow is shown in Fig. 82. In this figure only the bar centerlines are shown, with circles at the node points and small squares at the shear points. A number inside a circle or rectangle identifies the node or shear point to which reference is made. The left edge of the lattice model is to be considered a free edge or a centerline depending upon whether the lattice model represents an unsymmetrical or a symmetrical case respectively.

Example 1: Unsymmetrical Crack Propagation. In this example the crack propagates in four jumps starting at the right edge and extending to the left edge of the lattice model. The crack was started by separating node 1 in Fig. 82 at time zero. After intervals of 0.180 millisecc, nodes 2, 3, and 4 were separated. After 0.720 millisecc, nodes 1 to 4 were separated and node 5 was still intact but just ready to separate to complete propagation of the crack across the lattice model. Integration was carried out with the Runge-Kutta Method using the integration time $h = 2 \times 10^{-6}$ sec as mentioned previously.

Strain-time curves for all nodes and shear points of the lattice model (Fig. 82) are presented in Figs. 83 to 122. Horizontal and vertical strains are given at the node points as indicated on the figures except at nodes where the horizontal strain values cannot be calculated as at the edges. When a node is separated to extend the crack, the point of separation is indicated on the appropriate vertical strain curve in Figs. 83 to 86 by an X. It can be seen by examining Figs. 83 to 86 that in the nodes ahead of the crack in the lattice model the vertical strain increases in value as the crack approaches a node until the node is separated to extend the crack. Node 4, shown in Fig. 85, shows a slight relaxation of the initial positive vertical strain before the increase resulting from the approaching crack. Figure 86 shows a fairly large decrease of initial vertical strain at node 5 until the crack reaches node 4, whereupon a sharp increase of strain takes place. The horizontal strain in nodes 2, 3, and 4, as shown in Figs. 83 to 85, goes from a negative value to a positive value as the crack approaches and passes one of the nodes. This creates a zone of biaxial tension ahead of the crack. After separation of node 2, a definite oscillation on the horizontal strain value occurs because of a strain wave reflection off the right side of the lattice model.

Vertical strains in nodes 7 to 9 (Figs. 88 to 90) show a small peak as the crack passes by a node and then a rapid decrease in strain magnitude. After the crack has passed by a node, an oscillation in the strain values oc-

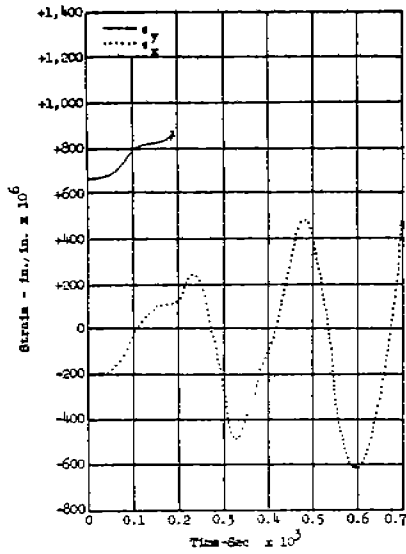


FIG. 83 STRAIN-TIME BEHAVIOR
NODE 2 - EXAMPLE 1

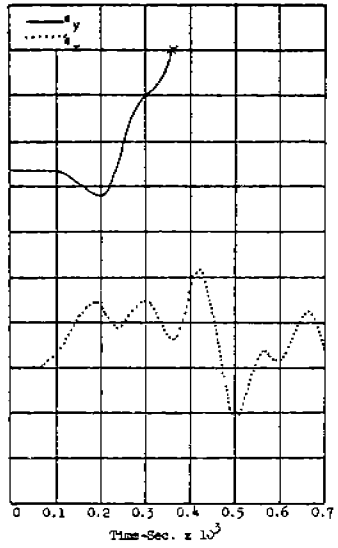


FIG. 84 STRAIN-TIME BEHAVIOR
NODE 3 - EXAMPLE 1

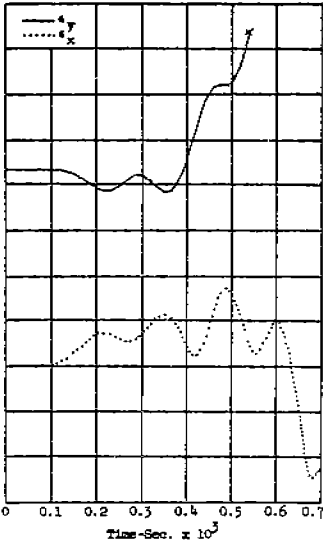


FIG. 85 STRAIN-TIME BEHAVIOR
NODE 4 - EXAMPLE 1

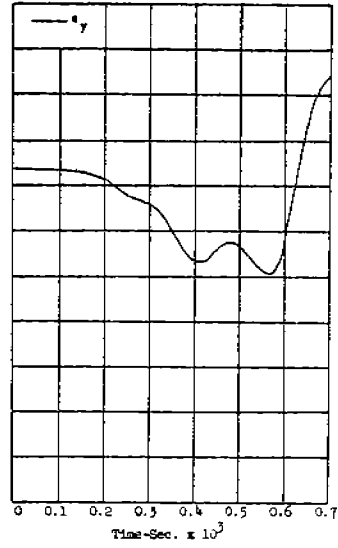


FIG. 86 STRAIN-TIME BEHAVIOR
NODE 5 - EXAMPLE 1

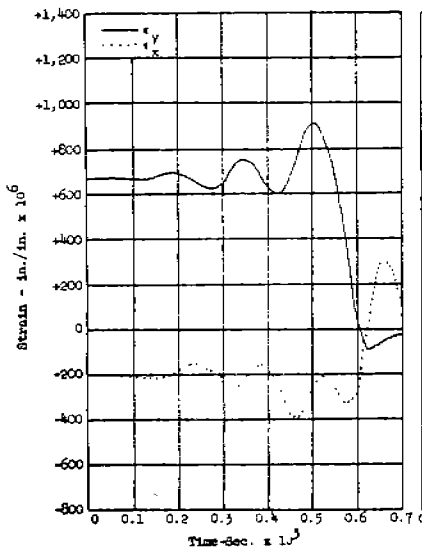


FIG. 88 STRAIN-TIME BEHAVIOR
NODE 7 - EXAMPLE 1

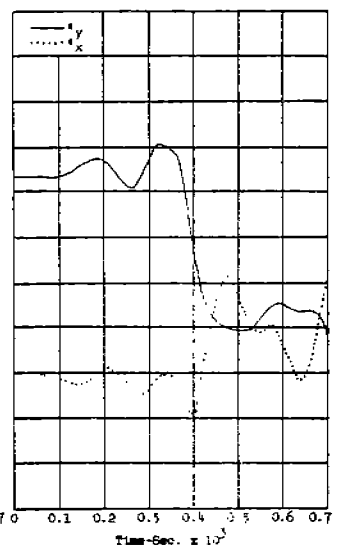


FIG. 89 STRAIN-TIME BEHAVIOR
NODE 8 - EXAMPLE 1

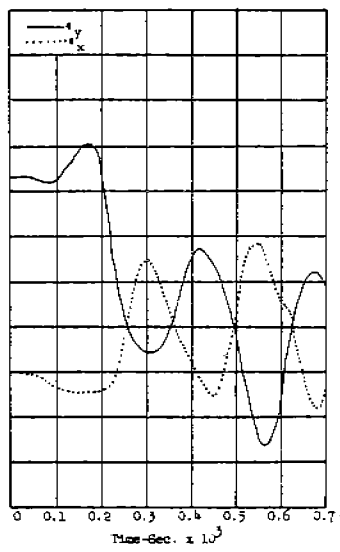


FIG. 90 STRAIN-TIME BEHAVIOR
NODE 9 - EXAMPLE 1

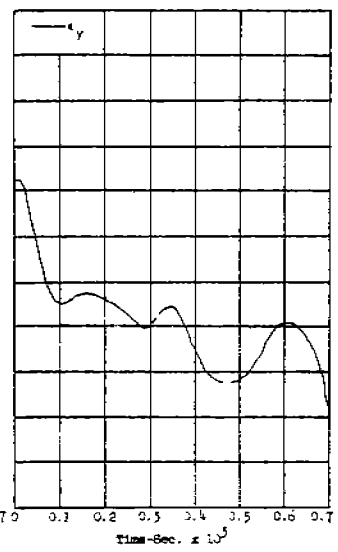


FIG. 91 STRAIN-TIME BEHAVIOR
NODE 10 - EXAMPLE 1

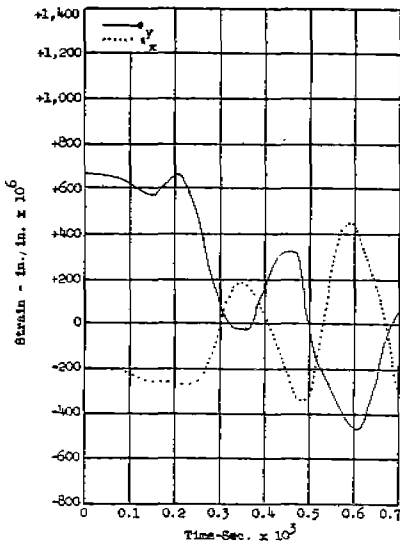


FIG. 93 STRAIN-TIME BEHAVIOR
NODE 12 - EXAMPLE 1

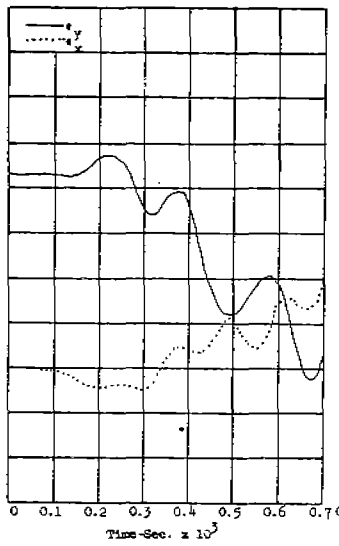


FIG. 94 STRAIN-TIME BEHAVIOR
NODE 13 - EXAMPLE 1

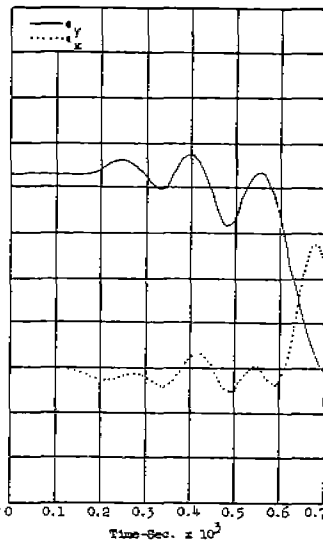


FIG. 95 STRAIN-TIME BEHAVIOR
NODE 14 - EXAMPLE 1

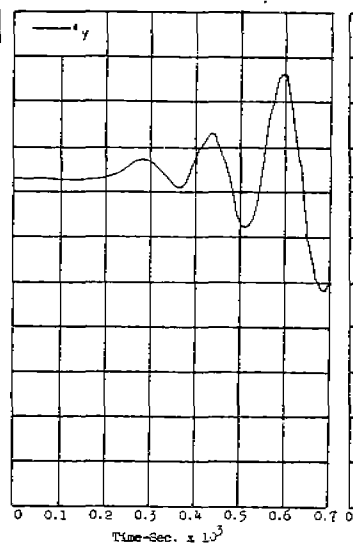


FIG. 96 STRAIN-TIME BEHAVIOR
NODE 15 - EXAMPLE 1

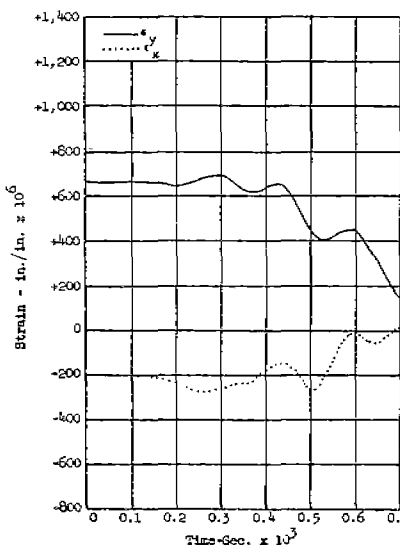


FIG. 98 STRAIN-TIME BEHAVIOR
NODE 17 - EXAMPLE 1

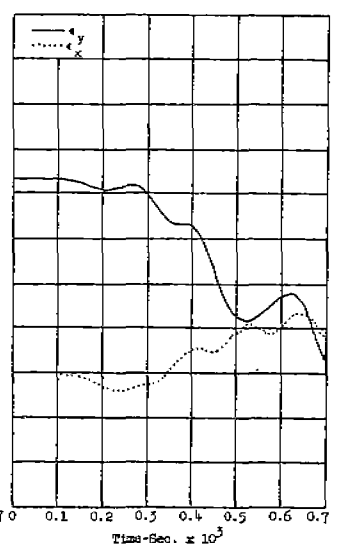


FIG. 99 STRAIN-TIME BEHAVIOR
NODE 18 - EXAMPLE 1

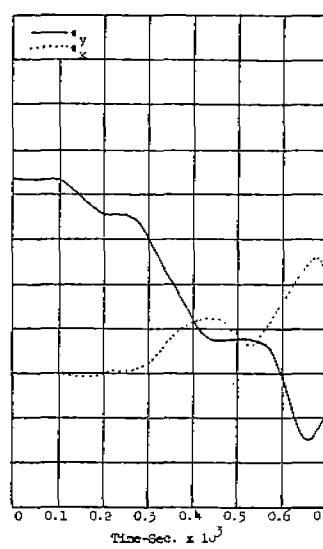


FIG. 100 STRAIN-TIME BEHAVIOR
NODE 19 - EXAMPLE 1

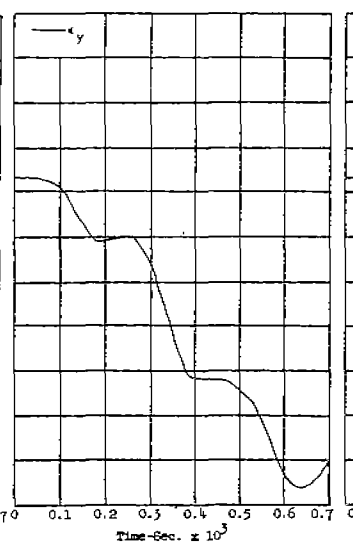


FIG. 101 STRAIN-TIME BEHAVIOR
NODE 20 - EXAMPLE 1

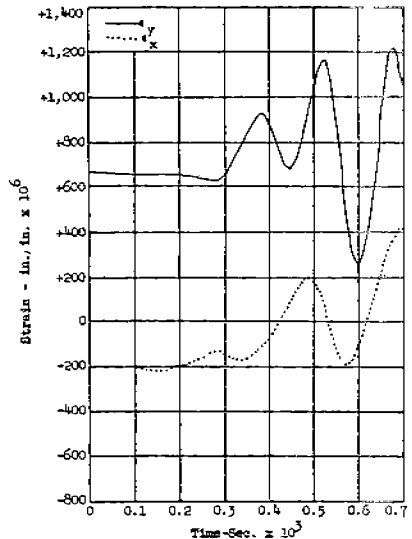


FIG. 103 STRAIN-TIME BEHAVIOR
NODE 22 - EXAMPLE 1

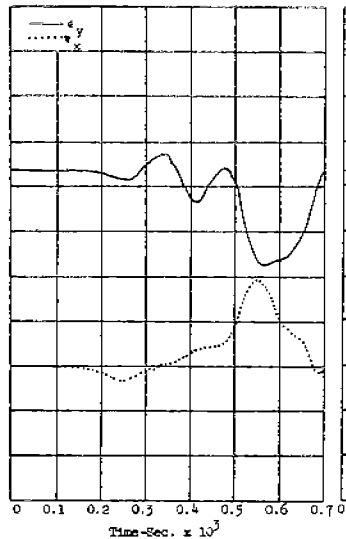


FIG. 104 STRAIN-TIME BEHAVIOR
NODE 23 - EXAMPLE 1

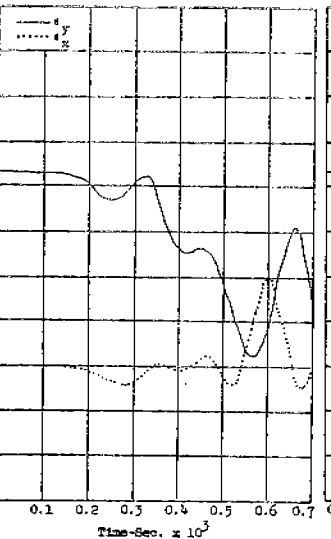


FIG. 105 STRAIN-TIME BEHAVIOR
NODE 24 - EXAMPLE 1

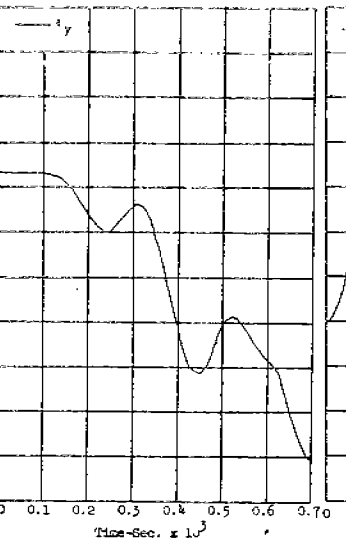


FIG. 106 STRAIN-TIME BEHAVIOR
NODE 25 - EXAMPLE 1

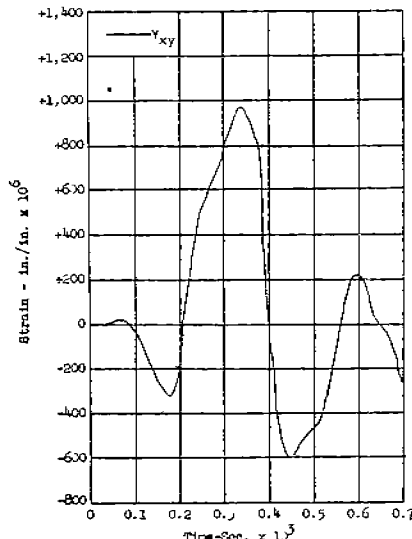


FIG. 108 STRAIN-TIME BEHAVIOR
SHEAR POINT 2 - EXAMPLE 1

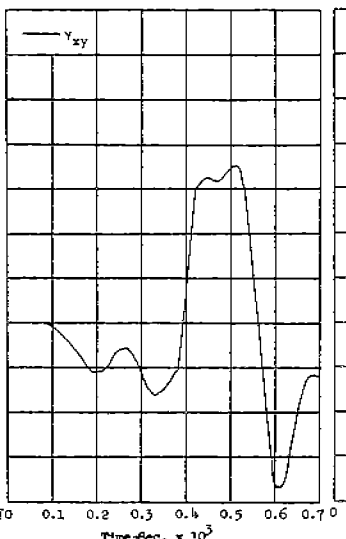


FIG. 109 STRAIN-TIME BEHAVIOR
SHEAR POINT 3 - EXAMPLE 1

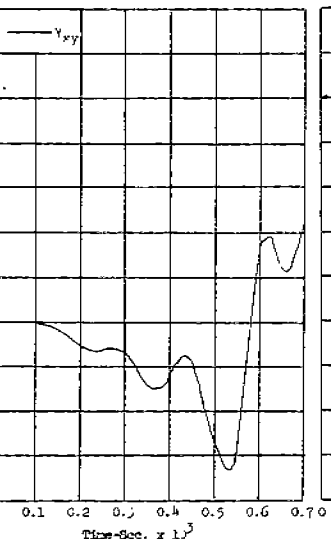


FIG. 110 STRAIN-TIME BEHAVIOR
SHEAR POINT 4 - EXAMPLE 1

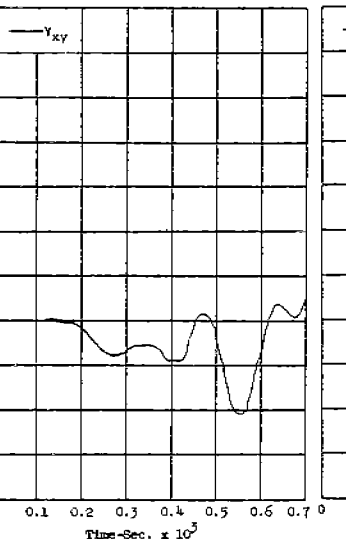


FIG. 111 STRAIN-TIME BEHAVIOR
SHEAR POINT 5 - EXAMPLE 1

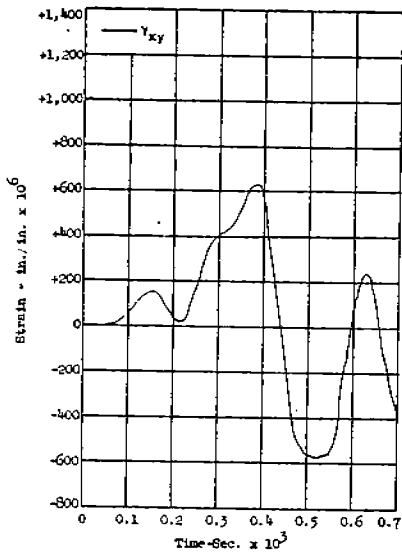


FIG. 113 STRAIN-TIME BEHAVIOR
SHEAR POINT 7 - EXAMPLE 1

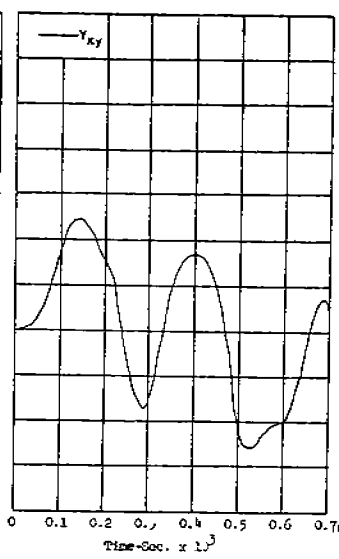


FIG. 114 STRAIN-TIME BEHAVIOR
SHEAR POINT 8 - EXAMPLE 1

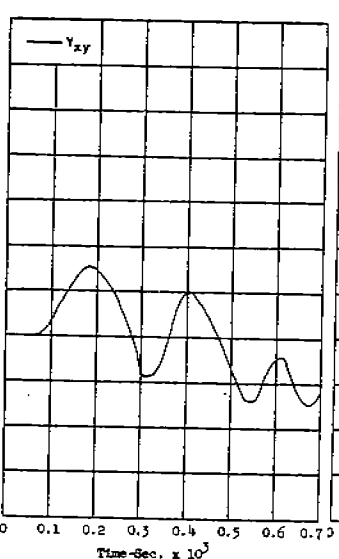


FIG. 115 STRAIN-TIME BEHAVIOR
SHEAR POINT 9 - EXAMPLE 1

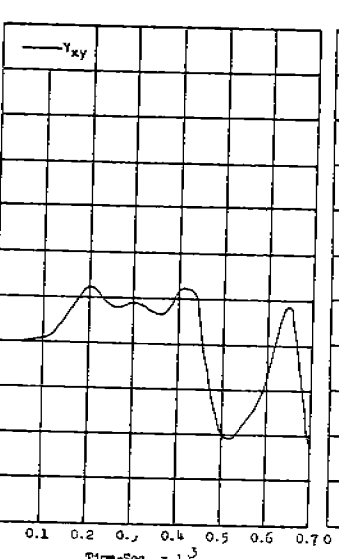


FIG. 116 STRAIN-TIME BEHAVIOR
SHEAR POINT 10 - EXAMPLE 1

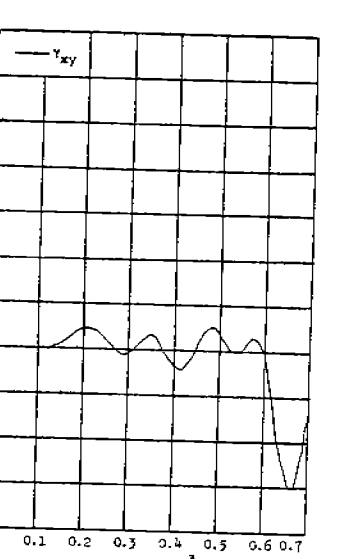


FIG. 117 STRAIN-TIME BEHAVIOR
SHEAR POINT 11 - EXAMPLE 1

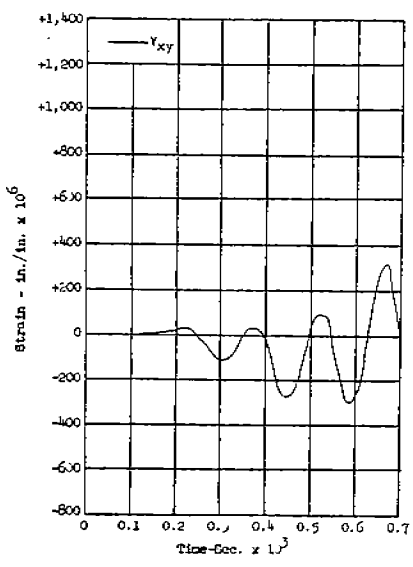


FIG. 118 STRAIN-TIME BEHAVIOR
SHEAR POINT 12 - EXAMPLE 1

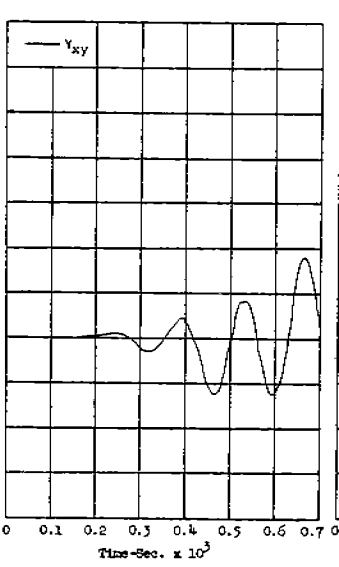


FIG. 119 STRAIN-TIME BEHAVIOR
SHEAR POINT 13 - EXAMPLE 1

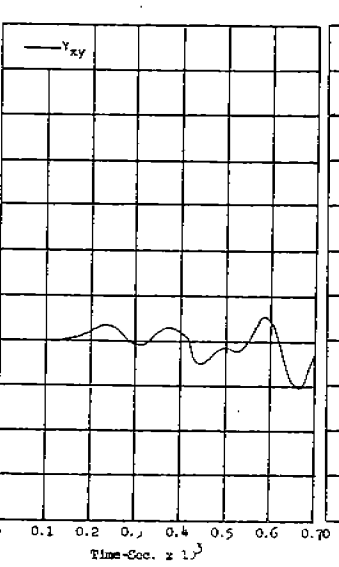


FIG. 120 STRAIN-TIME BEHAVIOR
SHEAR POINT 14 - EXAMPLE 1

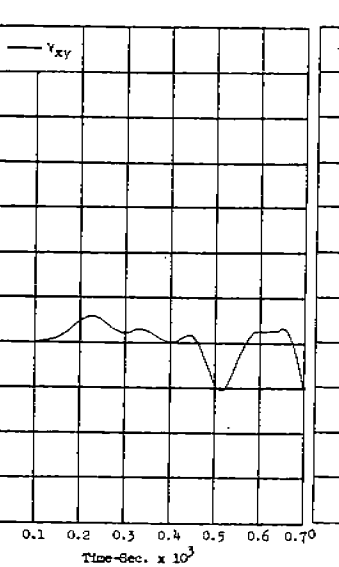


FIG. 121 STRAIN-TIME BEHAVIOR
SHEAR POINT 15 - EXAMPLE 1

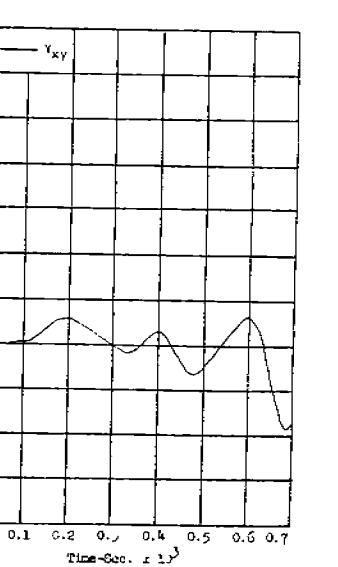


FIG. 122 STRAIN-TIME BEHAVIOR
SHEAR POINT 16 - EXAMPLE 1

curs because of reflections from the boundaries formed by the crack surface and because of reflections at the right edge of the model. Node 6, situated on the left side of the lattice model, is affected by reflections from the left edge of the lattice model, and the strain value starts to oscillate sooner than the strain values in interior nodes.

In general, the group of nodes (12-14 and 17-19) situated in the interior of the lattice model tends to show only a slight peaking of the strain values; oscillations begin after the first small peak, as shown in Figs. 93-95 and 98-100. After the crack has passed beneath one of the nodes, the strain values begin to relax and release stored strain energy in the form of strain waves that eventually reflect from the lattice model boundaries. After a period of time the strain values all oscillate within the spectrum of the natural frequencies of the lattice model as the strain waves reflect and re-reflect from the lattice model boundaries.

Strain values in nodes along the lattice model boundaries show the effects of reflected strain waves from the boundaries, and the strain values tend to oscillate quite a bit. At some nodes, such as 15 and 22 shown in Figs. 96 and 103, the reflections reinforce each other and produce quite high positive strain values.

Shear strains are shown in Figs. 107 to 122 for the shear points in the lattice model. The shear strains at shear points 1, 2, 3, and 4 adjoining the crack path become positive as the crack approaches and then rapidly drop to a negative value as the crack passes. Shear points 5, 6, 7, and 8 follow the same trend as shear points 1, 2, 3, and 4. As the distance from the crack path increases, the shear strain varies in an oscillatory manner, showing the effect of wave reflections from the lattice model boundaries.

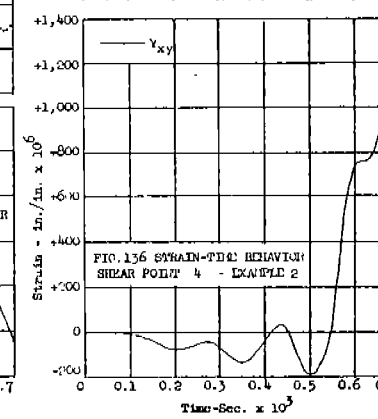
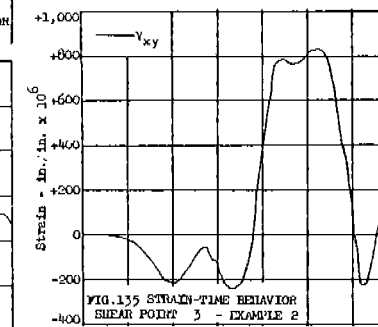
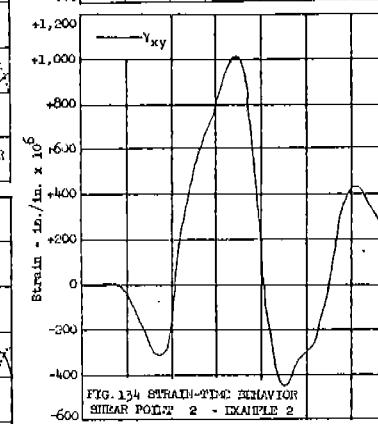
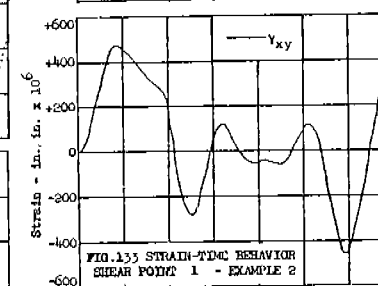
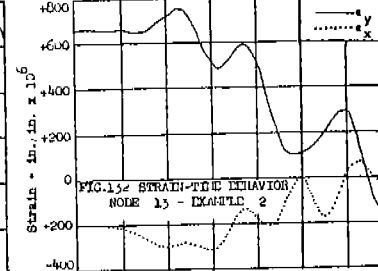
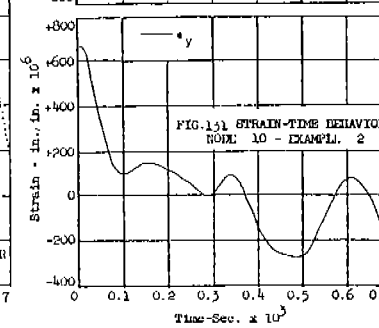
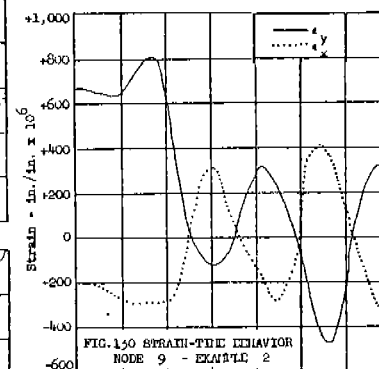
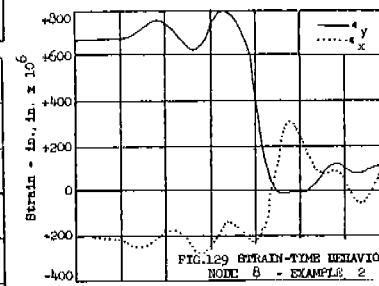
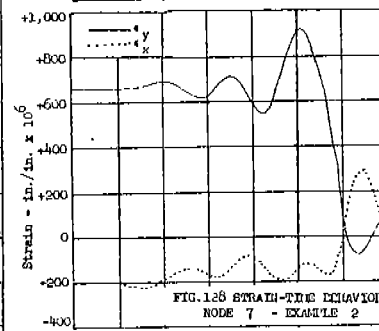
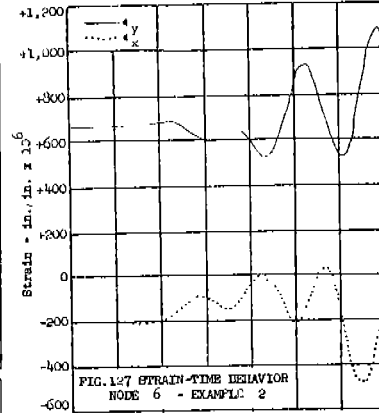
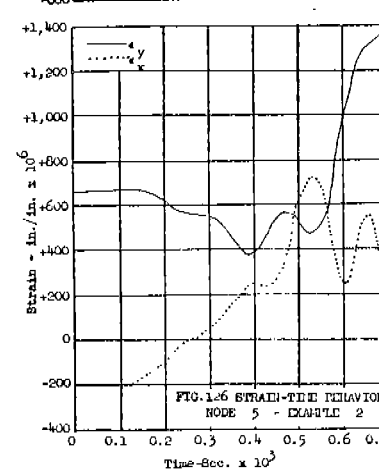
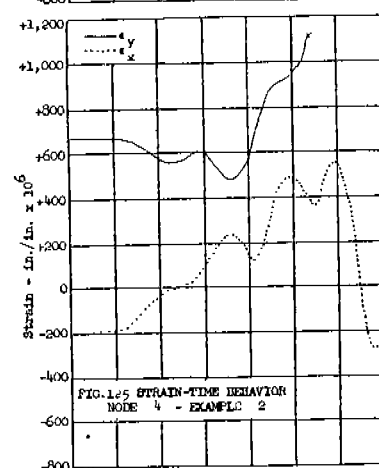
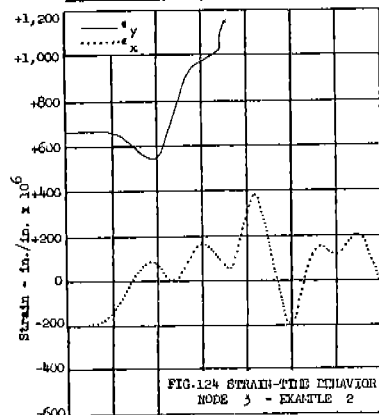
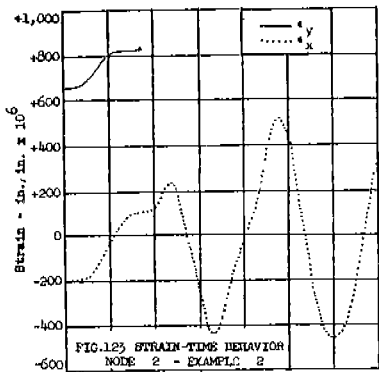
A general picture of the strain redistribution associated with crack propagation is as follows: A tension pulse is generated when strain energy is released by crack formation and propagates away from the source, creating a zone of biaxial tension ahead of the crack. As the crack approaches a particular point, the shear strain becomes positive in value and then decreases in

value as the crack goes past. Because the lattice model used is purely elastic and dissipates no energy, the strain energy released by the crack formation must be stored in the lattice model as kinetic energy of the bars and changes in strain of nodes and shear points. After the initial pulse resulting from separation of a node has passed, the bars of the lattice model develop an oscillatory motion because of strain wave reflection from boundaries.

Example 2: Symmetrical Crack Propagation. In this example a pair of cracks propagate from each edge of a square plate toward the center. As in Example 1 each of the cracks propagate toward the center in four jumps spaced at equal intervals of 0.180 millisecc. Both cracks start at time zero and reach the center of the plate after 0.720 millisecc. Integration was carried out with the Runge-Kutta Method with the time interval $h = 2 \times 10^{-6}$ sec.

Strain-time curves for nodes 1 to 10, node 13, and shear points 1 to 4 (as shown in Fig. 82) are presented in Figs. 123 to 136. A comparison of the strain-time curves for nodes 1 to 10 and node 13 of this symmetric crack-propagation case with strain-time curves for the same nodes of the unsymmetrical case in Example 1 show that there is very little difference in vertical strain response. There is some slight difference in magnitude, but the shapes of the curves are about the same. The horizontal strains are affected markedly because of the continuity at the left side of the symmetrical lattice model. Shear strains toward the right edge of the lattice model are the same for both the unsymmetrical and the symmetrical cases; however, toward the left side of the lattice model, the symmetrical-case shear strains at shear points 3 and 4 do not decrease to negative values in the same manner as shear points 3 and 4 in the unsymmetrical case, again showing the effect of continuity at the left side of the model (which is the center of the square plate represented by the lattice model).

Example 3: Comparison of Values Calculated by Two Numerical Integration Methods. The same problem discussed in Example 1 was solved using



the Newmark Beta-Method of integration with $\beta = 1/6$. As nearly as possible, all auxiliary data required for the numerical integration process are supplied by the same computer routines used for the solution with the Runge-Kutta Method. All starting conditions also were made identical, so that any difference in calculated values could be attributed to the integration method.

The time interval used was very conservative as far as limits of stability and convergence are concerned. As worked out in Ref. 18, the limits of stability and convergence for a single-degree-of-freedom system can be expressed in terms of h/T , where h is the integration time interval and T is the period of vibration. If a multi-degree-of-freedom system is considered, then T is taken as the period of a particular mode of vibration. For $\beta = 1/6$, the stability limit is $h/T = 0.551$ and the convergence limit is $h/T = 0.389$. Because the largest value of h/T is desired, the smallest period would be used when considering a multi-degree-of-freedom system.

The smallest period for the four-division unsymmetrical lattice model is $T = 0.31 \times 10^{-3}$ sec as shown in Table 2. As the bar spacing and bar mass are the same for the symmetrical model as for the unsymmetrical model, the shortest period of vibration is about the same in each case. Using the values $h = 2 \times 10^{-6}$ sec and $T = 0.31 \times 10^{-3}$ sec, the ratio h/T is 0.006, which is only a fraction of either the stability or convergence limit. Stability and convergence are therefore not a problem in carrying out the integration of this example with the Beta Method.

A comparison of extensional and shear strains at all node shear points of the unsymmetrical lattice model, as calculated with the Runge-Kutta and Newmark Beta-Methods of integration, is given in Table 4. Locations of the node and shear points listed in the table are shown in Fig. 82. Values are compared at times of 0.180, 0.360, 0.540, and 0.700 millisecc after a crack initiation; the latter value was chosen because it fell just before complete separation.

Referring to Table 4, it can be seen that at $t = 0.180$ millisecc the

TABLE 4 COMPARISON OF STRAINS CALCULATED WITH TWO INTEGRATION METHODS

Method	Runge-Kutta				Newmark Beta				Runge-Kutta				Newmark Beta				Runge-Kutta				Newmark Beta			
	Time 0.180 millisec.								Time 0.360 millisec.								Time 0.540 millisec.							
	Extensional Strains - in./in. x 10 ⁶								Extensional Strains - in./in. x 10 ⁶								Extensional Strains - in./in. x 10 ⁶							
Node	(ϵ_y)	(ϵ_x)	(ϵ_y)	(ϵ_x)	(ϵ_y)	(ϵ_x)	(ϵ_y)	(ϵ_x)	(ϵ_y)	(ϵ_x)	(ϵ_y)	(ϵ_x)	(ϵ_y)	(ϵ_x)	(ϵ_y)	(ϵ_x)	(ϵ_y)	(ϵ_x)	(ϵ_y)	(ϵ_x)				
1	-----	+0.00	-----	+0.00	-----	+0.00	-----	+0.00	-----	+0.00	-----	+0.00	-----	+0.00	-----	+0.00	-----	+0.00	-----	+0.00				
2	+852.69	+111.23	+845.20	+114.36	-----	-303.61	-----	-318.99	-----	-199.61	-----	-208.69	-----	-215.45	-----	-215.45	-----	-215.45	-----	-215.45				
3	+553.60	+81.49	+546.90	+86.58	+1206.74	-79.02	+1211.43	-88.05	-----	-217.66	-----	-215.45	-----	-215.45	-----	-215.45	-----	-215.45	-----	-215.45				
4	+610.04	-83.98	+610.72	-82.76	+566.29	+25.14	+555.33	+27.82	+1270.73	-107.83	+1280.55	-107.76	-----	-107.76	-----	-107.76	-----	-107.76	-----	-107.76				
5	+646.33	+0.00	+648.79	+0.00	+380.82	+0.00	+380.84	+0.00	+241.96	+0.00	+278.91	+0.00	+0.00	+0.00	+0.00	+0.00	+0.00	+0.00	+0.00	+0.00				
6	+676.87	+0.00	+676.18	+0.00	+599.62	+0.00	+606.85	+0.00	+770.75	+0.00	+802.48	+0.00	+815.74	+0.00	+815.74	+0.00	+815.74	+0.00	+815.74	+0.00				
7	+695.06	-203.65	+696.30	-206.71	+749.94	-191.97	+764.40	-193.05	+804.48	-231.72	+794.86	-215.28	+794.86	-215.28	+794.86	-215.28	+794.86	-215.28	+794.86	-215.28				
8	+751.98	-210.99	+758.02	-212.57	+777.30	-233.00	+772.41	-226.52	+20.57	-18.41	+0.89	-43.28	+20.57	-18.41	+0.89	-43.28	+20.57	-18.41	+0.89	-43.28				
9	+813.51	-286.53	+820.93	-285.81	+32.45	+7.97	+13.11	+1.76	-402.43	+375.44	-436.07	+411.27	-402.43	+375.44	-436.07	+411.27	-402.43	+375.44	-436.07	+411.27				
10	+147.26	+0.00	+144.95	+0.00	+71.73	+0.00	+86.60	+0.00	-132.31	+0.00	-155.49	+0.00	-132.31	+0.00	-155.49	+0.00	-132.31	+0.00	-155.49	+0.00				
11	+338.55	+0.00	+340.59	+0.00	+18.86	+0.00	+14.88	+0.00	-567.60	+0.00	-599.37	+0.00	-567.60	+0.00	-599.37	+0.00	-567.60	+0.00	-599.37	+0.00				
12	+621.62	-255.74	+617.95	-255.49	-5.70	+180.28	-18.45	+199.19	-227.57	+150.67	-235.64	+160.36	-227.57	+150.67	-235.64	+160.36	-227.57	+150.67	-235.64	+160.36				
13	+688.24	-281.88	+684.16	-284.69	+560.51	-128.44	+565.52	-118.70	+125.98	-110.00	+132.22	-155.79	+125.98	-110.00	+132.22	-155.79	+125.98	-110.00	+132.22	-155.79				
14	+675.86	-235.69	+673.54	-235.60	+650.26	-258.26	+637.99	-270.01	+650.73	-191.99	+673.95	-163.16	+650.73	-191.99	+673.95	-163.16	+650.73	-191.99	+673.95	-163.16				
15	+666.80	+0.00	+667.85	+0.00	+636.66	+0.00	+618.48	+0.00	+562.96	+0.00	+498.88	+0.00	+562.96	+0.00	+498.88	+0.00	+562.96	+0.00	+498.88	+0.00				
16	+665.10	+0.00	+665.33	+0.00	+790.72	+0.00	+794.19	+0.00	+671.30	+0.00	+619.57	+0.00	+671.30	+0.00	+619.57	+0.00	+671.30	+0.00	+619.57	+0.00				
17	+660.35	-215.48	+660.53	-213.78	+629.34	-230.41	+621.21	-232.72	+410.67	-178.20	+412.33	-186.38	+410.67	-178.20	+412.33	-186.38	+410.67	-178.20	+412.33	-186.38				
18	+632.50	-235.95	+632.17	-238.01	+468.19	-171.91	+459.29	-174.04	+48.43	+14.69	+56.84	+28.29	+48.43	+14.69	+56.84	+28.29	+48.43	+14.69	+56.84	+28.29				
19	+530.95	-211.91	+528.33	-213.64	+187.26	-20.34	+189.45	-17.46	-54.91	-70.48	-45.73	-66.84	-54.91	-70.48	-45.73	-66.84	-54.91	-70.48	-45.73	-66.84				
20	+387.86	+0.00	+380.61	+0.00	-109.14	+0.00	-120.57	+0.00	-371.77	+0.00	-361.00	+0.00	-371.77	+0.00	-361.00	+0.00	-371.77	+0.00	-361.00	+0.00				
21	+432.81	+0.00	+432.84	+0.00	-27.35	+0.00	-12.21	+0.00	-171.06	+0.00	-92.75	+0.00	-171.06	+0.00	-92.75	+0.00	-171.06	+0.00	-92.75	+0.00				
22	+665.46	-202.86	+665.83	-204.48	+898.50	-149.05	+913.45	-160.49	+1081.36	-45.12	+1212.56	-43.10	+1081.36	-45.12	+1212.56	-43.10	+1081.36	-45.12	+1212.56	-43.10				
23	+660.75	-217.85	+661.89	-216.05	+707.95	-189.58	+730.80	-190.64	+530.85	+163.50	+290.41	+210.54	+530.85	+163.50	+290.41	+210.54	+530.85	+163.50	+290.41	+210.54				
24	+634.32	-206.40	+637.74	-205.06	+514.60	-194.74	+527.45	-183.12	-78.57	-211.32	-109.37	-273.64	-78.57	-211.32	-109.37	-273.64	-78.57	-211.32	-109.37	-273.64				
25	+548.48	+0.00	+553.71	+0.00	+322.12	+0.00	+339.26	+0.00	+10.36	+0.00	+30.49	+0.00	+10.36	+0.00	+30.49	+0.00	+10.36	+0.00	+30.49	+0.00				

Shear Point	Shear Strain, γ_{xy}	Shear Strain, γ_{xy}	Shear Strain, γ_{xy}	Shear Strain, γ_{xy}	Shear Strain, γ_{xy}	Shear Strain, γ_{xy}	Shear Strain, γ_{xy}	Shear Strain, γ_{xy}
1	+295.32	+290.33	-29.87	-39.09	-21.17	-28.26	+300.37	
2	-312.61	-321.84	+939.48	+968.66	-246.45	-260.99	-255.71	
3	-197.91	-203.76	-274.54	-272.05	+554.46	+620.45	-239.79	
4	-66.17	-66.94	-284.90	-291.98	-642.87	-662.26	+446.70	
5	-7.32	-3.56	-175.70	-174.08	-398.20	-454.76	+98.04	
6	-10.71	-3.73	-138.07	-159.77	-185.11	+191.22	-249.55	
7	+100.79	+106.40	+562.29	+559.90	-585.74	-617.89	-402.12	
8	+404.50	+410.18	+237.81	+261.83	-500.15	-538.70	+108.87	
9	+315.96	+326.08	+17.18	+13.89	-283.85	-297.45	-229.14	
10	+215.65	+221.92	+123.83	+108.73	-386.39	-384.50	-436.26	
11	+69.34	+69.83	+47.96	+63.72	-3.00	-45.84	-265.86	
12	+15.16	+14.34	+18.34	+27.14	+52.15	+90.32	+11.88	
13	+5.15	+4.25	+24.50	+15.60	+166.45	+278.06	+62.40	
14	+25.09	+23.06	+61.56	+75.55	-37.21	-70.38	-59.51	
15	+75.90	+74.98	+43.46	+51.38	-137.56	-157.95	-208.02	
16	+99.86	+102.57	+6.76	-10.01	-2.04	+17.32	-346.95	

values calculated by the two methods agree very well, with the Runge-Kutta Method giving a slightly greater response ahead of the crack than the Beta Method. As the time increases, the values begin to deviate a little more, and the Beta Method starts giving a larger response ahead of the crack. At $t = 0.700$ millisecc one of the differences in values, at node point 23 which is on the fixed boundary, is 117×10^{-6} in./in. which is 18 per cent of the initial vertical strain value. In the vicinity of the crack tip, the values calculated by the two methods do not differ by more than 7 per cent of the initial strain value. The reason for the differences is that the Runge-Kutta Method has a truncation error for one step of the order of h^5 , and the ILLIAC computer code for the Runge-Kutta Method of integration has a provision for reducing round-off errors, whereas the Newmark Beta-Method, with $\beta = 1/6$, has a truncation error for one step of the order of h^3 , and the computer routine written for this method did not have a special provision to reduce round-off. As a result, in this particular case the Runge-Kutta Method of integration has a smaller truncation error and could carry more significant figures than the Beta Method.

Comparison of the values calculated with the two methods of integration shows that the same general results are obtained with each method. After a large number of integration steps there are some deviations in values, but these deviations do not change the overall picture of the transient strain distribution in the lattice model. Either method of integration provides a satisfactory solution for the problem.

SUMMARY AND CONCLUSIONS

This report has presented a physical lattice model suitable for investigating strain-wave propagation in two dimensions and for investigation of the transient strain redistribution associated with a crack that propagates in finite jumps. Equations expressing elastic behavior of the model under plane-stress conditions were developed for both static and dynamic conditions. The purpose of this type of model is to provide an approximate solution for problems to which

it is difficult or impossible to apply classical methods of analysis.

It was shown that the lattice model presented can be related to finite differences of an Airy stress function for linearly elastic conditions. Static equilibrium equations in terms of displacements were developed for plane-stress conditions. Equations can be developed for plane-strain conditions by using the stress-strain relationships applying to the plane-strain assumptions. The lattice model can also be used to investigate non-linear elasticity by using an appropriate stress-strain relationship in developing the equilibrium equations. A high-speed digital computer of large memory capacity is virtually a necessity for numerical solution of problems of any complexity with the lattice model.

Several statically loaded plates were analyzed with lattice models having different numbers of subdivisions. One case, a square plate loaded with parabolically distributed end tension, was solved by an energy method and with a lattice model having three different sizes of subdivision. Averaged energy-method stresses were compared to stresses calculated from the lattice models. It was found that for this comparison the lattice model gave excellent results. The greatest difficulty encountered with the lattice model was in duplicating the boundary deformation where the end loads were applied. Finer subdivision of the lattice model produced a better approximation of the loaded boundary deformation and gave more accurate results at other points of the lattice model.

Two examples of concentrated effects, a plate with a pair of concentrated loads and plates containing a crack or pair of cracks, were presented to show how the lattice model represents the strain distribution associated with such effects and to get some indication of the change in representation of strain distribution as the number of model-subdivisions changes. If steep strain gradients are involved in a problem, a finely divided lattice model is required to give a satisfactory representation of these strain gradients.

The differential equations expressing the dynamic behavior of the lat-

tice model were developed by adding time-dependent terms to the static equilibrium equations of the lattice model. Application of these equations to a steady-state condition, and the calculation of natural frequencies of lattice models are discussed. Frequencies for two examples and mode shapes for one example are also given. Two methods of numerical integration were used in the analysis of crack propagation in lattice models. It was found that the two methods of numerical integration gave essentially the same results after a small number of time intervals. After a large number of time intervals one value differed by 18 per cent of the initial vertical-strain value, while in the vicinity of the crack, differences were about 7 per cent of the initial strain value; however, these differences did not change the overall picture of strain redistribution in the lattice model. The computer used for the integration of the differential equations expressing the transient behavior of the lattice model could not be used for lattices having more than 40 bars without the calculation time becoming excessive. A lattice model with only 40 bars is much too coarse to adequately represent the steep strain gradients associated with a crack, and therefore such a coarse lattice can only give a rough qualitative picture of the transient strain redistribution associated with crack propagation. In spite of the coarseness of the lattice model used, a general picture of transient strain redistribution was given by the lattice model.

Only undamped elastic behavior of the lattice model was considered because of the limitations imposed by the available computer. Damping and non-linear deformational behavior could be treated with the lattice model if a very large computer is used for solution of the problem.

Several problems arise in solving dynamic problems with a lattice model. One problem is that bars can be set into oscillatory motion when energy is fed into or released in the lattice model. This has the effect of modulating strain waves passing through the lattice model. Bar oscillations also occur as a result of reflections of strain waves from the lattice model boundaries. A second problem, of more importance for strain waves originating from external dynamic

loads than for transient strains associated with a crack, is that the elastic lattice model has an electrical analog in the form of an L-C filter. Such electrical filters have the property of offering a varying resistance to the passage of electrical disturbances of varying frequencies, passing some frequencies with little resistance while stopping passage of other frequencies. Therefore, if the lattice model is to be used for investigation of strain-wave propagation resulting from external loading, the possibility of the existence of passing and stopping bands must be considered.

It is concluded that the lattice model presented in this report can be used for the investigation of strain-wave propagation problems in two-dimensions. The use of the lattice-model method of analysis is contingent upon the availability of a large high-speed computer. It was not possible with the computer available for this investigation to use lattice models having very many bars, and only a crude picture could be formed of the transient strain distribution in a plate with a propagating crack. When larger and faster computers are used, the lattice-model method for investigating transient strains associated with a propagating crack can be used to theoretically investigate different aspects of the fracture process in an ideal plate replaced with a lattice model by assuming fracture criteria for nodes in the lattice model and determining whether a crack would propagate or arrest. The fracture criteria assumed could include internal damping, strain rates, strain magnitudes, non-linear stress-strain relationships, and previous deformation history.

REFERENCES

1. Shank, M. E., A Critical Survey of Brittle Fracture in Carbon Plate Steel Structures Other Than Ships (Ship Structure Committee Report Serial No. SSC-65), Washington: National Academy of Sciences-National Research Council, December 1, 1953.
2. Rolfe, S. T., Lynam, T. M., and Hall, W. J., Studies of the Strain Distribution in Wide Steel Plates During Brittle Fracture Propagation (Civil Engineering Studies, Structural Research Series No. 151), Urbana: University of Illinois, April 1958. (Also available as Ship Structure Committee Report Serial No. SSC-118, Washington: National Academy of Sciences-National Research Council, December 30, 1959.)
3. Inglis, C. E., "Stresses in a Plate Due to the Presence of Cracks and Sharp Corners," Trans. Inst. Naval Arch. (London), vol. 55, (1913).
4. Westergaard, H. M., "Bearing Pressures and Cracks," Journ. App. Mech., vol. 6 (1939).
5. Griffith, A. A., "The Phenomenon of Rupture and Flow in Solids," Trans. Royal Society (A), vol. 221 (1921).
6. Orowan, E., "Fracture and Strength of Solids," Reports on Progress in Physics, vol. 12, p. 214 (1948-49).
7. Irwin, G. R., "Fracture Dynamics," Trans. Am. Soc. Metals, vol. 40A, pp. 147-166 (1948).
8. Neuber, H., Theory of Notch Stresses. Ann Arbor, Mich.: J. W. Edwards, 1946.
9. Irwin, G. R., "Analysis of Stresses and Strains Near the End of a Crack Traversing a Plate," Journ. App. Mech., 24:3 (Sept. 1957).
10. McClintock, F. A., "Ductile Fracture Instability in Shear," Journ. App. Mech., 25:4, pp. 582-8 (Dec. 1958).
11. Mott, N. F., "Brittle Fracture in Mild Steel Plates--II," Engineering, 165:4275, pp. 16-18 (Jan. 2, 1948).
12. Roberts, D. K., and Wells, A. A., "The Velocity of Brittle Fracture," Engineering, 178:4639, pp. 820-821 (Dec. 24, 1954).

13. Yoffe, E. H., "The Moving Griffith Crack," Philosophical Magazine, vol. 42, 7th series, No. 330 (July 1951).
14. Hrennikoff, A., "Solution of Problems in Elasticity by Framework Method," Journ. App. Mech., 8:4, p. A169 (Dec. 1941).
15. McHenry, D., "Lattice Analogy for Solution of Stress Problems," Journ. Institution of Civil Engineers, pp. 59-82, Dec. 1943.
16. Timoshenko, S., and Goodier, J. N., Theory of Elasticity (2nd Edition). New York: McGraw-Hill Book Co., 1951.
17. Newmark, N. M., "Numerical Procedure for Computing Deflections, Moments, and Buckling Loads," Trans. ASCE, vol. 108, p. 1161 (1943).
18. Newmark, N. M., "Computation of Dynamic Structural Response in the Range Approaching Failure," Proc. of the Symposium on Earthquake and Blast Effects on Structures, pp. 114-129. Los Angeles: Earthquake Engineering Research Institute and University of California, June 1952.
19. Newmark, N. M., and Chan, S. P., A Comparison of Numerical Methods for Analyzing the Dynamic Response of Structures (Civil Engineering Studies, Structural Research Series No. 36), Urbana: University of Illinois, Oct. 1952.
20. Tung, T. P., and Newmark, N. M., A Review of Numerical Integration Methods for Dynamic Response of Structures (Civil Engineering Studies, Structural Research Series No. 69), Urbana: University of Illinois, March 1954.
21. Nystrom, E. J., "Uber die Numericshc Integration von Differentialgleichungen," Aeta Soc. Sci. Fennicae, 50:13, p. 56 (1926).
22. Gill, S., "A Process for the Step-by-Step Integration of Differential Equations in an Automatic Digital Computing Machine," Proc. of the Cambridge Philosophical Society, vol. 47, pp. 96-108 (1951).
23. Hildebrand, F. B., Introduction to Numerical Analysis. New York: McGraw-Hill Book Co., 1956.
24. Levy, H., and Baggott, E. A., Numerical Solution of Differential Equations. New York: Dover Publications, Inc., 1950.
25. Brillouin, L., Wave Propagation in Periodic Structures (2nd Edition). New York: Dover Publications, Inc., 1953.

COMMITTEE ON SHIP STRUCTURAL DESIGN

Chairman:

Professor N. J. Hoff
Head, Department of Aeronautical Engineering
Stanford University
Stanford, California

Vice Chairman:

Mr. M. G. Forrest
Vice President - Naval Architecture
Gibbs and Cox, Inc.
21 West Street
New York, New York

Members:

Dr. C. O. Dohrenwend
Provost and Vice President
Rensselaer Polytechnic Institute
Troy, New York

Professor J. Harvey Evans
Department of Naval Architecture and Marine Engineering
Massachusetts Institute of Technology
Cambridge 39, Massachusetts

Dr. J. M. Frankland
Mechanics Division
National Bureau of Standards
Washington 25, D. C.

Professor J. W. Miles
Department of Engineering
University of California
Los Angeles 24, California

Professor William Prager
Brown University
Providence 12, Rhode Island

Professor Dana Young
School of Engineering
Yale University
New Haven, Connecticut